Advances in Energy Transition

8th Colloquium of the Munich School of Engineering
July 19, 2018

Organizers of the Colloquium:
Christian Aigner, M.Sc.
Julia Bergermeier
Felix Fischer, M.Sc.
Stephanie Horstmeier
Anurag Mohapatra, M.Sc.
Nitin Saxena, M.Sc.
Iryna Takser, B.Sc.
Dr.-Ing. Christoph Wieland

Picture Credits:
Title page; Uli Benz, TUM, 2017 Page 1; Astrid Eckert

Editor:
Prof. Dr. rer. nat. Thomas Hamacher
Director Munich School of Engineering

Technische Universität München
Munich School of Engineering

Lichtenbergstr. 4a
85748 Garching
http://www.mse.tum.de

Jurors:
Andreas Albrecht, M.Sc.
Dr. Katharina Aubele
Marco Bobinger, M.Sc.
Prof. Dr. Christoph Hackl
Akhila Jambagi, M.Eng.
Michael Kramer, M.Sc.
Dr. Volker Körstgens
Dr. Petra Liedl
Dr. Dr. Christina de la Rue Lope
Dr. Konrad Schönleber
Dr. Lin Song
Dr. Annelies Vandersickel

Date of Publication:
July 2018

Download:
https://mediatum.ub.tum.de/1449240
DOI: 10.14459/2018md1449240

In 2001 Michael Grubb published in the Journal Energy Policy a paper with the title: “Who’s afraid of atmospheric stabilisation? Making the link between energy resources and climate change”. In the paper he confronts the carbon budgets, which may still be released by emissions to the atmosphere, with the carbon stored in the conventional fossil fuel base. He concludes that the resource base of conventional oil and gas could to a great extent be used up without challenging the climate goals. It is the use of coal on one side and of unconventional oil resources on the other side, which will lead to high emission levels. His paper was meant as an offer to oil and gas companies to use their assets, if already in operation, by refraining from investments especially in unconventional resources. Today 17 years later we know the companies did not follow the suggestion of Mr. Grubb. On the 20th of June this year CNN titled an article, “Shale exec: US will be the world's biggest oil producer by the fall” and most of this new production is unconventional oil. This demonstrates that the route to go for a low emission path is certainly not followed these days and that it is rather unlikely that the 2°C goal will be reached, not to talk about a 1.5°C goal. Some people have hope that “negative” emissions from e.g. biomass plants, where emissions are stored in geological formation, can solve the problem. However, it is time that the problem is addressed by all means. Slow incremental changes will no longer be able to fix the problem; it is time for new radical changes! Since we are in the last phase of the additional time, science either scores some extraordinarily pretty goals or the game is lost.

Thomas Hamacher
Director Munich School of Engineering

Munich School of Engineering (MSE)

The **Munich School of Engineering (MSE)** of the Technische Universität München is an open platform for all researchers and students at TUM to combine knowledge and visions for the energy systems of tomorrow. The MSE bundles competencies from TUM's faculties to develop comprehensive research programs tackling as well fundamental as applied questions in the areas of energy production, distribution and storage. To ready upcoming generations of engineers and scientists to respond to the challenges of tomorrow, programs on undergraduate, graduate and postgraduate (PhD) level have been developed and are continuously refined. Exceptionally talented students are equipped with a fundamental scientific tool box and an interdisciplinary mindset to become the future leaders in energy research.

TUM.Energy is a cross-departmental research initiative within the MSE, which offers a platform for the so-called "Green Technologies", in particular energy research in the segments Electromobility, Power Plant Technologies, Renewable Energies, and Energy Efficiency. These main topics are represented in networks in which researchers of different departments are working in detail on the challenges within these fields:

- The ***Geothermal-Alliance Bavaria*** combines interdisciplinary research strategies in order to strengthen deep geothermal as a sustainable and controllable source of renewable energy.
- In the ***Center for Power Generation*** the efficiency and the environmental sustainability of existing and future power plants is increased and improved by modern and innovative technologies.
- The ***Network for Renewable Energy*** is doing research in both, fundamental research in the field of new technologies and materials as well as improvements of existing technologies increasing their applicability.
- The ***Science Center for Electromobility*** contains a wide spectrum of topics from fundamental battery research, development and design of electric vehicles as well as future mobility concepts.
- The ***Center for Sustainable Building*** is dedicating itself to energy efficiency during the use of buildings and its consideration during planning. Thereby not only technical but also socio-ecologic aspects are integrated in urban planning approaches.
- The ***Combined Smart Energy Systems Center*** focuses on modeling the interdependency of electricity distribution, heat and communication networks. The goal of the center is to develop strategies for integrating extensive distributed energy sources in the energy grid of the future, the smart micro grid.

Munich School of Engineering
Technische Universität München

8th Energy Colloquium of the Munich School of Engineering

Advances in Energy Transition

July 19, 2018 – 8:30 a.m. to 8:00 p.m.
TUM – Quantum, Garching-Hochbrück

8:30 – 9:00 a.m.
Registration

9:00 – 9:15 a.m.
Opening: Prof. Thomas Hamacher
Director Munich School of Engineering

9:15 – 9:45 a.m.
Keynote: Shell Hydrogen Study – Energy of the Future?
Dr. Jurgen Louis, Shell Global Solutions GmbH

9:45 – 11:00 a.m.
Electrochemical Energy Storage: From Fundamentals to Experiments
Session Chair: **Prof. Peter Müller-Buschbaum**

Watching Metal Nanolayer Growth on Functional Polymer Thin Films for Lithium-Ion Battery Applications
Simon Schaper, Chair of Functional Materials

Towards Graphite/V2O5 Na Ion Batteries
Lukas Seidl, Electrochemical Research Group

Activity of Oxygen and Hydrogen Evolution Reaction Electrocatalysts under Industrially Relevant Conditions
Sebastian Watzele, Physics of Energy Conversion and Storage

11:00 – 11:30 a.m.
Poster Presentation and Coffee Break

11:30 – 12:45 p.m.
Power Generation and Storage: From Micro to Macro
Session Chair: **Prof. Hartmut Spliethoff**

Monitoring a Commercial µ-CHP SOFC-Stack by Electrochemical Impedance Spectroscopy
Tobias Herrmann, Chair of Plant and Process Technology

Biomass Combustion from Lab-Scale to Full-Scale: A Holistic Approach for CHP Plants
Richard Nowak Delgado, Chair of Energy Systems

Distributed Residential Battery Energy Storage Systems in a Microgrid Environment
Stefan Englberger et al., Institute for Electrical Energy Storage Technology

12:45 – 2:00 p.m.
Poster Presentation and Lunch Break

Please register: **http://www.mse.tum.de**

2:00 – 2:30 a.m.
Keynote: Potential of Sustainable Campuses in Driving Energy Transition
AStA Umweltreferat, TUM

2:30 – 3:45 p.m.
Renewable Energies: From Prediction to Market
Session Chair: **Prof. Carlo L. Bottasso**

An Analytical Weather Generator: Energy Source Data for Renewable Energy Models
Franz Christange, Chair of Renewable and Sustainable Energy Systems

Numerical Simulation of a Scaled Wind Farm
Chengyu Wang, Chair of Wind Energy

Renewable Auctions – A Real Options Approach
David Matthäus, Chair of Management Accounting

3:45 – 4:15 p.m.
Poster Presentation and Coffee Break

4:15 – 5:30 p.m.
Energy-Water-Nexus: From Munich to Harare
Session Chair: **Prof. Werner Lang**

Multi Energy Management and Aggregation Platform
Alexandre Capone, Chair of Renewable and Sustainable Energy Systems

Thermal Use of Shallow Groundwater in Munich's Energy Planning
Fabian Böttcher, Chair of Hydrogeology

Promoting Rural Electrification in Sub-Saharan Africa: Least-Cost Modeling of Decentralized Energy-Water-Food Systems
Johannes Winklmaier, Chair of Renewable and Sustainable Energy Systems

5:30 – 6:00 p.m.
Keynote: Designing with Nature -The Potentials of Green Technologies in the Context of Climate Change and the Transition to Renewable Energy
Prof. Ferdinand Ludwig, TUM

6:00 – 6:15 p.m.
Summary and Closing

6:15 – 8:00 p.m.
Poster and Presentation Award with Colloquium Dinner

Abstracts

1. Oral Presentations

Watching metal nanolayer growth on functional polymer thin films for lithium-ion battery applications

Simon Schaper[a], Franziska C. Löhrer, Volker Körstgens, Matthias Schwartzkopf, Pallavi Pandit, Alexander Hinz, Oleksandr Polonskyi, Thomas Strunskus, Franz Faupel, Stephan V. Roth, and Peter Müller-Buschbaum[b]

[a]simon.schaper@ph.tum.de, [b]muellerb@ph.tum.de

Understanding the interface between metals, commonly used as current collectors, and ion-conducting polymers used in polymer lithium-ion batteries (LIBs) is crucial to develop highly reproducible, low-cost and reliable devices. To address these issues, sputter deposition is the technique of choice to fabricate scalable, reproducible and controllable nanometer and sub-nanometer metal layers on polymer thin films. The sputter deposition process, being well understood and controlled, offers advantages over chemical methods to tailor metal thin-flim morphologies on the nanoscale and offers a superior adhesion of the deposited material.[1] We use in-situ grazing incidence small angle X-ray scattering (GISAXS) to investigate the formation, growth and, self-assembled structuring on polymer thin films used in LIBs.[2]

The growth of gold on silicon and homopolymer substrates was investigated by Schwartzkopf et al. [1],[2]. Continuing these studies having a polymer solid state battery in mind, the growth of gold and copper on polystyrene-*block*-poly(ethylene oxide) (PS-*b*-PEO), a diblock copolymer with a glassy PS block providing mechanical stability and a soft, ion-conducting PEO block, used for polymer electrolytes and composite battery electrodes is investigated. Using the hemispherical growth model by Schwartzkopf et al. [3] and a modified model with hemispheroids, the gold and copper growth can be described, respectively (see Figure 1).
A selective growth of gold and copper is also found in the GISAXS measurements. Thus, this work gives valuable insight into understanding the growth mechanism of copper current collectors on polymer composite electrodes for LIBs.

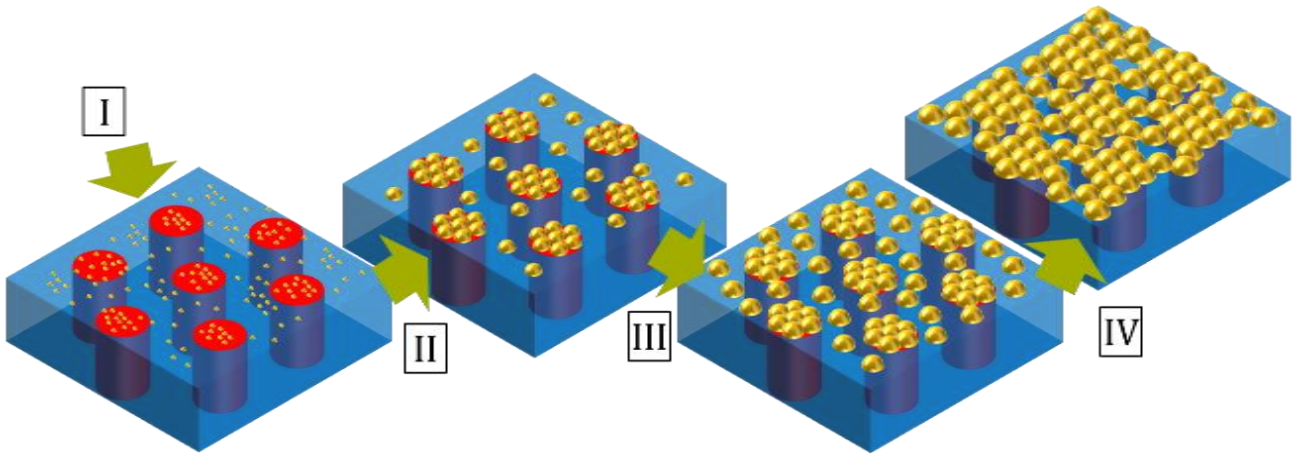

Figure 1: Model for the selectieve growth of gold/copper thin-films on polystyrene-*block*-poly(ethylene oxide) (PS-*b*-PEO) templates. PS domains are shown in red, PEO domains in blue, respectively. I) nucleation of metal particles, II) diffusion driven metal-cluster growth, III) enhanced growth on PEO domains, IV) cluster growth due to adsorption and attainment of the percolation thershold.

[1] Schwartzkopf et al., ACS Appl. Mater. Interfaces 9, 5629 (2017).
[2] Schwartzkopf et al., ACS Appl. Mater. Interfaces 7, 13547 (2015).
[3] Schwartzkopf et al., Nanoscale 5, 5053 (2013).

Towards Graphite/V_2O_5 Na Ion batteries

L. Seidl[a], H. Si[b], E. M. Ling Chu[c], S. Martens[d], J. Ma[e], X. Qiu[f], A. Knoll[g], U. Stimming[h], O. Schneider[i]

[a]lukas.seidl@tum.de, [b]shn_laurial@126.com, [c]eileen_chu90@hotmail.com, [d]sladjana.martens@tum.de, [e]jiwei.ma@tongji.edu.cn, [f]qiuxp@mail.tsinghua.edu.cn, [g]knoll@in.tum.de, [h]Ulrich.Stimming@newcastle.ac.uk, [i]oliver_m.schneider@tum.de

While Li ion batteries (LIBs) represent the state of the art battery system for use in mobile devices and in electric vehicles, they cannot satisfy the increasing need for energy storage in stationary applications [1]. Na ion batteries (NIBs) represent a viable alternative, because sodium is an abundant element and evenly distributed over the world. The typical energy density is still below those of LIBs, but for stationary application this disadvantage is compensated by the lower cost [2]. Materials from LIBs cannot be transferred immediately to NIBs, as the ion radius and the chemistry of the different crystallographic phases differ from the Li systems. In this work, studies aiming at a full NIB battery using graphite as the negative electrode material and V_2O_5 as the positive electrode materials are presented.

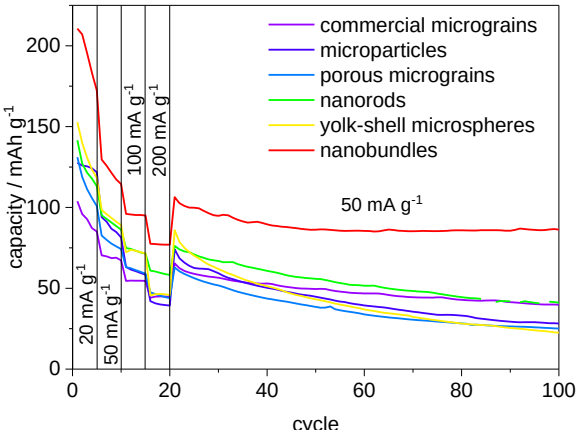

Figure 1: Capacities and rate capabilities of different V_2O_5 morphologies

In common battery electrolytes based on organic carbonate solvents, graphite cannot be used for sodium ion batteries, as no stable binary graphite intercalation compounds (GICs) can be formed [3]. However, it has been shown in literature that glyme based solvents do permit the formation of ternary GICs, i.e. the intercalation of solvated Na ions [4-6]. We studied this intercalation behavior in the first four glymes systematically using several *in-operando* techniques [7]. The general intercalation mechanism is very similar, forming eventually stage 1 GICs. However, in the triglyme the Na ion is intercalated with only a single solvent molecule, and thus not fully coordinated. This slows down the kinetics and lowers the capacity. For construction of a full cell, therefore tetraglyme was chosen as a solvent. V_2O_5 is not the best cathode material in LIBs, but it is rather versatile, can be easily fabricated in many different morphologies, and can also intercalate Na ions [8, 9]. First, we studied the impact of the morphology of the V_2O_5 on the Na (de)intercalation in standard battery electrolytes. Sono-chemically prepared nanostructured V_2O_5 clearly outperformed micron-sized materials with respect to capacity, rate capability, and energy efficiency (cf. Figure 1). A change of the solvent had little impact on the electrochemistry, indicating that Na is inserted without solvent into V_2O_5. For the construction of a full cell, the V_2O_5 electrode was pre-sodiated in another cell before assembly. The full cell performance (cf. Figure 2) and the contributions from the individual electrodes will be discussed in this presentation.

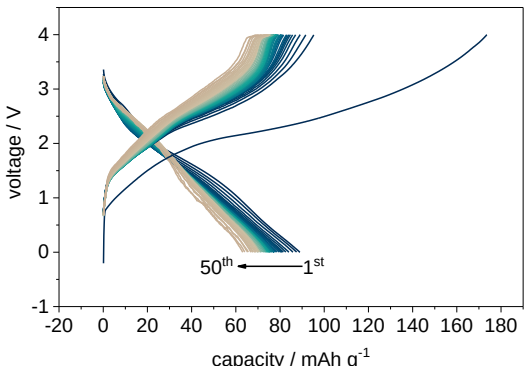

Figure 2: Charge-discharge curves of a full graphite|V_2O_5 cell in 1 M $NaClO_4$ in tetraglyme

References:

[1] R. E. Smalley, MRS Bull. 30 (2005) 412−417
[2] V. Palomares et al., Energy Environ. Sci. 5 (2012) 5884−5901
[3] K. Nobuhara et al., J. Power Sources 243 (2013) 585–587
[4] F. Klein et al., Phys. Chem. Chem. Phys. 15 (2013), 15876
[5] B. A. Jache et al., Phys. Chem. Chem. Phys. 18 (2016) 14299–14316
[6] H. Kim et al., Energy Environ. Sci. 8 (2015), 2963–2969
[7] L. Seidl et al., Energy Environ. Sci. 10 (2017) 1631-1642
[8] R. Haberkorn et al., Z. Anorg. Allg. Chem. 640 (2014) 3197–3202
[9] S. Tepavcevic et al., ACS Nano 6 (2012) 530–538

Intrinsic Activity of some Oxygen and Hydrogen Evolution Reaction Electrocatalysts under Industrially Relevant Conditions

Sebastian Watzele[a], Yunchang Liang[b], Aliaksandr S. Bandarenka[c],

[a]s.watzele@tum.de, [b]yunchang.liang@tum.de, [c]bandarenka@ph.tum.de

Water electrolysis to produce hydrogen fuel is one of the most important processes to optimize on the way to sustainable energy provision schemes. Its efficiency in both alkaline and acidic media is drastically limited by the sluggish kinetics of the oxygen evolution reaction (OER) taking place at the anode side of modern electrolyzers. Numerous electrocatalysts have been proposed recently to increase the activity of the anodes; most of them are transition metal oxides and perovskite materials. However, the activities reported in the literature for these electrodes are in the majority of cases measured at low overpotentials, low or moderate current densities (often 10-50 $mA \cdot cm^{-2}$), relatively dilute electrolytes (e.g. 0.1 M KOH) and at room temperatures. However, commercial electrolyzers operate at current densities, which are at least one order of magnitude larger, elevated temperatures and significantly higher pHs. In order to enable new generation of electrocatalysts it is important to evaluate their intrinsic activities under industrially relevant conditions. This is not a trivial task, neither in industry nor in research laboratories, particularly due to (i) formation of a non-conducting gas phase in the vicinity of the electrode under such conditions, (ii) limitations due to mass transfer and uncompensated resistances, and (iii) problems in determination of the real electroactive electrode surface area. In this work, with the use of microelectrodes we evaluate intrinsic OER catalytic activities of several state-of-the-art nickel-, cobalt- and nickel/iron-oxide/hydroxide thin films at different temperatures (up to 80 °C), in 5.4 M KOH and at current densities up to several $A \cdot cm^{-2}$. Additionally, Ni-modified Pt electrocatalysts for the hydrogen evolution reaction were also tested under similar conditions and compared with pure Pt and Ni electrodes.

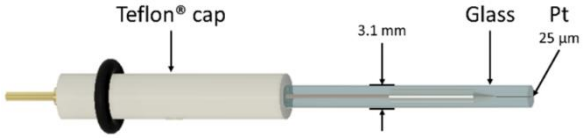

Figure 1: Sketch of the platinum microelectrode

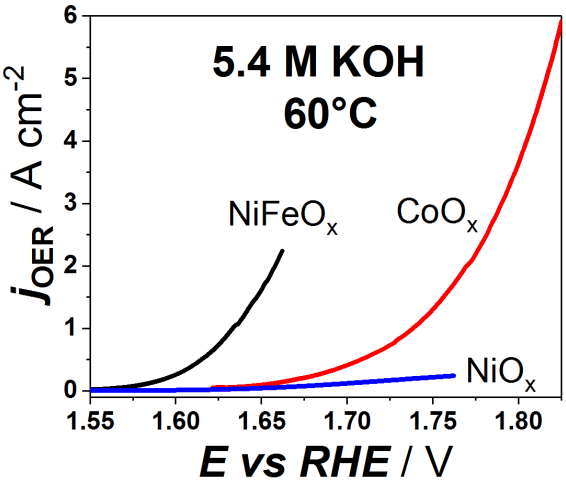

Figure 2: OER activity measurement of different catalysts at industrial relevant conditions

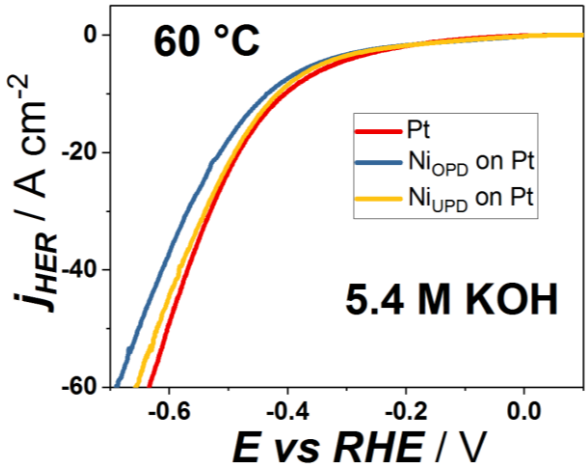

Figure 3: HER activity measurements

Reference:
S. Watzele, Y. Liang, A. S. Bandarenka, submitted

Monitoring a commercial µ-CHP SOFC-Stack by electrochemical impedance spectroscopy

Tobias Herrmann [a], Marius Dillig [b], Jürgen Karl [c]

[a]tobias.herrmann@fau.de, [b]marius.dillig@fau.de, [c]juergen.karl@fau.de

The use case of µ-CHP SO(F)C systems is not limited to the commonly applied natural gas fueled baseload operation. Transient reversible operation or the use of other fuels like producer gas from biomass could greatly extend the market penetration of SOC systems. However, in those advanced application scenarios lifetime, degradation and fuel utilization are major challenges which have to be addressed. For example, fuel fluctuations and remaining contaminants in the Biosyngas lead to unwanted processes like the reoxidation of nickel based anodes. In order to guarantee stable stack operation and to evaluate ongoing processes monitoring solutions are necessary.

The Chair of Energy Process Engineering at Friedrich-Alexander-University Erlangen-Nuremberg (FAU-EVT) investigates the integration of biomass gasification and solid oxide fuel cells. Here, we focus on an online monitoring of the stack behavior, which ultimately lays the foundation for a stack module control scheme. The research targets on developing a low ripple current power inverter with an integrated electrochemical impedance spectroscopy function. Evaluating the low-frequency response of the stack can give insights into the current availability of electrochemical active species, while other frequency domains address ion conduction or charge transfer.

A specifically engineered frequency response analyzer (NOVUM Engineering) has been implemented in our 1 kW-stack module test rig and delivers continuous impedance spectra. Based on a variation of different stack operation parameters (gas composition and flow rates, temperature, load), monitoring methods are currently developed and their suitability is evaluated.

This contribution to the Colloquium gives an overview about stack monitoring and presents results from EIS measurements from a 1 kW commercial SOFC stack. Those measurements are interpreted in terms of their usability as state-of-health monitoring tool.

Biomass Combustion from Lab-scale to Full-scale: A holistic Approach for CHP plants

Richard Nowak Delgado[b], Lynn Hansen, Sebastian Fendt, Hartmut Spliethoff

[a]richard.nowak.delgado@tum.de

The European Horizon 2020 project “Biofficiency” is dealing with the enhancement of biomass-fired CHP plants by handling ash-related problems. The project approach addresses current bottlenecks in solid biomass combustion, namely enhanced deposit formation, corrosion and ash utilization by a variety of new, promising technologies.

Three different pre-treatment methods in order to derive a more homogeneous fuel with improved properties (e.g. for pellet production, handling and combustibility) are investigated: torrefaction, hydrothermal carbonization and steam explosion. Additionally, the removal of corrosive components (such as potassium chloride) in the biomass fuel during the pre-treatment process is analysed. Potential feedstock are agricultural or wood industry residues such as straw or bark, fast-growing crops including miscanthus and wood pellets.

Efficiency increase of CHP plants can be achieved by generating steam at elevated temperatures through solving and understanding of ash-related problems – namely slagging, fouling and corrosion. Those problems can cause unscheduled power plant outages and unplanned maintenance work and therefore increase operation costs.

Detailed ash analysis in terms of chemistry and physical properties can help to widen ash utilization and nutrient recirculation. Therefore, ashes are taken from biomass-fired PF and FB experimental test rigs and power plants at different locations in order to explore new ideas to the European technical regulation for future biomass ash usage. New concepts are studied and possible utilization options are explored based on in-depth ash characterization.

Keywords: Pulverized fuel combustion of biomass, full-scale biomass combustion, biomass pre-treatment, biomass ash utilization.

Distributed residential battery energy storage systems in a microgrid environment

Stefan Englberger[a], Holger C. Hesse, Andreas Jossen

[a]stefan.englberger@tum.de

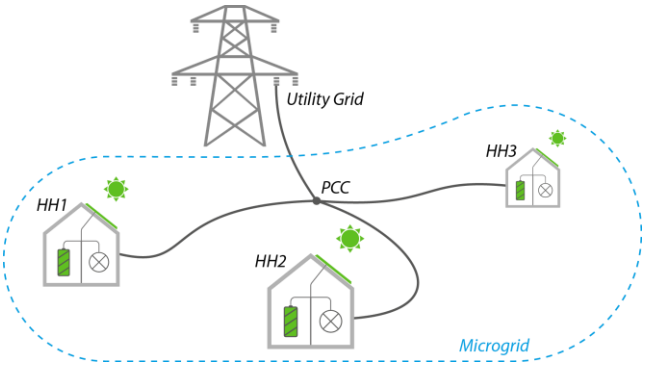

Figure 1: Three households that are connected to the superordinate utility grid

Residential battery energy storage systems are increasingly installed in households with solar photovoltaic generation. While self-consumption and self-sufficiency can be increased notably with PV-coupled battery systems, grid relief and profitability remain low in most scenarios investigated in the literature. At the same time, several announcements to electricity sharing and coordinated control of a "swarm" of multiple storage systems have been in the media recently (cf. Figure 1). However, these announcements come short in their technical analysis and economic value assessments.

In this contribution, two optimization and simulation approaches are combined: Firstly, a central controlled linear-programming optimization is applied to coordinate the power flow between the households and the superordinate utility grid. Multiple residential energy storage systems can thus be addressed simultaneously. All relevant electricity flows of the microgrid-connected PV-battery prosumer household are depicted and fundamental constraints as well as equalities summarized for the problem formulation (cf. Figure 2). Secondly, the proprietary storage simulation tool *SimSES* is used for in-depth analysis of profitability, aging, and efficiency for all individual energy storage systems. Apart from to the objective of maximizing the community profit, a peak-power and grid reliving constraint is considered suppressing power peaks between point of common coupling and utility grid.

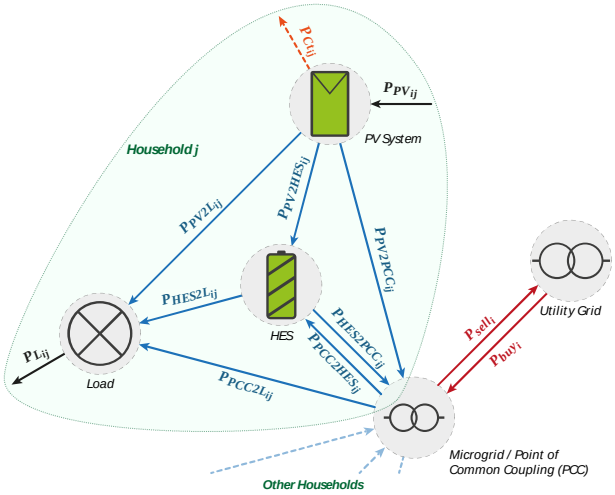

Figure 2: Overview of relevant nodes for the power flow optimization of an exemplary household *j*

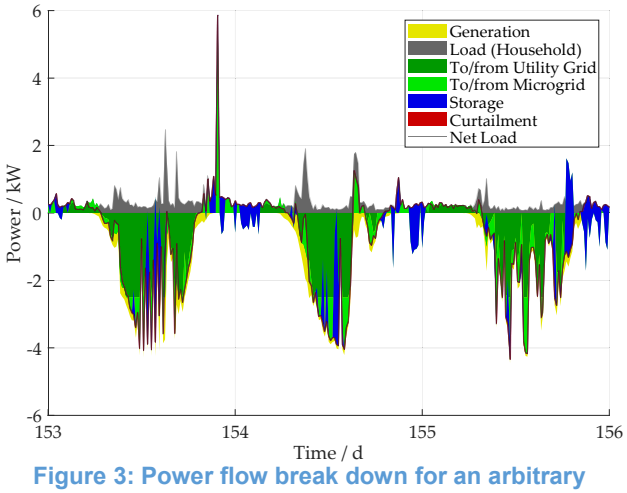

Figure 3: Power flow break down for an arbitrary household showing a three-day operation period

The overall economic benefit and the maximum grid relieving potential of sharing energy in the community microgrid is derived and compared to an autonomous operation of the same households. By allowing electricity trading between the households in the microgrid, the amount of purchased electricity from the utility grid per household was reduced in the microgrid setting. For the exemplary simulation data chosen, a profitability increase of 1.5% per household was achieved. Simultaneously, the average dissipation losses were reduced by 13.5% for the low-voltage power lines connecting the microgrid with the superordinate utility grid. At the same time, the charge throughput of all energy storages in the microgrid setting has decreased, which led to notably reduced battery aging and improved storage system efficiencies

An Analytical Weather Generator: Energy Source Data for Renewable Energy Models

Franz Christange[a], Thomas Hamacher[b]

[a]franz.christange@tum.de, [b]thomas.hamacher@tum.de

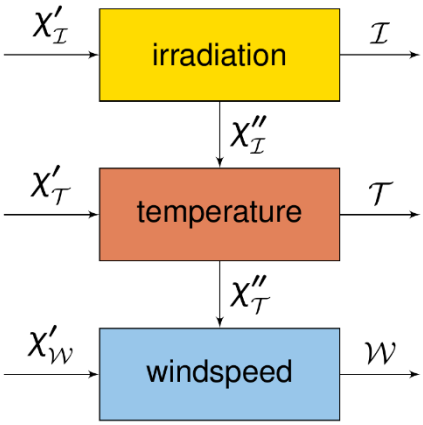

Figure 1: Interactions in the weather model with white noise input

The integration of significant amounts of renewable energy sources into the electricity system implicates its dependency on climate and weather, which has to be incorporated in its modeling. Three weather quantities emerge to be important. Irradiation is the main energy source for photovoltaic (pv) systems, windspeed is the energy source for wind power plants and temperature affects sparsely both processes. The main importance of the temperature to be considered is in the context of power to heat, as it highly affects the heat energy demand.

Renewable energy system models require accurate weather models as input. Conventional approaches showed results with limited accuracy. Using annual recorded time series shows typically deviations in the double-digit percentile range. Conventional weather generator approaches oversimplify by neglecting important properties of the weather, like the interdependency of individual weather quantities, realistic rates of change or the model's accurate time variance.

This work describes an improvement of our previous work's weather model. We use analytical mathematics to ensure its modularity and the ability to intuitively parameterize the model. It models solar irradiation, ambient temperature and wind speed which interdepend as illustrated in Fig. 1. Each weather quantity is computed in 4 individual steps as depicted in Fig. 2. The input into the system is standard normal distributed white noise. The first step is to execute a simplified interdependent dynamical system to incorporate the typical dependency of one sample on its preceding samples, what we call realistic rate of change. The dynamics also incorporate the interdependency of the weather quantities as illustrated in Fig. 1. The second step is to incorporate the time variance as a parameter function of the time dependent mean and standard deviation. The third step is to apply the time variance on the dynamics output. This results in a time variant colored normal distributed noise signal which is transformed into the final weather quantities as the last step.

This work contains in its full version a well-elaborated description of the mathematics and the behavior of the model. We propose a specific set of simple time variance functions with intuitive parameters. A detailed description of all required parameters ensures the ability to parameterize the model intuitively. An analysis of typical parameter spaces provides first references for the parameterization. To integrate this weather model into the picture of energy systems, this paper proposes methodologies mainly from literature to model the energy generation through wind and pv plants based on these weather quantities. The model with the proposed time variance function set showed accurate results for non-tropical regions. For regions in the intertropical convergence zone adaptions of this function set promise comparably accurate results. For maximum accuracy, the model requires location specific individual time variance functions.

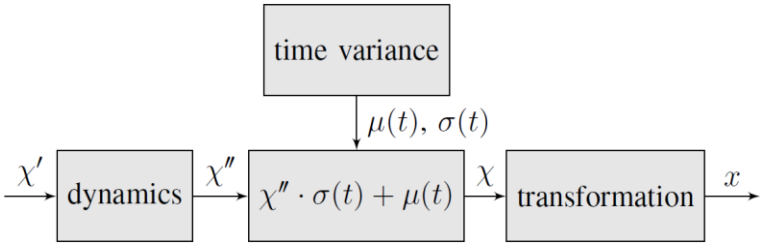

Figure 2: Unbalanced grid current reference tracking

Numerical Simulation of a Scaled Wind Farm

Chengyu Wang[a], Johannes Schreiber[b], Carlo Bottasso[c]

[a]cy.wang@tum.de, [b]johannes.schreiber@tum.de, [c]carlo.bottasso@tum.de

The development of large wind farms and improvement of wind farm's efficiency are important for the wind energy industry. Large wind farms necessitate the organization of multiple wind turbines into large arrays, which saves a lot of infrastructure and management costs. However, downstream wind turbines in a wind farm are usually exposed to the wake of upstream wind turbines, which decreases the power output and increases the fatigue loads of the turbines. Wind farm control is relatively new research topic aiming at mitigating the negative effects of turbine interaction and improving wind farm efficiency and reliability.

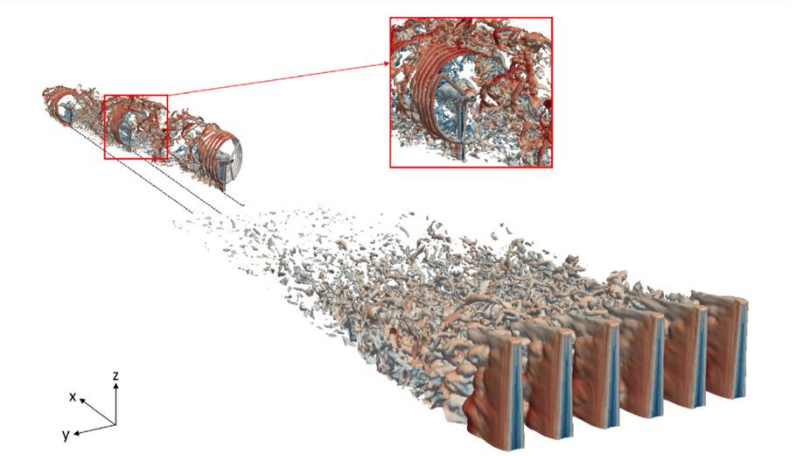

Figure 1: Visualisation of simulation result

Due to the sophisticated physics dominating a wind farm, the wake phenomenon has to be studied both experimentally and numerically. The Wind Energy Institute of TUM conducts quantities of experiments of a scaled wind farm in a wind tunnel. The experimental data is used to develop and validate a CFD framework. The validated CFD framework is then exploited to get insight into details of the flow field, turbine behaviors and so on.

This first part of the paper presents the validation of the CFD framework. Lifting-line large-eddy simulations of scaled wind turbines have been conducted. The results are validated against experimental measurements obtained in a boundary layer wind tunnel. The final goal of this effort is to develop a verified digital copy of the experimental facility, in support of wind farm control research. Three scaled wind turbine models are arranged in different waked configurations and yaw misalignment conditions. In the experiments, the wind turbine response is measured in terms of various operational parameters, while the flow is measured with two scanning LiDARs. Simulation and experimental results are compared with respect to flow characteristics, turbine states and wake behavior. The analysis of the results shows a good match between simulations and experiments. Besides this important verification, the numerical simulations are also used to explain a wake interference phenomenon observed in the experiments, which causes a modification in the path of the wake of shaded turbines.

The second part of the paper presents an example of exploiting the CFD framework, i.e., the validation of a wind state observer. The wind state observer utilizes turbine loads to estimate the ambient inflow speed at the rotor plane. However, the induction of the rotor changes the flow. Therefore, the real value of the ambient inflow speed cannot be measured directly in any experiments, making it hard to validate the wind state observer. Since the same inflow condition can be exactly reproduced in the CFD simulation. It can be used for this validation. To simulations with and without the wind turbine are conducted, so the estimated wind velocity from the first simulation and the sampled speed from the second simulation can be compared directly.

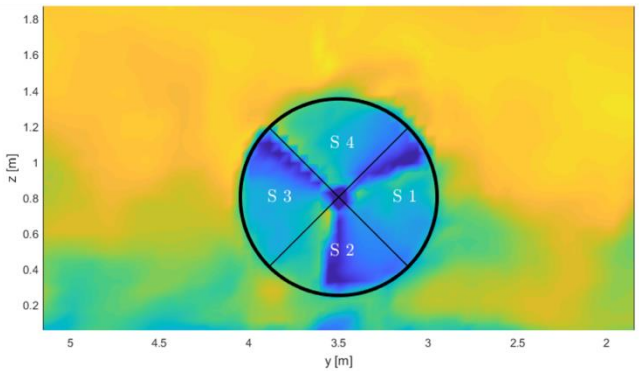

Figure 2: Wind state observer in the simulation

Multi-Energy Management and Aggregation Platform

Alexandre Capone

alexandre.capone@tum.de

Through the increased efforts to achieve a sustainable energy supply, particular interest has grown around the topic of building energy efficiency. Due to the development of new communication technologies and energy systems, buildings play an increasingly important role in enhancing the flexibility of energy networks, which in turn is vital for a succesful integration of renewable energy sources.
A commonly found technology which has largely contributed to the enhancement of building energy efficiency are energy management systems. These consist of software automation tools that optimize building energy performance while simultaneously guaranteeng consumer comfort. So far, energy management systems have been successfully marketed, and have attained high consumer acceptance. However, few tools exist which fully exploit synergies across whole city districts or even multiple buildings. Due to the increased presence of building automation systems, the building landscape is ripe for automation approaches which optimize the energy consumption among multiple buildings simultaneously.
The project “Multi-Energy Management and Aggregation Platform” (MEMAP) aims to develop a software platform, which coordinates building functions of whole city districts by communicating with each building’s energy management system. This way, synergies between buildings are to be identified and exploited, thus enabling a more efficient and environmentally friendly usage of energy resources.

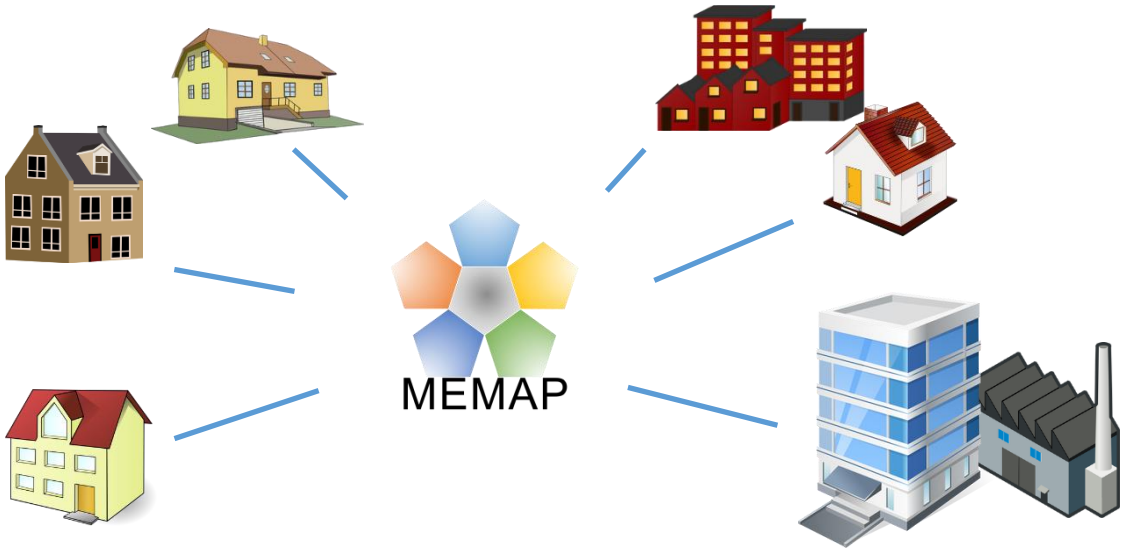

Figure 1: MEMAP Platform

Thermal use of shallow groundwater in Munich's energy planning

Fabian Böttcher[a], Kai Zosseder[b]

[a] fabian.boettcher@tum.de, [b] kai.zosseder@tum.de

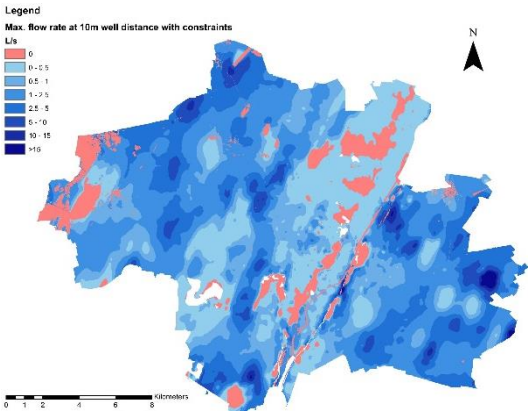

Figure 1: Sustainable flow rates in Munich.

The European Union consumes nearly half of its energy for heating & cooling. Nowadays, already 85 % electricity is produced from renewable energy sources, whereas the share in heating & cooling is only at 20 %. Especially the City of Munich fosters a continuous growth of this share and serves as a role model for other urban areas. Apart from ongoing constructions of deep geothermal plants for the district heating supply, the city already benefits from its shallow geothermal resources.
The quaternary sediments below Munich offer a highly productive aquifer, which can be used through extraction-injection well pairs for multiple heating & cooling applications. Most commonly households take advantage of the fairly constant groundwater temperatures (9-14°C) for heating with a heat pump. However, the largest users are cooling systems for datacenters and industry.

In the framework of the EU-Project GRETA, the Chair of Hydrogeology cooperates with the local authorities and energy planners to integrate the thermal use of groundwater in the spatial energy planning of the city. Therefore, a new spatial assessment method is developed. The method includes all relevant regulatory and operational constraints of two-well systems to provide technical potential estimates, which can be spatially applied (c.f. Fig. 2).

Major influences on constraining factors are governed by hydrogeological properties of the aquifer. In consequence, a resilient potential estimate relies on a detailed knowledge about groundwater-level, -gradient, -thickness and -temperature, as well as the hydraulic conductivity of the porous medium. This Data is available in outstanding resolution throughout the city area and was elaborated by the Chair of Hydrogeology in the Projects GEPO and GeoPot, funded by the Bavarian Ministry of Environment and Health.
Based on this data, the method calculates sustainable flow rates to get the volume flow potential (c.f. Fig. 1). This includes a drawdown threshold of 1/3 of the saturated groundwater thickness, an infiltration limit to prevent flooding and a restriction to prevent a hydraulic breakthrough between extraction and injection well. Further, the spatial hydraulic influence is considered to lower negative influences on neighboring well pairs.

As thermally altered water is reinjected into the same aquifer, a temperature anomaly occurs downstream of every injection well. This anomaly deteriorates the efficiency of similar usages and already approved users can claim unaffected conditions. Therefore, negative interactions have to be avoided. In the next step, regulatory thresholds on the temperature spread, the volume flow potential and significant hydrogeological parameters are merged to estimate the footprint of the anomaly and complete the analysis.

The method's mathematical relations have been derived through regression analysis of extensive parameter studies in FEM-models.

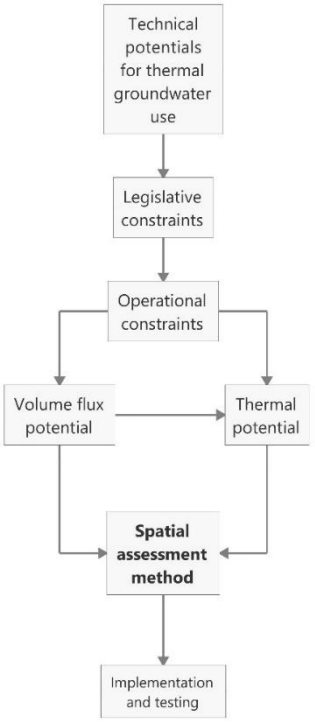

Figure 2: Overview of the workflow.

Promoting rural electrification in Sub-Saharan Africa: Least-cost modelling of decentralized Energy-Water-Food systems

J. Winklmaier[a], S. Bazan[b]

[a]johannes.winklmaier@tum.de, [b]adeli.bazan@tum.de

The outstanding solar potential in Sub-Saharan Africa (SSA) enables significantly cheaper levelized costs of electricity for decentral solar systems compared to the commonly used diesel generators. Yet, the limited purchase power in SSA impedes rural electrification by solar systems due to their high investment costs. Decentralized Energy-Water-Food systems have the potential to solve this problem. Using solar-powered water pumps, rural communities can supply water for drinking and irrigation. Thereby, agriculture does not depend on rainfall solely and can be done all over the year, which leads to increasing productivity. The increased crop production reduces the community´s expenses for nutrition and enables profit by sales, which in turn enables a payback of the initial investment costs of the solar system. The increased amount of biomass waste enables economically feasible small-scale biogas production. The biogas can be used for electricity production by biogas motors. These can supply private, social or small commercial loads, which enhance the local productivity even more.

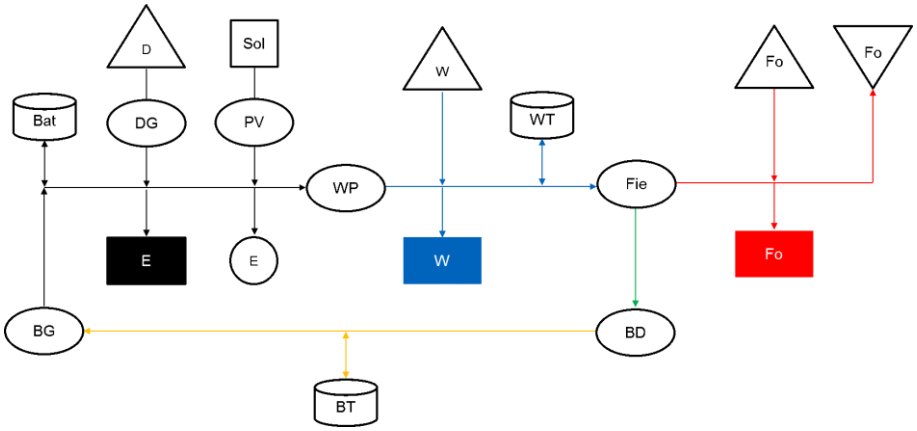

Figure 1: Scheme of Energy-Water-Food systems

To identify the least-cost system design regarding the supply of electricity, water and food for the rural village of St. Rupert Mayer, Zimbabwe, the linear optimization model *urbs* was adapted. *urbs* was developed for energy system model-ling, yet its sector coupling feature allows to add processes like water pumps and commodities such as biogas. The modelling results show that a holistic system including photovoltaics (PV), water pumps, enhanced agriculture and biogas production reduces the levelized costs of electricity (LCOE) from 0.45 USD/kWh by power supply from diesel generators to 0.16 USD/kWh. The modelling results shall support local governments and entrepreneurs in their decision-making.

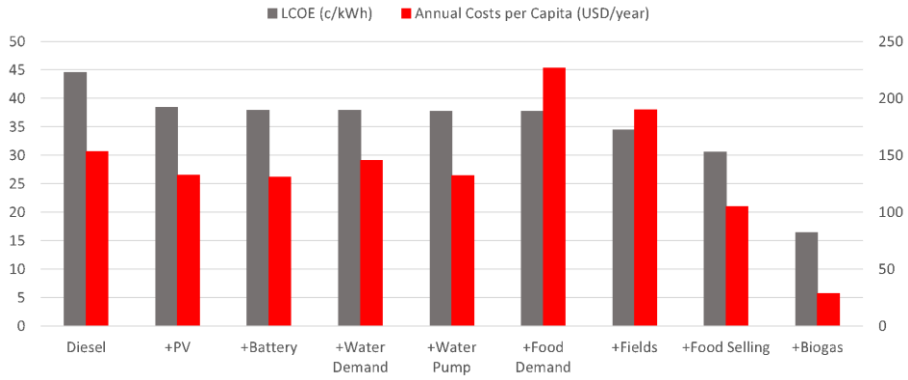

Figure 2: LCOE and annual costs per capita for each scenario

2. Posters

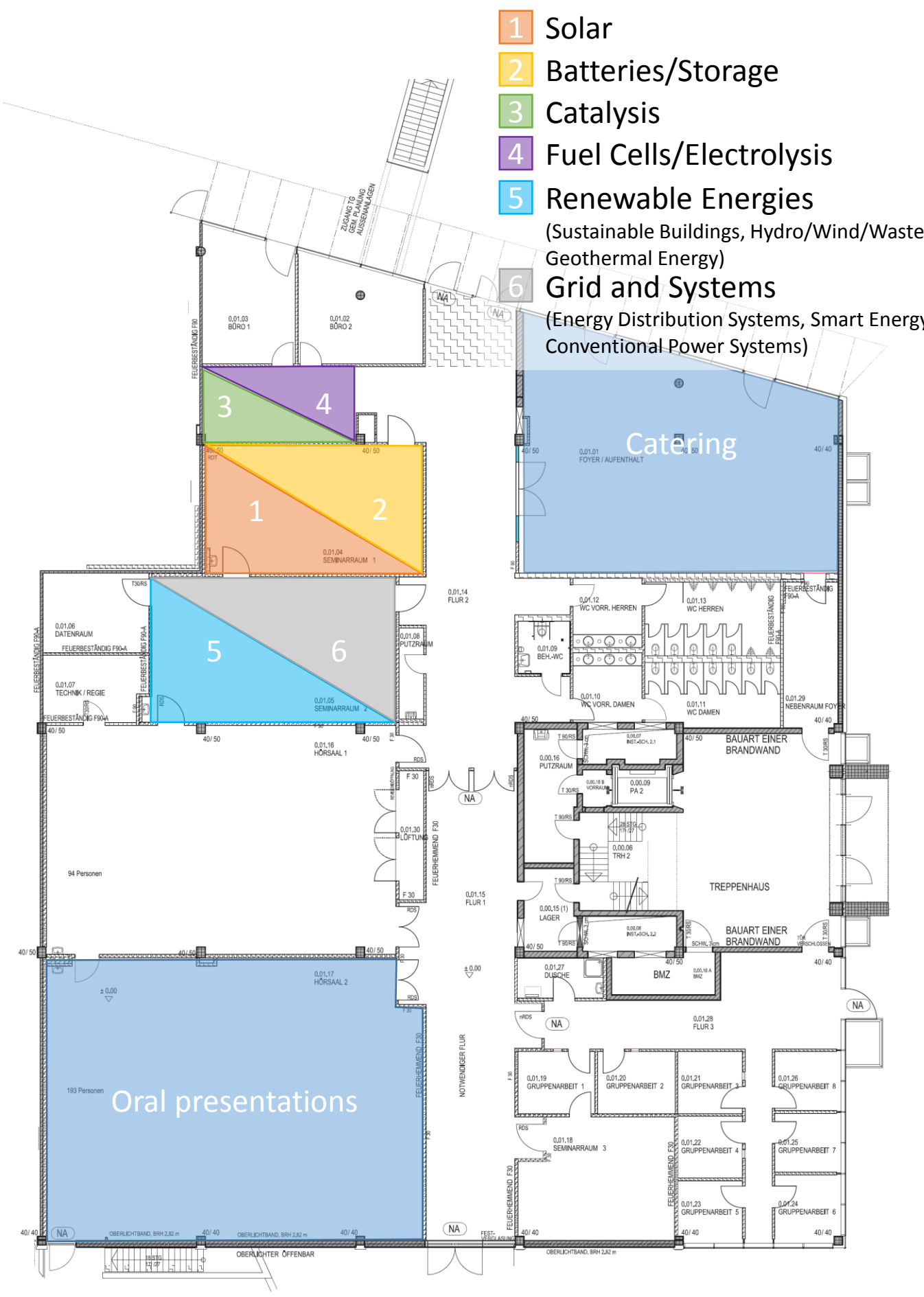
1 Solar
2 Batteries/Storage
3 Catalysis
4 Fuel Cells/Electrolysis
5 Renewable Energies
(Sustainable Buildings, Hydro/Wind/Waste/ Geothermal Energy)
6 Grid and Systems
(Energy Distribution Systems, Smart Energy, Conventional Power Systems)
Catering
Oral presentations
0,01,01 FOYER / AUFENTHALT
0,01,02 BÜRO 2
0,01,03 BÜRO 1
0,01,04 SEMINARRAUM 1
0,01,05 SEMINARRAUM 2
0,01,06 DATENRAUM
0,01,07 TECHNIK / REGIE
0,01,08 PUTZRAUM
0,01,09 BEH.-WC
0,01,10 WC VORR. DAMEN
0,01,11 WC DAMEN
0,01,12 WC VORR. HERREN
0,01,13 WC HERREN
0,01,14 FLUR 2
0,01,15 FLUR 1
0,01,16 HÖRSAAL 1
0,01,17 HÖRSAAL 2
0,01,18 SEMINARRAUM 3
0,01,19 GRUPPENARBEIT 1
0,01,20 GRUPPENARBEIT 2
0,01,21 GRUPPENARBEIT 3
0,01,22 GRUPPENARBEIT 4
0,01,23 GRUPPENARBEIT 5
0,01,24 GRUPPENARBEIT 6
0,01,25 GRUPPENARBEIT 7
0,01,26 GRUPPENARBEIT 8
0,01,27 DUSCHE
0,01,28 FLUR 3
0,01,29 NEBENRAUM FOYER
0,01,30 LÜFTUNG
0,00,06 TRH 2
0,00,09 PA 2
0,00,15 (1) LAGER
0,00,16 PUTZRAUM
BMZ
TREPPENHAUS
BAUART EINER BRANDWAND
NOTWENDIGER FLUR
94 Personen
193 Personen
OBERLICHTER ÖFFENBAR
OBERLICHTBAND, BRH 2,82 m

Electrodeposited $Na_2Ni[Fe(CN)_6]$ Thin Film Cathodes Exposed to Simulated Aqueous Na-Ion Battery Conditions

Philipp Marzak[a], Jeongsik Yun[b], Albrecht Dorsel[c], Armin Kriele[d], Ralph Gilles[e], Oliver Schneider[f], Aliaksandr S. Bandarenka[g]

[a]philipp.marzak@ph.tum.de, [b]jeongsik.yun@tum.de, [c]albrecht.dorsel@tum.de, [d]armin.kriele@hzg.de, [e]ralph.gilles@tum.de, [f]oliver_m.schneider@tum.de, [g]bandarenka@ph.tum.de

Secondary batteries employed as grid-scale energy storage systems are attractive to address the so-called generation versus consumption issue which is inevitably connected to the use of energy from naturally fluctuating renewable sources and the so-called Terawatt Challenge by 2050. Aqueous Na-ion batteries, in contrast to conventional Li-ion batteries, meet the economic demands, safety requirements and are environmentally more benign[1,2]. Among different types of electrode materials for those classes of batteries, so-called Prussian Blue Analogues (PBAs) are very attractive due to their comparatively simple and low-cost methods of synthesis coupled with a promising cycle performance. A state-of-the-art PBA battery materials, electrodeposited $Na_2Ni[Fe(CN)_6]$ (NiHCF) thin films, were tested under simulated battery conditions in aqueous and mixed (H_2O/organic) electrolytes[3]. Prolonged stability tests in aqueous electrolytes were performed together with in-operando electrochemical AFM monitoring. Further supported by XRD analysis, it is demonstrated that degradation of this material is not associated with noticeable morphological changes (mechanical stress). On the contrary, degradation is likely caused by changes in the chemical composition of the films. Intercalation and de-intercalation reversibility of Na^+ and thin film stability in aqueous electrolytes do not appear to be negatively affected by changes in the pH to values below 7. However, the films showed unstable behavior in alkaline media (pH > 10). Such electrolytes promote the degradation. Increasing the content of acetonitrile, which was used as an additive to simulate the influence of antifreezes in aqueous electrolytes, appears to primarily affect the de-intercalation of Na^+-ions in Na_2SO_4-based aqueous electrolytes [3].

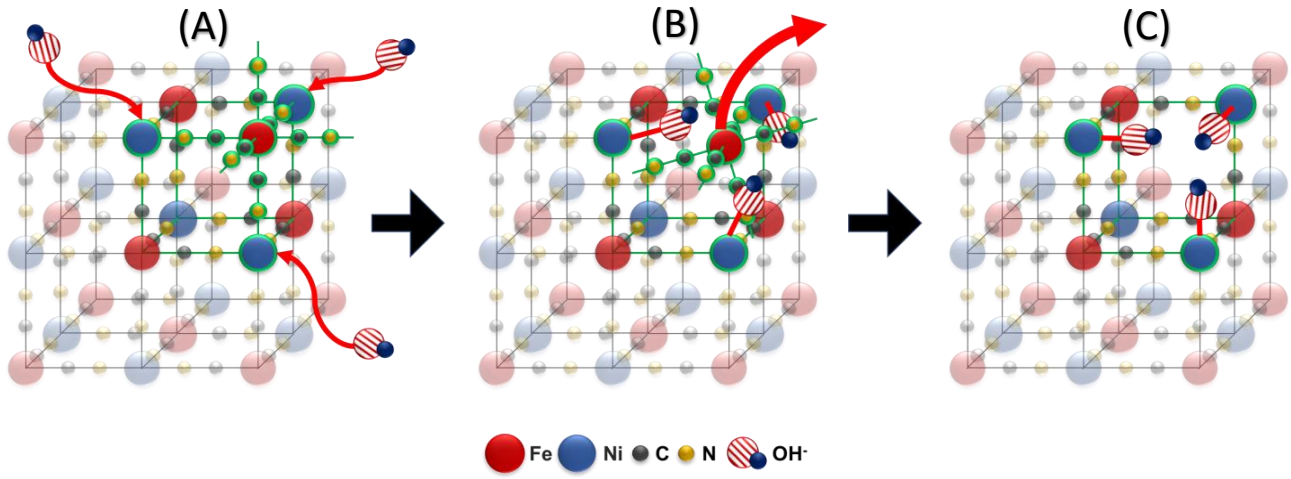

Figure 1: Aging of electrodeposited NiHCF thin film cathodes upon repeated (dis)charging appears not to result from mechanical degradation induced by changes in lattice parameters, but rather to be induced by changes in the chemical composition. Supposedly, (A) adsorbed OH^- (B) reacting with exposed nickel sites leads to (C) extraction of iron centers, the sources of the driving force for (de-)intercalation.

[1] Qian, J.; Wu, C.; Cao, Y.; Ma, Z.; Huang, Y.; Ai, X.; Yang, H. *Adv. Energy Mater*. **2018**, *1702619*.
[2] Wessells, C.; Peddada, S.; Huggins, R.; Cui, Y. *Nano Lett.* **2011**, *11*, 5421-5425.
[3] Marzak, P.; Yun, J.; Dorsel, A.; Kriele, A.; Gilles, R.; Schneider, O.; Bandarenka, A. S. *J. Phys. Chem. C* **2018**, Article ASAP, DOI: 10.1021/acs.jpcc.8b00395.

Neutron methods for battery research at the Heinz Maier-Leibnitz Zentrum (MLZ)

Stefan Seidlmayer[a], Neelima Paul[b], Ralph Gilles[c]

[a]stefan.seidlmayer@frm2.tum.de, [b]neelima.paul@frm2.tum.de, [c]ralph.gilles@frm2.tum.de

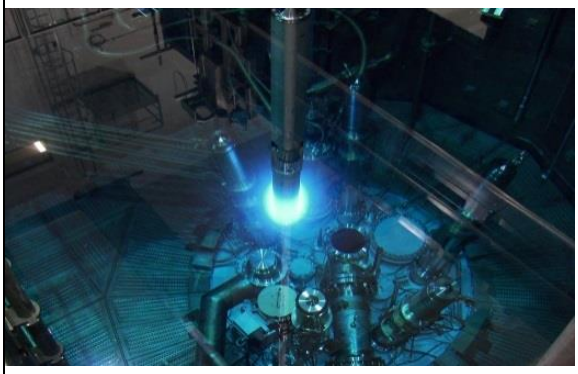

Figure 1: Neutron source FRM II at MLZ
Copyright W. Schürmann (TUM).

At MLZ, several neutron methods for non-destructive characterization of Li-ion batteries are available. Within the framework of ExZellTUM I, ExZellTUM II and EEBatt projects, the Advanced Materials Group headed by Dr. habil. Ralph Gilles is performing ex-situ, in-situ and operando measurements during charging/ discharging of batteries.

Diffraction methods provide information about the chemical composition, structure of the phases present in the battery electrodes and associated structural changes during the electrochemical processes [1-2]. Using techniques like small angle scattering and reflectivity, it is possible to obtain depth specific information about the average size (1- 300 nm), shape and distribution of lateral structures (and pores) with high statistical relevance upon ageing as well as during charging/discharging [3, 4]. Prompt Gamma-Ray Activation Analysis (PGAA) is being used for the determination of elemental composition and concentration of ions in electrodes (ca. down to ppm range) [5]. Radiography/Tomography are used to probe inner structures within batteries for dimensions greater than 50 µm as well as monitor electrolyte filling and gas evolution. Positron Annihilation Spectroscopy has been applied to study disorder and defect structures [6]. Complimentary to the neutron methods, X-ray diffraction is also established within our group for battery studies.

[1] N. Paul, J. Wandt, S. Seidlmayer, S. Schebesta, M.J. Mühlbauer, O. Dolotko, H.A. Gasteiger, R. Gilles, Journal of Power Sources, 345 (2017) 85-96.
[2] N. Paul, J. Keil, F. M. Kindermann, S. O. Schebesta, Dolotko, M. J. Mühlbauer, L. Kraft, S. V. Erhard, A. Jossen, R. Gilles, Journal of Energy Storage 17 (2018) 383-394.
[3] N. Paul, J. Brumbarov, A. Paul, Y. Chen, J.-F. Moulin, P. Müller-Buschbaum, J. Kunze-Liebhäuser, R. Gilles, Journal of Applied Crystallography, 48 (2015) 444 – 454.
[4] S. Seidlmayer, J. Hattendorff, I. Buchberger, L. Karge, H.A. Gasteiger, R. Gilles, J Electrochem Soc, 162 (2015) A3116-A3125.
[5] I. Buchberger, S. Seidlmayer, A. Pokharel, M. Piana, J. Hattendorff, P. Kudejova, R. Gilles, H.A. Gasteiger, J Electrochem Soc, 162 (2015) A2737-A2746.
[6] S. Seidlmayer, I. Buchberger, M. Reiner, T. Gigl, R. Gilles, H.A. Gasteiger, C. Hugenschmidt, Journal of Power Sources, 336 (2016) 224-230.

Exploring Novel Solid Electrolytes via Aluminum Substitution in Lithiumphosphido-germanates: Introducing Li_9AlP_4 and Solid Solution $Li_{9-x}Al_{1-x}Ge_xP_4$

Tassilo M. F. Restle [a], David Müller [b], Thomas F. Fässler [c]

[a]tassilo.restle@tum.de, [b]david.mueller@tum.de, [c]thomas.faessler@lrz.tum.de

Solid-state batteries have the potential to replace currently available liquid battery systems due to their higher energy and power density, their increased safety and mechanical stability. Solid electrolytes with high ionic conductivity and chemical stability are the key component for full-scale commercialization of solid-state batteries.[1] So far the highest ionic conductivity was achieved by the lithium thiophosphate $Li_{10}GeP_2S_{12}$ ($1.2\ 10^{-2}$ S cm^{-1}).[2]

Recently our group reinvestigated lithiumphosphidosilicates and germanates, which proved to be moderate lithium ion conductors with conductivities up to $1.2\ 10^{-4}$ Scm^{-1} at 75 °C.[3] In prominent examples, the ionic conductivity could be enhanced by the substitution of an element with an lower valence element, e.g. going from Li_3PS_4 to $Li_{3.25}Ge_{0.25}P_{0.75}S_4$ by replacing P^{5+} with Ge^{4+} or from $LiTi_2(PO_4)_3$ to $Li_{1.2}Al_{0.2}Ti_{1.8}(PO_4)_3$ by replacing Ti^{4+} with Al^{3+}.[4-5] Hereby, the Lithium concentration is increased and the bottleneck size of the charge carrier pathways can be changed.[6]

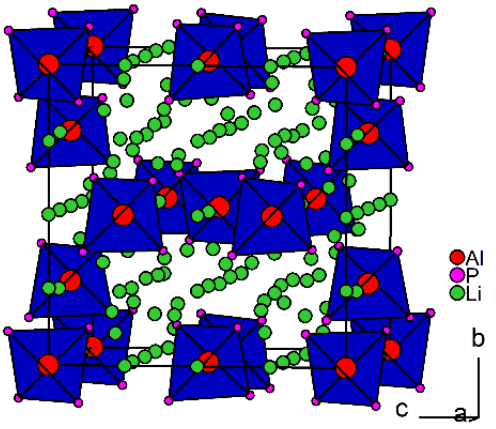

Figure 1. Crystal structure of Li_9AlP_4. Isolated $[AlP_4]^{9-}$ tetrahedra are highlighted in blue.

We succeeded in substituting β-Li_8GeP_4 with Al^{3+} yielding the solid solution $Li_{9-x}Al_{1-x}Ge_xP_4$. Furthermore, a total substitution leads to the new Lithiumphosphidoaluminate Li_9AlP_4. Phase pure samples were obtained by a two-step synthesis via ball milling of the elements to reactive mixtures and subsequently annealing of the reactive mixtures. The structure of Li_9AlP_4 was solved via SC-XRD, resulting in a cubic closed packing of P atoms which form with Al isolated $[AlP_4]^{9-}$ tetrahedra (Fig. 1). Li_9AlP_4 crystallizes in the same structure as β-Li_8GeP_4, though the Lithium content in the tetrahedral and octahedral voids is higher. Rietveld-Analysis of PXRD patterns proofs a complete substitution in the solid solution $Li_{9-x}Al_{1-x}Ge_xP_4$. Here, the lattice parameters behave linear according to Vegard's law (Fig. 2). In further investigations, we will determine the bulk ionic conductivity by impedance spectroscopy and the Lithium ion mobility by ^{7}Li-NMR.

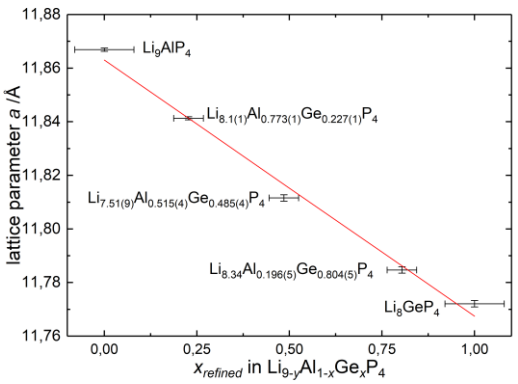

Figure 1. Vegard plot of the lattice parameters of $Li_{9-x}Al_{1-x}Ge_xP_4$. Al can completely substitute Ge in β-Li_8GeP_4 resulting in larger lattice parameters.

[1] J. Janek, W. G. Zeier, *Nat. Energy* **2016**, *1*, 16141.
[2] N. Kamaya, K. Homma, Y. Yamakawa, M. Hirayama, R. Kanno, M. Yonemura, T. Kamiyama, Y. Kato, S. Hama, K. Kawamoto, A. Mitsui, *Nat. Mater.* **2011**, *10*, 682-686.
[3] L. Toffoletti, H. Kirchhain, J. Landesfeind, W. Klein, L. van Wüllen, H. A. Gasteiger, T. F. Fässler, *Chem. - Eur. J.* **2016**, *22*, 17635-17645.
[4] R. Kanno, M. Murayama *J. Electrochem. Soc.* **2001**, *148*, A742-A746.
[5] H. Aono, E. Sugimoto, Y. Sadaoka, N. Imanaka, G. y. Adachi, *J. Electrochem. Soc.* **1990**, *137*, 1023-1027.
[6] J. C. Bachman, S. Muy, A. Grimaud, H.-H. Chang, N. Pour, S. F. Lux, O. Paschos, F. Maglia, S. Lupart, P. Lamp, L. Giordano, Y. Shao-Horn, *Chem. Rev.* **2016**, *116*, 140-162.

Preparation of TiO_2/SnO_2 composites via PS-b-PEO assisted sol-gel process for LIBs anodes

Shanshan Yin[a], Lin Song, Peter Müller-Buschbaum[b]

[a]shanshan.yin@ph.tum.de, [b]muellerb@ph.tum.de

Metal oxides, for example TiO_2 and SnO_2, have been widely studied as anode materials of lithium ion batteries, recently. TiO_2, as one of the alternative anode materials of lithium ion batteries, possesses superior stability on electrochemical performance and flexibility on structural regulation. However, its moderate conductivity and lithium ion migration still need to be improved to meet further requirement of energy storage equipment. Furthermore, regarding the lower theoretical specific capacity of 330 $mAhg^{-1}$, different composite have been developed to increase the lithium storage quantity of the TiO_2 anode. For example, TiO_2/Si, TiO_2/ZnO, TiO_2/SnO_2 were developed [1]. SnO_2, as another alternative anode material for lithium ion batteries, affords higher theoretical specific capacity of 1494 $mAhg^{-1}$. However, the big volume change and the formation of the thick SEI film during the cycling caused serious capacity recession thus greatly hindered its practical application. Therefore, after comparing the characteristic of TiO_2 and SnO_2, a novel amphiphilic block copolymer assisted sol-gel process toward the preparation of TiO_2/SnO_2 porous composite anode has been proposed by us, due to the big potential on the fabrication of 3D structures resulting from the microphase separation of the di-block copolymer in the solution. The obtained porous structure is not only favorable to the permeation of the electrolyte, but also suitable to accommodate the stress generated by the active material, especially for SnO_2 anode, during the lithiation and de lithiation process. In our work, the di-block copolymer PS(20500)-b-PEO(8000) was used as the structure directing agent, TTIP (Titanium tetraisopropanolate) and $SnCl_4$ were selected as the precursors of TiO_2 and SnO_2. THF was used as good solvent for both PS block and PEO block, HCl was used as a poor solvent for PS block and catalyst of the hydrolytic condensation process of TTIP and $SnCl_4$. Depending the hydrogen-bond interaction between the precursors and PEO block, the TTIP and $SnCl_4$ species specifically filled the PEO part of the block co-polymer. As a consequence, the hydrolysis and condensation of the precursors could be confined in the hydrophilic PEO domain. Through the spin coating and calcination process, the organic matter could be fully removed, and the 3D metal oxide structure could be obtained simultaneously. Other than pure TiO_2 and SnO_2 thin films, TiO_2/SnO_2 composite thin films with different TiO_2 to SnO_2 ratios were also designed and studied. In order to obtain similar structure, the total mass of TiO_2 and SnO_2 in each composite was kept consistent. The crystalline and morphology characterization were performed through X-ray diffraction (XRD) and scanning electron microscope (SEM). The conductivity of the thin film were confirmed by the four probe method. The band gap of the thin films could be extrapolated by the UV-Vis spectra according to the Tauc equation [2]. The inner structure of the thin film could be studied by GISAXS measurement.

Figure 1..Preparation process of the TiO_2/SnO_2 composite and evaporation induced self-assemble of the mixture

[1] J Mater Sci (2012) 47:2519-2534.
[2] Applied Catalysis B: Environmental (2018) 222:133-145.

Mixed Alkali Effect in PEO Based Electrospun Solid Polymer Electrolytes

Patrick Walke[a], Amy Wuttke[b], Tom Nilges[c]

[a]patrick.walke@tum.de, [b]MSE bachelor student, [c]tom.nilges@lrz.tu-muenchen.de

Solid polymer electrolytes used in lithium ion batteries could be a more stable and safer alternative to conventional liquid electrolytes.[1] In the wide field of polymer chemistry it has been discovered more than 40 years ago that poly (ethylene oxide) mixed with alkali metal salts shows ionic conductivity and good ion mobility.[2] Combined with electrospinning as preparation technique, membranes consisting of thin composite fibers of PEO mixed with $LiBF_4$ and succinonitrile can reach conductivities up to 10^{-4} S/cm at room temperature.[3] While investigating alternatives to lithium based battery systems, it has been shown that the system could be transferred to sodium ion batteries. Here membranes of PEO mixed with $NaBF_4$ and succinonitrile reached ionic conductivities of 10^{-4} S/cm at room temperature.[4] With these two known systems it is of general interest to investigate the mixed alkali effect, which is known from crystalline materials and glasses. Herein the ionic conductivity shows a minimum at A_1/A_2-ratio equal to 1. This is due to the blocking of diffusion pathways in the conducting material. A prominent example for the mixed alkali effect is $Li_xRb_{1-x}PO_3$.[5]

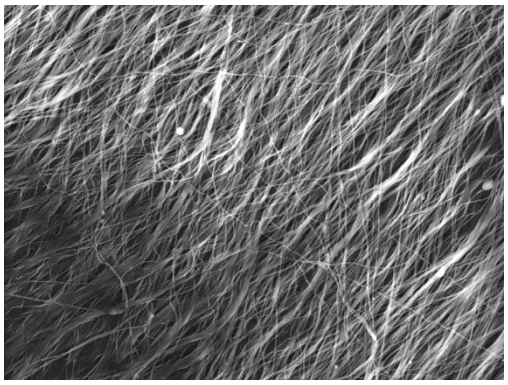

Figure 1: Scanning electron microscope image of electrocpun PEO.

PEO mixed with $LiBF_4$ and $NaBF_4$ without any succinonitrile were chosen to investigate the mixed alkali effect for this system. Therefore a molar ratio of PEO/$LiBF_4$ equal to 36/1 and 18/1 has been applied, subsequently $LiBF_4$ was substituted by $NaBF_4$ in 10% steps. After electrospinning the polymer solutions, the obtained membranes were characterized by means of SEM, XRD, DSC and impedance spectroscopy. The mixing of alkali metal salts has no influence on neither the morphology, the crystallinity, nor the thermal behavior. The conductivity derived from impedance data shows a minimum in conductivity for a Li^+/Na^+ ratio equal to 1/1. In contrast to the mixed alkali effect known from literature, it seems like adding small amounts of $LiBF_4$ to a system with the composition PEO:$NaBF_4$ has a positive effect on the ionic conductivity.

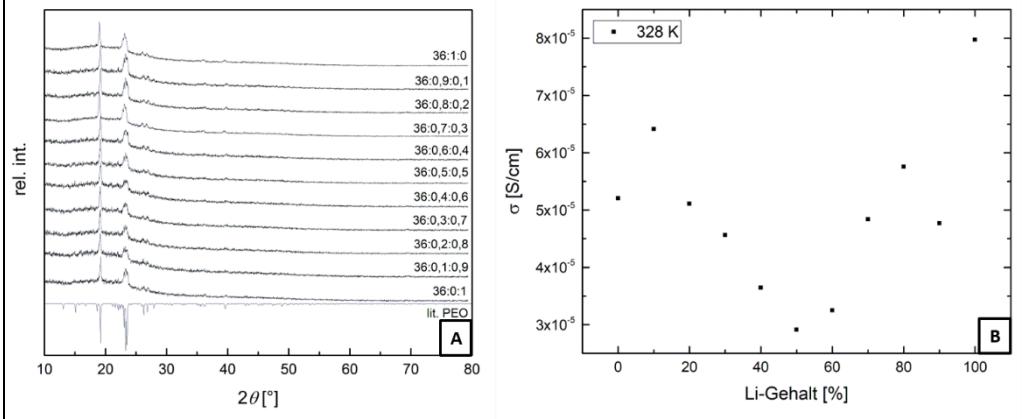

Figure 2: A) XRD-patterns of electrospun PEO:$LiBF_4$:$NaBF_4$ (36:1-x:x); B) Conductivity calculated from impedance dependent on relative Li content. Measured at 328 K.

[1] W.H. Meyer, *Adv. Mater.* **1998**, 10, No. 6
[2] D.E. Fenton, J.M. Parker, P.V. Wright, *Polymer*, **1973**, 14, 589
[3] K. Freitag *et.al*., *Inorg. Chem*., **2017**, 56, 2100−2107
[4] K. Freitag *et.al*., *J. Power Sources,* **2018**, 378, 610–617
[5] C. Karlsson *et. al*. Phys. Rev. B, **68**, 064202, 2003

Model Compounds with Diamond-Structure Type for Potential Lithium-Ion-Conductors

Jasmin Dums[a], Tassilo Restle,[b] Alexander Henze, and Thomas F. Fässler[c]

[a]jasmin.dums@tum.de, [b]tassilo.restle@tum.de, [c]thomas.faessler@mytum.de

Among solid ionic conductors, salts containing lithium and silver ions show rather high ion conduction. It had been shown that the substitution of Ag^+ by Li^+ in silver argyrodites leads to a new innovative family of fast lithium ion conductors.[1] Recently we investigated lithium silicides and germanides[2] which are discussed as active anode materials with high capacity. In this context we were interested in the properties of silver in contrast to lithium in intermetallic compounds and investigated the Li−Ag−Ge phase diagram.[3] Various new ternary compounds such as Li_2AgGe, $Li_{2.53}AgGe_2$ and $Li_2Ag_{0.8}Ge_{1.2}$ were discovered and a general rule that Ag prefers to substitute Ge atoms rather than lithium was found. As a basic structural unit in all new structures Ag and Ge form a diamond-like or wurtzite-type network, hosting lithium atoms in its cavities or channels. Some phases show temperature-dependant phase transitions.

In Li_2AgGe (space group $R\bar{3}m$) and $Li_{2.53}AgGe_2$ (space group $I4_1/a$) all atomic positions are fully occupied and ordered, besides the latter, that shows defects on Li positions. $Li_2Ag_{0.8}Ge_{1.2}$ forms at higher temperatures a cubic NaTl-type structure (space group $Fd\bar{3}m$) with a statistical occupation of Ag/Ge atomic position, at lower temperature (space group $I4_1/amd$) an ordered superstructure with an enhanced c-axes is observed.

We present synthesis, characterization and phase transitions of the novel lithium-silver germanides. Structural relationships are demonstrated using the Bärnighausen family tree formalism.[4] In addition the results of quantum chemical calculations based on CRYSTAL14 will be shown.

[1] H.-J. Deiseroth, S.-T. Tong, H. Eckert, J. Vannahme, C. Reiner, T. Zaiß, M. Schlosser, *Angew. Chem. Int . Ed.* **2008**, *47*, 755-758.

[2] M. Zeilinger, I. Kurylyshyn, U. H. ussermann, T. F. Fässler, *Chem. Mater.* **2013**, *25*, 4623-4632. M. Zeilinger, D. Benson, U. Häussermann, T. F. Fässler, *Chem. Mater.* **2013**, *25*, 1960-1967.

[3] A. Henze, V. Hlukhyy, T. F. Fässler, *Inorg. Chem* **2015**, *54*, 1152-1158.

[4] H. Bärnighausen, *Commun. Math. Chem.* **1980**, *9*, 139.

Prussian Blue Analogues: Electrode Materials for High Voltage Aqueous Na-Ion Batteries

Jeongsik Yun[a], Daniel Scieszka[b], Philipp Marzak[c], Florian Schiegg[d], Jonas Pfisterer[e], Paul Scheibenbogen[f], Alexander Wieczorek[g], Radu Bors[h], Aliaksandr Bandarenka[i]

[a]jeongsik.yun@tum.de, [b]daniel.scieszka@ph.tum.de, [c]philipp.marzak@ph.tum.de, [d]florian.alexander@gmail.com, [e]pfisterer@mpip-mainz.mpg.de, [f]paul.scheibenbogen@tum.de, [g]alexander-wieczorek@gmx.net, [h]radu.bors@gmail.com, [i]bandarenka@ph.tum.de

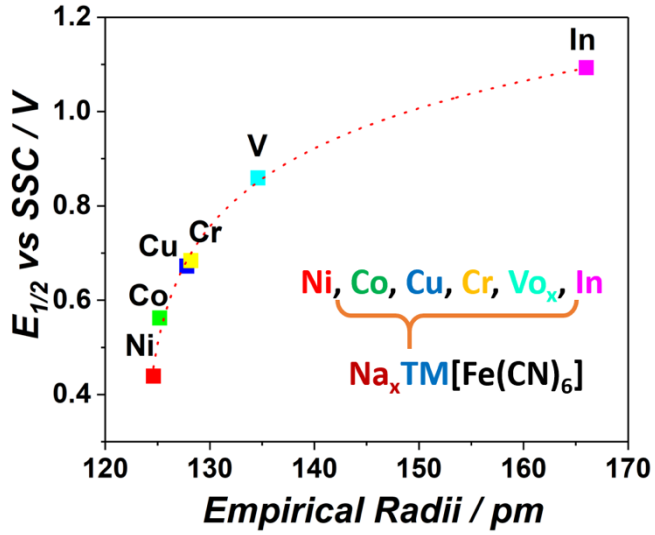

Figure 1: Half-charged potentials of different PBA electrodes as a function of the empirical radii of N-coordinated transition metals

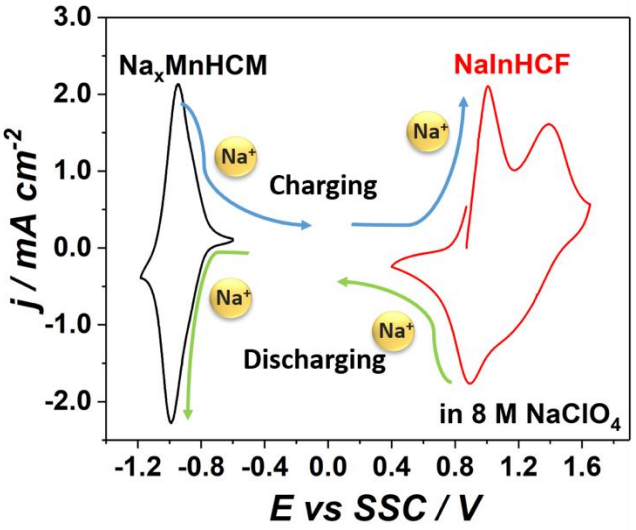

Figure 2: Cyclic voltammogramms of NaxHCM (black) and NaInHCF (red) electrodes in 8 M NaClO4, respectively

Recently, aqueous Na-ion batteries have drawn attention as promising energy storage systems (ESSs) to mitigate power fluctuation of renewable energies. For large scale stationary applications, the focus should be placed more on the costs and the availability of resources rather than energy density; i) battery materials should be affordable at reasonable prices, ii) manufacture of the battery should be cost-efficient and iii) batteries' cycle life and charge/discharge efficiency should be high and iv) they should be able to operate at high rate.[1] Among different classes of electrode materials, Prussian Blue analogues (PBAs) appear to be very attractive as electrode materials for aqueous Na-ion batteries fulfilling aforementioned requirements.

PBAs have large channels that can accommodate relatively larger Na ions than Li ions without significant volume swelling or shrinkages which are main problems of the Li-ion battery degradation.[2] Commonly accepted chemical formula of PBAs can be written as $A_xTM_1[TM_2(CN)_6]$ (where A is intercalating cations, TM_1 and TM_2 (usually Fe) are N-linked and C-linked transition metals, and $0 < x < 2$). We have demonstrated various electrodes based on electrochemically deposited PBAs and their interesting characteristics. By changing the chemical compositions of electrode materials and/or electrolytes, the electrochemical properties of Na-ion batteries vary significantly.[3,4,5] For instance, the "half-charged potential" can be tuned with some modifications of electrode compositions as shown in Figure 1. The half-charged potentials of different PBA based electrodes seem to have a certain correlation with the empirical radii of the used transition metals. With state of the art cathode and anode materials, namely indium hexacyanoferrate (InHCF) and manganese hexacyanomanganate (MnHCM), a high voltage (over 2V) aqueous Na-ion battery can be realized (see Figure 2).

[1] H. Kim, J. Hong, K.-Y. Park, H. Kim, S.-W. Kim and K. Kang, *Chem. Rev.*, **2014**, 114, 11788–11827
[2] M. Pasta, C. D. Wessells, R. A. Huggins and Y. Cui, *Nat. Commun.*, **2012**, 3, 1149.
[3] Yun, J.; Pfisterer, J.; Bandarenka, *Energy Environ. Sci.* **2016**, 9, 955−961.
[4] J. Yun(1), F. Schiegg(1), Y. Liang, D. Scieszka, B. Garlyyev, A. Kwiatkowski, T. Wagner, A.S. Bandarenka. *ACS App. Energy Mater.* **2018**, 1, 123–128.
[5] R. Bors, J. Yun, P. Marzak, J. Fichtner, D. Scieszka, A.S. Bandarenka. *ACS Omega*, **2018** (Accpeted).

Investigation of structural changes over long-term cycling of Ni-rich layered oxides used as cathode materials in Li-ion batteries

Franziska Friedrich [a], Benjamin Strehle [b], Hubert A. Gasteiger [c]

[a]franziska.friedrich@tum.de, [b]benjamin.strehle@tum.de, [c]hubert.gasteiger@tum.de

Layered oxides ($LiNi_xCo_yMn_zO_2$, x+y+z=1) with a rhombohedral structure are commercially used cathode materials in lithium-ion batteries because they offer high energy and power densities, high gravimetric capacities and good cycling stability. However, depending on the ratio Ni:Co:Mn, the electrochemical performance of the material varies a lot. Increasing the Ni content allows for the utilization of more lithium at a given cell potential, thereby improving the specific capacity. However, Ni-rich layered oxides are subjected to severe structural changes upon (de)lithiation, which adversely affect the cycling stability.[1,2]

In this context, we study the structural processes within the Ni-rich layered oxide $LiNi_{0.8}Co_{0.1}Mn_{0.1}O_2$ upon long-term cycling. Electrochemical measurements are complemented with *in-situ* synchrotron X-ray powder diffraction experiments. For this purpose, pouch cells with the above mentioned cathode material versus a graphite counter-electrode are cycled at a synchrotron facility. Within the scope of a long-duration experiment, an XRD analysis is conducted in regular intervals at 100% and 0% state-of-charge to study structural changes continuously over 1000 cycles. The Rietveld refinement technique was successfully applied for the structural characterization of the electrode materials as a function of fatigue. The observed changes in lattice parameters of the layered cathode materials indicate a loss of active lithium over the entire charge-discharge curve, which was correlated to the capacity fading of the cells upon cycling. The loss of active lithium can be further verified by the refinement results of the graphite phases (LiC_6 and LiC_{12}) of the anode. Furthermore, the development of strain in the layered oxide was investigated. Another parameter of interest is the cation disorder. It was found to be fairly constant in the range of error over 1000 cycles in the discharged state and was considerably decreased upon delithiation indicating a (partially) reversible transition metal migration. The obtained results provided better understanding of structural changes in layered oxides upon long-term cycling.

References

[1] D. Andre, S.-J. Kim, P. Lamp, S. F. Lux, F. Maglia, O. Paschos, B. Stiaszny, J. Mater. Chem. A3, 6709 (2015).

[2] S. Choi, A. Manthiram, J. Electrochem. Soc. 149, A1157 (2002).

Next Generation Electrolytes for Safer Sodium Ion Batteries

Pauline Fischer[a], Do Minh Phuong[b], Madhavi Srinivasan[c], Fritz Kühn[d]

[a]pauline.fischer@tum.de, [b]DOMINHPH001@e.ntu.edu.sg, [c]Madhavi@ntu.edu.sg, [d]fritz.kuehn@ch.tum.de

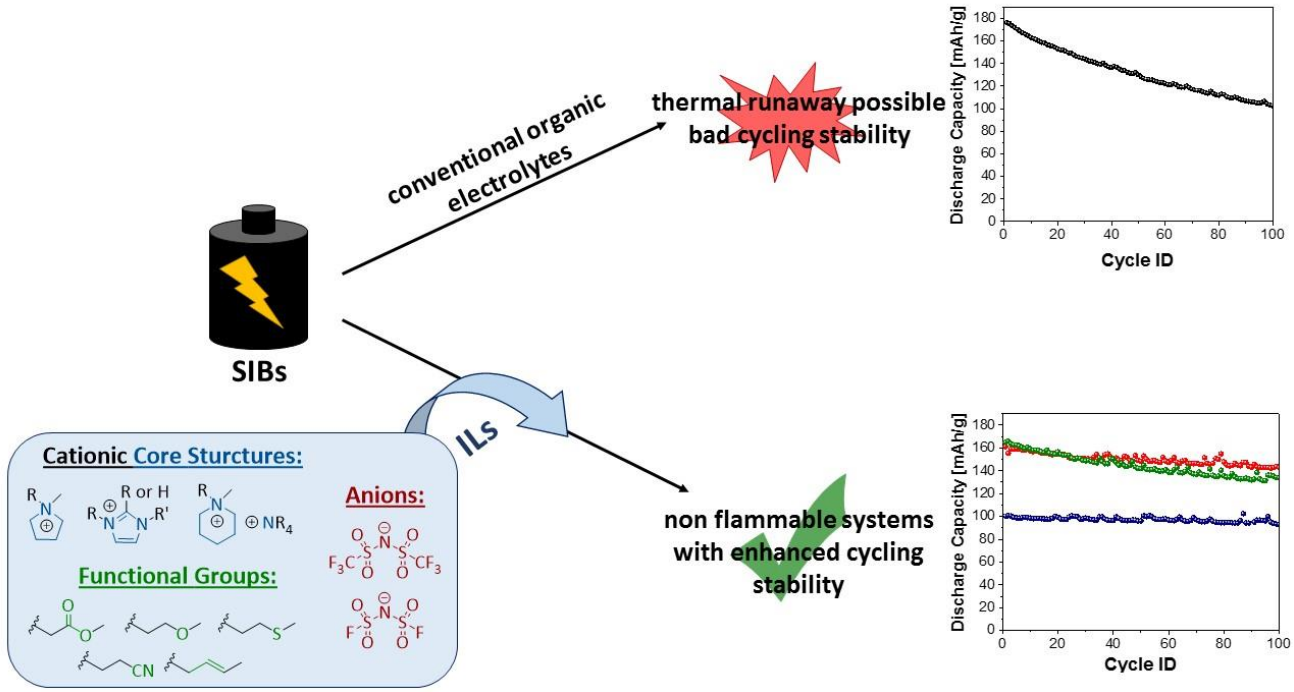

Sodium Ion Batteries (SIBs) are expected to be promising alternatives to the well established but cost-intensive Lithium Ion Batteries (LIBs), which eventually have to be replaced due to depleting lithium reserves. However, various extensively examined SIB systems still suffer from poor cycling stability, which is mainly due to unwanted decomposition of the conventionally applied organic carbonate based electrolytes. Furthermore, these electrolytes exhibit high volatility and flammability and therefore pose a serious safety issue. Featuring negligible vapor pressure combined with non-flammability on the one hand and wide electrochemical stability windows (ESWs) on the other hand, Ionic Liquids (ILs) represent promising alternatives to overcome these drawbacks. To comparably study the effect of the nature of the IL (cationic core structure, anion, presence of functional groups) on important parameters like thermal stability, viscosity, conductivity and ESW, a broad library of various ILs was synthesized and uniformly characterized. All ILs show significantly higher thermal stability compared to conventional organic electrolytes and enhanced ESWs. Viscosity and conductivity were found to be very susceptible towards structural changes in the ILs, covering broad ranges in both cases. Finally, the electrochemical performance of selected ILs tested in sodium half cells with a sodium manganese cobalt oxide as cathode material show clearly enhanced cycling stabilities compared to organic carbonates. This uniform investigation enables the comparison of different IL based systems and a rational design of ILs, being suitable alternatives for conventional electrolytes, paving the way to powerful SIBs.

Modeling Li_3OCl glass-electrolytes for all-solid-state Li ion batteries

Sina Stocker[a], Hendrik H. Heenen[b], Christoph Scheurer[c], Karsten Reuter[d]

[a]sina.stocker@tum.de, [b]hendrik.heenen@mytum.de, [c]christoph.scheurer@ch.tum.de, [d]karsten.reuter@ch.tum.de

All-solid-state Li ion batteries are facilitated by using glass superionic electrolytes that combine very high Li ion conductivity and mechanical ductility. One material that has attracted much excitement is the recently reported glass-amorphous Li_3OCl. Already a superionic conductor in its crystalline form, a glass transition increases its room temperature conductivity by an order of magnitude to an outstanding 25 mS cm^{-1} [1]. The elevated mobility likely originates from a lowered density of the liquid-like glass structure for which the ion transport mechanism has however not yet been elucidated. Based on a classical force-field [2] we explore Li_3OCl glass structures in simulation cells large enough to account adequately for long-range disorder. Via systematic melt-quench procedures qualitatively different glass ensembles are created allowing for structural heterogeneity. We use molecular dynamics simulations to analyze the ion mobility with emphasis on clarifying the influence of the structural relaxation associated with the glass transition.

[1] M. H. Braga, *et al*., J. Mater. Chem. A **2**, 5470 (2014)
[2] R. Mouta, *et al*., Chem. Mater. **26**, 7137 (2014)

In Situ DRIFTS Characterization of Surface Contaminants on Cathode Active Materials

Christian Sedlmeier[a], Johannes Sicklinger[b], Hubert A. Gasteiger[c]

[a]c.sedlmeier@tum.de, [b]johannes.sicklinger@tum.de, [c]hubert.gasteiger@tum.de

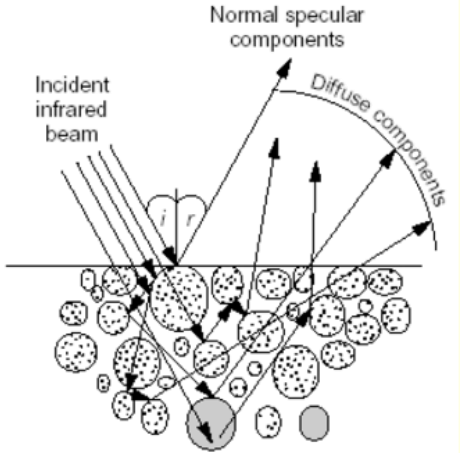

Figure 1: Diffuse reflection of the incident beam in the sample. Active material displayed as grey particels, nonabsorbing powder for dilution in white.[4]

Next generation Li-ion batteries (LIBs) aim higher capacities, higher energy densities as well as enhanced battery lifetime.[1] In this context, surface contaminants on metal oxide based cathode active materials (CAMs), *viz*. residual LiOH and Li_2CO_3 from the synthesis and basic transition metal (TM) hydroxides and carbonates formed upon air exposure of the CAM during battery manufacturing, are a serious issue w.r.t. cathode slurry processing as well as battery lifetime.[2,3]
In the study at hand, we present the necessity of surface sensitive characterization methods for investigating surface contaminants on CAMs by comparing Transmission Fourier Transform Infrared (T-FTIR) and Attenuated Total Reflection Fourier Transform Infrared (ATR-FTIR) Spectroscopy with the very surface sensitive Diffusive Reflectance Infrared Fourier Transform Spectroscopy (DRIFTS). In the case of DRIFTS, the radiation is diffusely reflected in different directions (*cf*. figure 1). The surface sensitivity raises from the low penetration depth of the IR beam into the material (typically 1 – 10 µm) and multiple remission due to diffuse reflection of the beam on the sample surface. It is predestined for powdered samples and is even capable of monitoring IR active species on the surface of highly absorbing materials with a rough surface like carbon or metal oxides.[5,6]
With our new setup for *in situ* DRIFTS we can directly observe the surface contaminants while being formed. Furthermore, we evaluate the surface reactivity upon exposure of cathode materials to different gases (CO_2 and O_2) and the influence of the relative humidity (RH) on the formation of surface carbonate and hydroxide species. With the help of *Kubelka-Munk* theory, the formation of surface contaminants can be assessed in a semi-quantitative manner.[7] By this, the CAMs can be classified in terms of storage stability and as an outcome, the optimum gas atmospheres for handling and processing especially the novel high-energy cathode materials can be defined.

References:

1. G. E. Blomgren, *J. Electrochem. Soc.* **2016**, *164*, A5029 – A5025.
2. D.-H Cho, C.-H. Jo, W. Cho, Y.-J. Kim, H. Yashiro, Y.-K. Sun, S.-T. Myung, *J. Electrochem. Soc.* **2014**, *161*, A920 – A926.
3. M. Metzger, B. Strehle, S. Solchenbach, H. A. Gasteiger, *J. Electrochem. Soc.* **2016**, *163*, A1219 – A1225.
4. V. Setnička, *Lecture on IR reflection techniques*, VFUB, Brno, Czech 2012.
5. M. P. Fuller, P. R. Griffiths, *Anal. Chem.* **1978**, *50*, 1906.
6. B. C. Smith, *Fundamentals of Fourier transform infrared spectroscopy*, CRC Press, Boca Raton, Fla., **1996**.
7. P. Kubelka, *J. Opt. Soc. Amer.* **1948**, *38*, 448.

ExZellTUM II – Cluster of Battery Research at the Technical University of Munich

Tanja Zünd[a], Fabian Linsenmann[a], Gunther Reinhart[b], Michael F. Zäh[b], Andreas Jossen[c], Ralph Gilles[d], Hubert A. Gasteiger[a]

[a] Lehrstuhl Technische Elektrochemie (TEC): tanja.zuend@tum.de, [b] Institut für Werkzeugmaschinen und Betriebswissenschaften (iwb),[c] Lehrstuhl für Elektrische Energiespeichertechnik (EES), [d] Forschungs-Neutronenquelle Heinz Maier-Leibnitz (FRM II)

ExZellTUM II is a joint research project where we follow the material from the first characterization steps up to the performance in industrial sized Li-ion battery cells.
The process chain starts with the material evaluation at the chair of technical electrochemistry (TEC) where we first investigate promising non-commercialized battery materials in laboratory cells. Additionally to the electrochemical performance, a special focus also lies on the processability and economical reasonability of the materials.
In the next step, the upscaling properties of the materials are optimized according to the requirements of the individual production step of the TUM pilot production line at the Institute for Machine Tools and Industrial Management (iwb). On the semi-automatic production line, we aim to produce 5 Ah pouch cells with 150 Wh/kg at a cycling rate of 1C out of the new materials, verifying their viability for large-scale production. To fulfill this requirement, each production step is fine-tuned to reach the optimized production parameters of the upscale calculations.

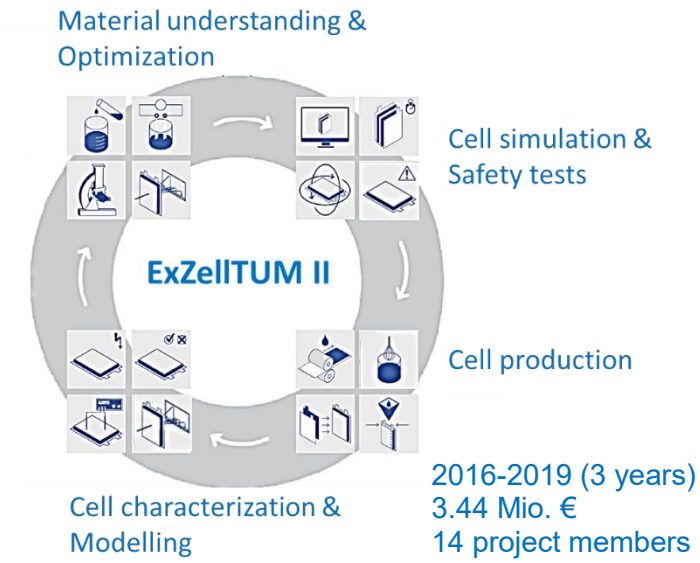

Figure 1: schematic representation of the cell development within the ExZellTUM II project.

Parallel to the production we simulate the electrochemical behavior of the cell and try to understand possible aging and failure mechanism at the chair for electrical energy storage systems (EES). In the second part of our project, we plan to compare the safety behavior of our cells with state of the art batteries. Additionally we will characterize the cell behavior with neutron methods at the Hans Maier Leibnitz neutron source (frmII).

Now, at half of the project term, we want to show the pathway of the material from the laboratory coin cells to the 5Ah pouch cells. Different electrode optimization steps such as cathode composition, mixing, drying, calendaring, and balancing will be shown. Parallel to the electrode production also the cell design to characterize the material was improved and an up scalable formation procedure could be established.
We will show how we transferred the acquired material understanding to the semi-automatic production line and show the similarities and differences of the laboratory and industrial production process of the material. Finally, we show the electrochemical performance of our first 5 Ah cells and compare them with our laboratory results and upscale calculations.

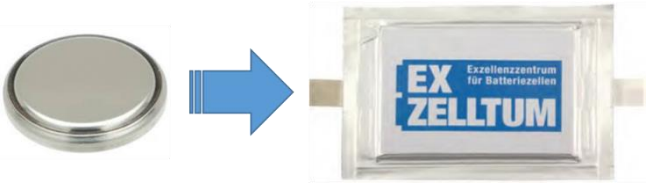

Energy Balanced by Urban Design \\ Towards Net Zero Energy Optimization of Dense Mediterranean Districts

Jonathan Natanian[a]

[a]j.natanian@tum.de

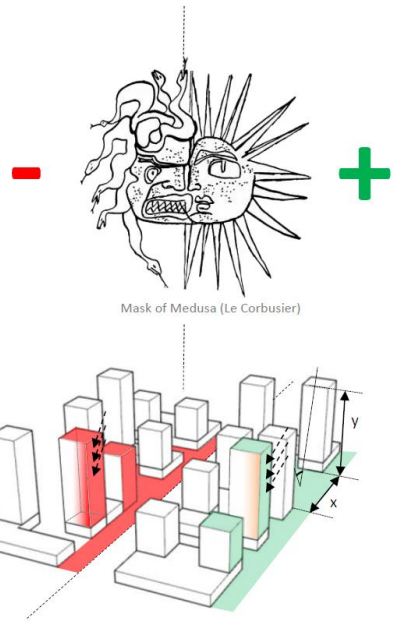

Figure 1: The contrasting effect of solar radiation at the urban scale

Despite the growing focus of contemporary research on environmentally responsive urban design, the longstanding question regarding the extents to which we will be able to densify our future cities without sacrificing energy performance and comfort, remains mostly unanswered. The quantitative evaluation of the effect of urban density on various environmental parameters is still lacking, particularly in the context of hot climatic regions where the future demographic challenge lies. Within these regions, the tradeoff constantly extends from the basic passive tradeoff between the contrasting effects of solar exposure (Figure 1), to energy production, Urban Heat Island considerations and recently to technological developments of district energy systems; all of which are changing the performative reference point and potentially leading to new results. With new challenges and opportunities opening as part of the growing debate on the district scale, more research is thus needed in order to inform urban design schemes on their performative consequences. Environmentally responsive urban design approach is specifically relevant to hot climatic regions, in which demography imposes rapid urban densification whereas environmental aspects of urban design are always one step behind.

This presentation will report on a PhD research conducted at the chair of Building Technology and Climate Responsive Design at TUM. Based on observations from a detailed environmental performance analysis of urban typologies in Israel, this research aims to highlight new district configurations which will deliver both density, comfort and energy balance in different land use, density and technology urban scenarios. The main working hypothesis is that performance driven urban design approach for Mediterranean climates will balance between energy demand and supply without sacrificing indoor environmental quality. This research is expected to conclude with a design road map for dense Mediterranean districts towards higher energetic balance and lower environmental impact.

Following a comprehensive literature review and in-depth contextual data acquisition, the analytic part of this research is divided into two phases: The first analytic part (ongoing), focuses on different urban typologies and explores the performance of Israel's common practices using the following criteria: heating and cooling demand, energy balance between supply and demand and natural daylight. Based on findings from this part, the second analytic part will focus on district studies, in which the evaluation of the same environmental criteria mentioned above will be conducted for different density, mix-use scenarios and energy systems (Figure 2). This part will conclude in an urban case study in which both approach, workflow and results will be tested. As the outcome of this research, findings from both analytic parts will be gathered systematically and presented in an appropriate platform, possibly through an interactive on-line interface towards responsive zero energy district design in hot climates.

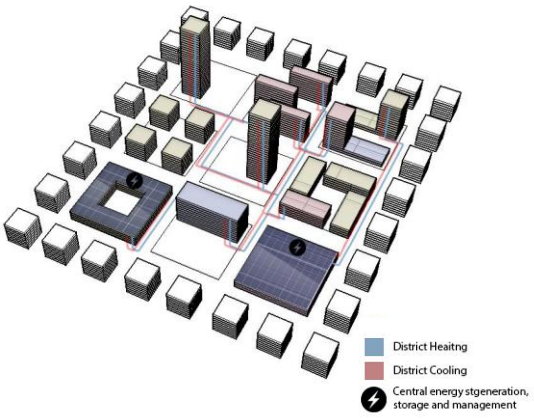

Figure 2: From block scale typologies to district energy scale studies

Investigations on PEDOT:PSS polymeric electrodes for OLED applications

Lorenz Bießmann[a], Nitin Saxena, Kun Wang, Dan Yang, Christoph Bilko,
Sigrid Bernstorff, Peter Müller-Buschbaum[b]

[a]lorenz.biessmann@ph.tum.de, [b]muellerb@ph.tum.de

Figure 1: Example for room lighting (Osram)

In the last years the efficiency and the life expectancy of organic light emitting diodes (OLEDs) reached values which make them suitable for industrial applications. OLEDs are able to cover a wide range of the color spectrum due to a large variety of different organic emitters. Combined with high color rendering and their energy saving potential, OLEDs became of high interest not only for display manufacturers. Additionally, OLEDs are based on thin-film technology which makes the device – depending on the substrate – transparent and flexible. Moreover, the production is also less energy demanding. As a consequence, OLEDs enable new possibilities in energy saving, e.g. for room lighting.

However, common OLEDs are prepared on rigid Indium doped Tin oxide or Fluorine doped Tin oxide coated glass substrates. These ITO and FTO substrates provide high transparency and electrical conductivity, but as well a high rigidity, which excludes such substrates for flexible organic electronic devices such OLEDs or organic solar cell applications. In addition, the fabrication of such metal oxide electrodes requires high energy consumption compared to solution processed alternatives.

One very promising approach to overcome the rigidity and the high costs of such common used metal oxide electrodes is the use of polymeric electrodes like PEDOT:PSS. This abundant material itself is inherently flexible, optical transparent and provides good conductivity, which makes it to an ideal candidate to replace its rigid metal oxide counterparts like ITO and FTO. Poly(3,4-ethylenedioxythiophene):polystyrene sulfonate (PEDOT:PSS) is a polyelectrolyte complex, which thin films can be easily deposited from aqueous solution. This allows the usage for large scale applications like spray deposition or printing. According to the treatment of the PEDOT:PSS solution or the thin films, it is possible to tune the work function and the conductivity of the final film and therefore tailor its functionality regarding the specific needs of the desired application, e.g. as blocking layer or polymeric electrode.

The conductivity of thin films highly depends on the interplay between PEDOT and PSS and its mixing ratio, which has an influence on the morphology and crystallinity. In this work the effect of different treatments on the film structure and conductivity is investigated. Different acid treatments were compared to the commonly used ethylene glycol post-treatment and the pristine PEDOT:PSS thin films. In order to examine the influence of the treatments on the crystal structure and orientation, grazing incidence wide angle X-ray scattering (GIWAXS) measurements were performed.

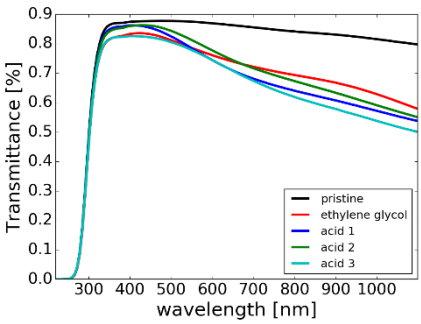

Figure 2: Transmittance of pristine PEDOT:PSS films compared to different post-treated films. Deposition on glass substrates.

Taking into account the findings of UV-Vis spectroscopy and 4-point measurements a figure of merit is calculated to link the film transparency and conductivity with the crystallite size and orientation of the PEDOT:PSS thin films.

TUMino: Modular platform for sensor networks

Almudena Rivadeneyra[a], Michael Haider[b], Vijay Bhatt[c], Andreas Albrecht[d], Jose F. Salmeron[e], and Markus Becherer[f]

[a]almudena.rivadeneyra@tum.de, [b]michael.haider@tum.de, [c]vijay.bhatt@tum.de, [d]andreas.albrecht@tum.de, [e]jf.salmeron@tum.de, [f]markus.becherer@tum.de

TUMino is dedicated for specialized sensing tasks in the research laboratories (temperature, humidity, air-quality, etc.) and for long-term monitoring of custom-made research devices (gas sensors, magnetic sensors, humidity sensors, among others). In this project, we concentrate on the realization of specifications like e.g. high-precision sensing, high-accuracy A/D conversion, energy autark sensors or low-power applications on printed-circuit-board (PCB) and prototyping level. The Cypress PSoC Analog Coprocessor development hardware platform will be a further building block for the TUMino project (see Figure 1).

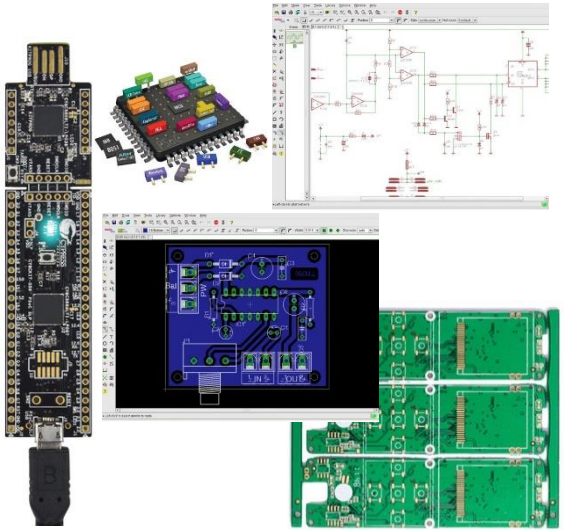

Figure 1. Workflow: reconfigurable electronics (PSoC from Cypress), PCB design and soldering.

The idea is to have a generic platform where different type of sensors can be connected according to the requirements of each environment or application. Therefore, All sensor nodes fit the same area (Arduino UNO geometry) and contain the same external pins: GND, VDD, SDA and SCL. The master board receive the data from the different sensor boards using I2C protocol. We have demonstrate the feasibility of using such a platform to integrate cost-effective sensors manufactured by printing techniques on flexible substrates.

Figure 2. Resistive sensor for temperature measurements based on Laser scribbing of Graphene oxide.

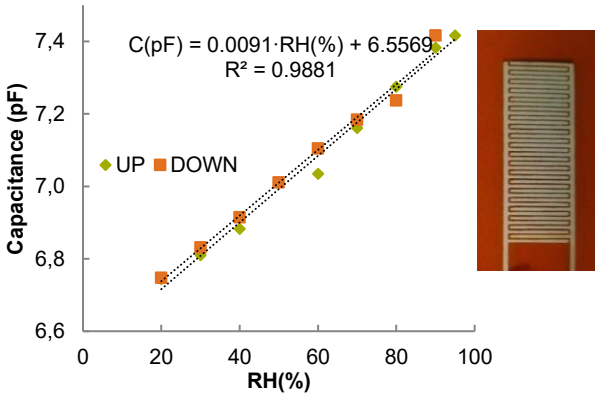

Figure 3. Capacitive sensor for relative humidity (RH) monitoring. Silver screen printed electrodes on polyimide (sensing layer).

Thermo-responsive polymer as smart surface coatings and their potential use as passive cooling system

Nawarah Aldosari[a], Lucas Kreuzer[b], Peter Müller-Buschbaum[c]

[a]nawarah.aldosari@ph.tum.de, [b]lucas.kreuzer@ph.tum.de, [c]muellerb@ph.tum.de

Energy consumption of cooling commercial and residential buildings has been steadily increasing in the past few years. With the current trends of energy consumption even higher percentages are expected to be reached within the next thirty years. The urbanization, emerging economies of developing countries and the global growth in population are some of the main factors behind this trend [1].

Passive cooling using thermo-responsive polymer thin films as smart surface coatings offers an easily integratable and economical solution to cool down and increase the energy efficiency of buildings. Polymers are flexible, readily available and customizable for different interfaces making them easy to integrate into existing structures. The absence of electricity and electrical components will reduce the risk factor of system failure associated with the conventional cooling systems.

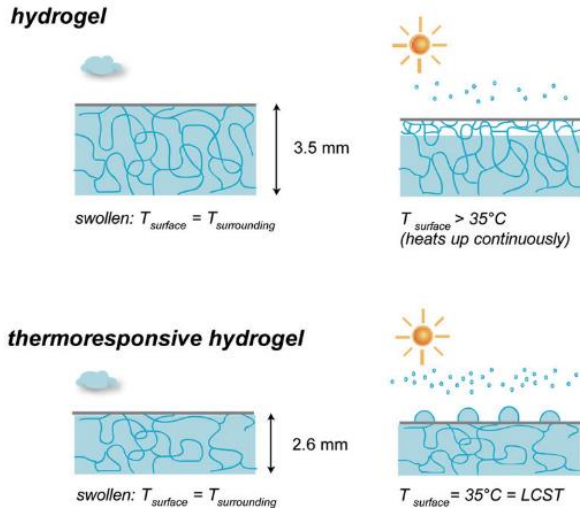

Figure 1: Conventional hydrogels are known for their ability to reversible store large amounts of water. However, upon drying a dense top layer is formed which considerably lowers the cooling rate. Thermo-responisve hydrogels do not show such top layer and maintain a surface temperature around the LCST due to a fast water evaporation based on irradiation [2].

One of the most extensively studied thermo-responsive polymers is poly(N-isopropylmethacrylamide) (PNIPAM) which has the ability to change its water affinity spontaneously in correspondence to changes in temperature. When the temperature is below its lower critical solution temperature (LCST), the polymer is able to sorb considerably high amounts of water and its thickness increases. As the temperature further increases above LCST, PNIPAM becomes hydrophobic and collapses releasing its water content. If this polymer is used as a coating on the external surfaces of windows, this water can precipitate and cool down buildings in a similar mechanism to how sweat cools down the body temperature [2].

To fully utilize this evaporative cooling technique, a deep understanding of the swelling kinetics of this polymer is required. In the present work, we investigate the cyclic water storage in a newly synthesized PNIPAM-based block copolymer. By using white light interferometry and Fourier transform infrared spectroscopy, we are able to follow in-situ the swelling and drying behavior and determine the underlying fundamental processes.

[1] Santamouris, M., 2016. Energy and Buildings 128, 617–638.
[2] Rotzetter, A.C.C., Schumacher, C.M., Bubenhofer, S.B., Grass, R.N., Gerber, L.C., Zeltner, M., Stark, W.J., 2012. Advanced Materials 24, 5352–5356.

Rate enhancement of stearic acid hydrodeoxygenation over bimetallic Ni_xFe_{1-x}/SiO_2 catalyst

Christoph Denk[a], Yue Liu[b], Eszter Baráth[c], Johannes A. Lercher[d]

[a]Christoph.Denk@tum.de, [b]Yue.Liu@tum.de, [c]Eszter.Barath@tum.de, [d]Johannes.Lercher@tum.de

The utilization of microalgae oil as a transportation fuel requires its hydrodeoxygenation (HDO) to form oxygen free green diesel.[1a] The HDO in this reaction network is mainly occurring via hydrogenation and decarbonylation to the respective alkane.[2] These mainly occur on supported metal sites.[1] Cu-Fe_2O_3 supported on SiO_2 is reported for the formation of fatty alcohols.[3] In the present work, we want to investigate the influence of Fe alloyed in Ni supported on mesoporous SiO_2. Hereby we found a promotion of both model reactions at different Ni_xFe_{1-x} compositions.

Seven Ni_xFe_{1-x}/SiO_2 catalysts with different Ni_xFe_{1-x} compositions (x = 0, 0.1, 0.22, 0.43, 0.71, 0.89, 1, 22–18 wt. % total metal loading) were prepared. The alloy formation was proven by the observation of alloy diffraction peaks by XRD. The initial reaction rate for the hydrogenation of stearic acid to 1-octadecanol shows a volcano-shaped curve, with a maximum at $Ni_{0.43}Fe_{0.56}/SiO_2$ (Fig.1 left). In contrast, the decarbonylation reaction is enhanced over higher Ni contents.

Catalytic reactions were carried out in an autoclave (Parr, 300 mL). Substrate and catalyst were mixed with 100 mL Cis, trans-Decaline, and pressurized with H_2 (40 bar). Typically, reactions were performed at 260 °C with stirring speed of 600 rpm. Samples were collected *in situ* during the reaction and analyzed on a GC-MS.

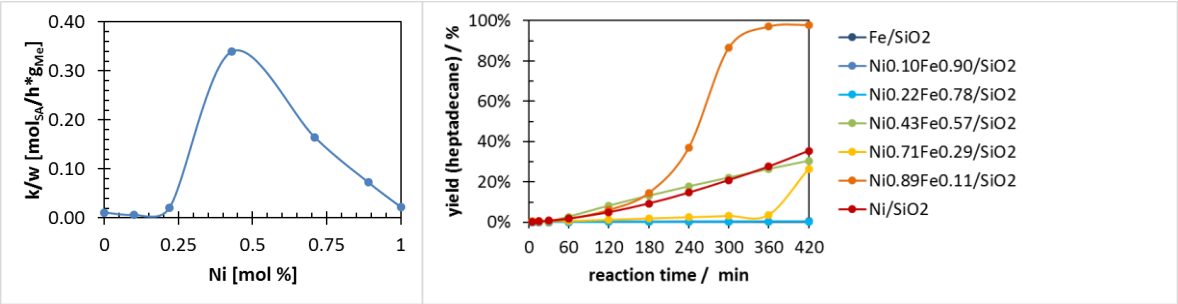

Figure 1: Initial reaction rate versus molar ratio of Ni (left), yield of *n*-heptadecane versus reaction time (right) for Ni_xFe_{1-x}/SiO_2 (x = 0, 0.1, 0.22, 0.43, 0.71, 0.89, 1).

Based on these observations, it can be concluded, that the hydrogenation of stearic acid to 1-octadecanol and the decarbonylation of the alcohol to *n*-heptadecane require two different active sites. Hydrogenation reaction is favored at a 1:1 ratio of Ni and Fe, however, the decarbonylation is preferred over Ni rich Ni-Fe-alloys.

Conclusion

HDO of stearic acid as model compound to its corresponding alkane was studied in the presence of Ni_xFe_{1-x} alloy materials supported on SiO_2. A suitable combination has been found for a fast hydrogenation of stearic acid to 1-octadecanol with $Ni_{0.43}Fe_{0.56}/SiO_2$, while a highly selective decarbonylation activity was observed for $Ni_{0.89}Fe_{0.11}/SiO_2$. Due to the different electronic properties present in the Ni-Fe-alloys, the selectivity to 1-octadecanol and *n*-heptadecane can be influenced significantly by adjusting the Ni_xFe_{1-x} ratio.

References

[1] (a) C. Zhao, T. Brück, J. A. Lercher, *Green Chem.* **2013**, *15*, 1720-1739. b) J. Lee, Y. T. Kim, G. W. Huber, *Green Chem.* **2014**, *16*, 708-718; c) M. Toba, S. Tanaka, S. Niwa, F. Mizukami, Z. Kopp. ny, L. Guczi, K.-Y. Cheah, T.-S. Tang, *Appl. Catal. A* **1999**, *189*, 243−250; d) B. Rozmysłowicz, A. Kirilin, A. Aho, H. Manyar, C. Hardacre, J. Wärnå, T. Salmi, D. Y. Murzin, *J. Catal.* **2015**, *328*, 197−207; e) H. G. Manyar, C. Paun, R. Pilus, D. W. Rooney, J. M. Thompson, C. Hardacre, *Chem. Commun.* **2010**, *46*, 6279−6281.

[2] S. Foraita, Y. Liu, G. H. Holler, E. Baráth, C. Zhao, J. A. Lercher, *ChemCatChem* **2017**, *9*, 195-203. (a) B. Peng, X. Yuan, C. Zhao, J. A. Lercher, *J. Am. Chem. Soc.* **2012**, *134*, 9400-9405; (b) B. Peng, Y. Yao, C. Zhao, J. A. Lercher, *Angew. Chem., Int. Ed.* **2012**, *51*, 2072−2075.

[3] K. Kandel, U. Chaudhary, N. Nelson, I. Slowing, *ACS Catal*. **2015**, *5*, 6719−6723

Catalyst development for CO_2 methanation

Thomas Burger[a], Olaf Hinrichsen[b]

[a]thomas.burger@ch.tum.de, [b]hinrichsen@tum.de

The power-to-gas concept (shown in Figure 1) represents a CO_2-neutral cycle to cope with future challenges arising from limited supply of fossil energy carrier feedstock and increasing energy consumption. Renewables are utilized to generate H_2 by electrolysis, which is then reacted with CO_2 to generate synthetic natural gas (SNG). SNG can act as a long-term chemical energy carrier that can be stored and distributed in the natural gas grid and be used in mobile applications or for the generation of heat and electricity on demand. Besides electrolysis, the key step is the highly exothermal, commonly heterogeneously catalyzed (Ni-Al catalysts) Sabatier reaction. [1]

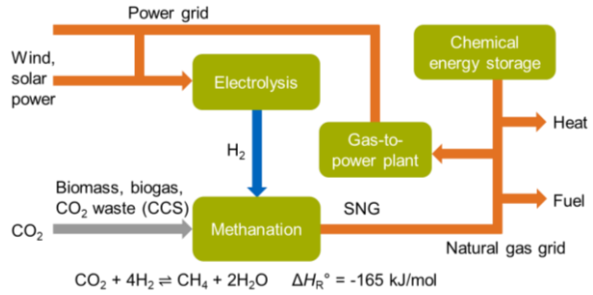

Figure 1: Power-to-gas concept.

From thermodynamics, two basic requirements for adequate catalysts are set: First, they are desired to feature a high catalytic activity in order to achieve decent CH_4 yields at low temperatures and pressures. Moreover, they should exhibit a superior stability under operating condition in order to increase catalyst life-time and reduce operating costs.

To develop original catalysts that feature a superior performance, detailed material characterization studies must be carried out to get insights into structure-activity relationships. By gaining a deeper understanding of effects of material parameters, novel and improved Ni-Al-based methanation catalysts can be designed. Material parameters that have shown to play an essential role in CO_2 methanation are illustrated in Figure 2. Different preparation procedures like incipient-wetness impregnation, precipitation, and co-precipitation were found to have a very high impact on the material properties of the final catalyst. Co-precipitated, highly loaded Ni-Al catalysts exhibit the best performance, which is attributed to the superior stabilization of small Ni crystallites on a partly reduced Ni-Al mixed oxide, where Ni oxide species further modify the catalyst basicity.

The catalytic activity of Ni-Al catalysts was found to increase by Mn doping, which leads to an increase of medium and strong basic site densities, that have been claimed to be essential for CO_2 methanation. [2] In contrast, Fe doping increases the stability of the co-precipitated Ni-Al catalyst by changing the electronic properties of the active Ni phase (formation of a surface alloy). [3] By co-doping Mn and Fe, highly stable CO_2 methanation catalysts with an improved catalytic activity can be synthesized (Figure 3).

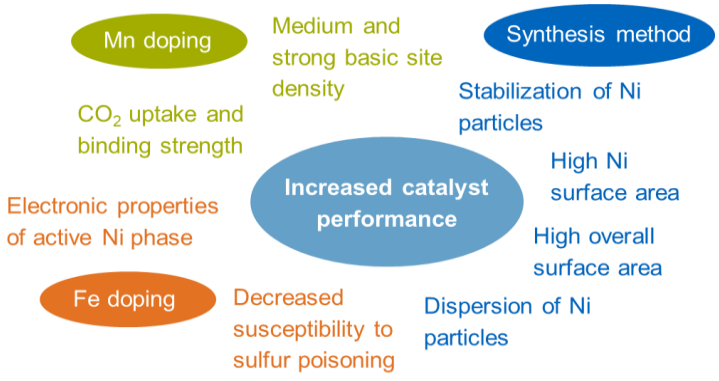

Figure 2: Influence parameters on catalyst performance.

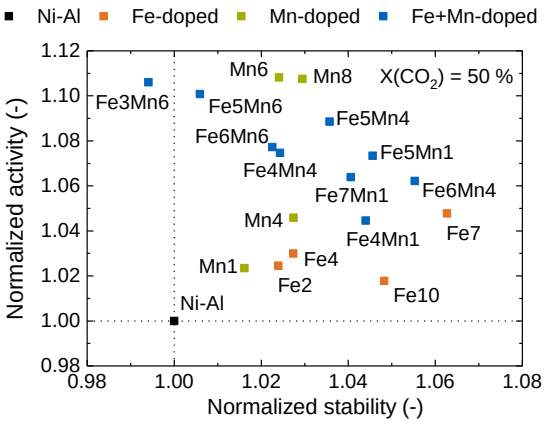

Figure 3: Promoter effects on the performance of a co-precipitated Ni-Al catalyst, numbers denote promoter loading, molar Ni/Al ratio: 1.

[1] P. Sabatier, J.B. Senderens, C.R. Acad. Sci., 134 (1902) 689–691.
[2] Q. Pan, J. Peng, T. Sun, S. Wang, S. Wang, Catal. Commun., 45 (2014) 74–78.
[3] T. Burger, F. Koschany, O. Thomys, K. Köhler, O. Hinrichsen, Applied Catalysis A: General, 558 (2018) 44–54.

Deactivation of Ni-Al catalysts for CO_2 methanation

Stefan Ewald[a], Michael Kolbeck[b], Olaf Hinrichsen[c]

[a]stefan.ewald@ch.tum.de, [b]michael.kolbeck@tum.de, [c]olaf.hinrichsen@ch.tum.de

CO_2 methanation plays a key role in the power-to-gas process, a promising technology in renewable energy storage [1]. The development of efficient catalysts for the methanation step requires knowledge of the governing deactivation mechanisms. However, studies on deactivation are scarce and a kinetic description of deactivation is lacking. In this contribution, a comprehensive deactivation study comprising both catalyst characterization and a kinetic description is presented. Ni-Al catalysts are used as model catalysts.

Ni-Al catalysts were synthesized via incipient wetness impregnation (IC17) and co-precipitation (PC13, PC11, PC31). For deactivation, catalyst samples were treated up to 165 h at elevated temperatures and 8 bar in feed gas with $H_2/CO_2/Ar/N_2$ = 8/2/5/1 under equilibrium conditions. Periodic activity measurements were performed at 523 K under differential conditions to reveal the catalyst deactivation behavior. The power law model (PLM) given in equation 1 was applied for the kinetic description. The apparent activation energy was determined before and after aging. Fresh and deactivated catalyst samples were characterized by means of H_2-TPD, pulsed H_2 adsorption, CO_2-TPD, XRD and N_2 physisorption.

$$\frac{da_{rel}}{dt} = -k_d \cdot a_{rel}(t)^m \qquad \text{with} \qquad a_{rel}(t) = \frac{WTY\,(t)}{WTY\,(t=0)} \tag{1}$$

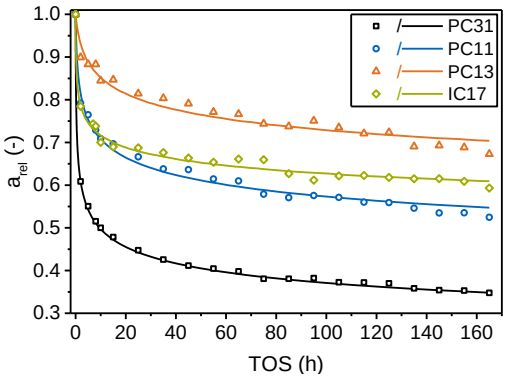

Figure 1: Deactivation behavior during aging at 623 K (m_{cat} = 50 mg, m_{SiC}= 450 mg, Ni loading: PC31>PC11> PC13 ≈ IC17).

We found the catalytic activity increasing with rising Ni content whereas the catalyst stability decreases. The stability of co-precipitated catalysts is higher as compared to impregnated systems. Results from the PLM fit match the experimental data (Figure 1 and Table 1). The kind of the active sites does not change during aging but the site density decreases, since the apparent activation energy remains constant within experimental error.

Table 1: Results from the PLM fit of catalyst deactivation at 623 K.

	k_d (h^{-1})	m (-)
PC31	3.08 ± 0.41	8.86 ± 0.81
PC11	0.31 ± 0.10	11.30 ± 0.87
PC13	0 05 ± 0 02	14.30 ± 2.18
IC17	1.78 ± 1.13	18.21 ± 1.78

The loss of Ni surface area and CO_2 adsorption capacity are predominant deactivation mechanisms. However, a linear correlation between activity and Ni surface area or CO_2 adsorption capacity is not observed, which might (at least partly) be explained by the stronger reduction of medium basic sites with increasing Ni content as evident from CO_2-TPD results (Figure 2). Medium basic sites have been described to be essential for catalytic activity [2]. H_2-TPD indicates a reduction of defects in the Ni phase upon aging and the BET surface area of all catalysts decreases. No correlation between BET surface area and activity is observed. The average pore diameter and the pore volume remain unchanged during aging for the impregnated samples while the pore diameter of precipitated samples increases at constant pore volume, indicating that catalyst deactivation is not accompanied by transport limitations. XRD results show the formation of mixed oxides in the precipitated samples. Upon aging, structural changes are observed due to the further reduction of the catalysts. No structural changes are observed for impregnated samples.

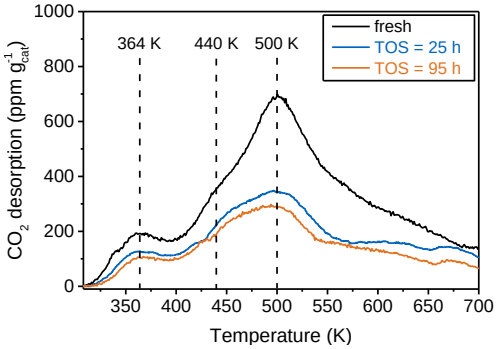

Figure 2: Exemplary CO_2-TPD results (PC31, T_{Aging} = 623 K).

[1] M. Sterner, *Dissertation*, Kassel University, **2009**.
[2] Q. Pan et al., *Catal. Commun.* **2014**, *45*, 74-78.

Contactless temperature measurements under static and dynamic reaction conditions in a single-pass fixed bed reactor for CO_2 methanation

C. Schüler[a], M. Wolf[b] and O. Hinrichsen[c]

[a]chris.schueler@ch.tum.de, [b]moritz.wolf@ch.tum.de, [c]olaf.hinrichsen@ch.tum.de

In this study, the heat evolution during CO_2 methanation reaction over a $NiAlO_x$ catalyst was monitored under static and dynamic reaction conditions by means of thermography. Therefore, industrial relevant $NiAlO_x$ catalysts were prepared by the reverse co-precipitation method at constant pH. The molar ratio of Ni/Al was set to 1/5 for static and 1/1 for dynamic experiments. Contactless temperature measurements were carried out in an optical accessible reactor setup, equipped with a SC-2500 near-infrared camera (FLIR). Most of the experiments were conducted at standard conditions (table 1).

Table 1: Standard reaction conditions for the CO_2 methanation reaction

$m_{catalyst}$ (mg)	m_{SiC} (mg)	T_{oven} (°C)	$\dot{V}$ (sccm)	$H_2/CO_2/Ar$	p (bar)	activation procedure
50	450	400	62.5	4/1/5	1.013	10 % H_2/Ar, 450 °C, 4 h

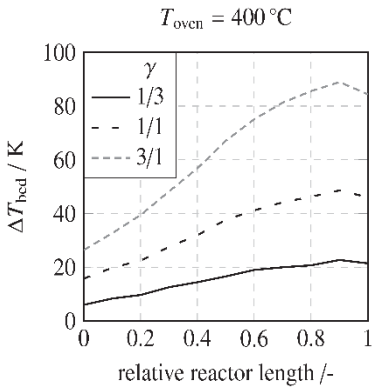

Figure 1: Bed temperature elevation at 240 sccm at 400 °C oven temperature with different feed gas dilutions *γ* for NiAl15.

In the case of the static experiments, the volume flow $\dot{V}$, feed gas dilution γ ($\gamma = p_{reactants}/p_{Argon}$) and furnace temperature T_{oven} were varied. For the dynamic experiment, the activation procedure was followed by an aging period of 24 h at standard conditions. Afterwards, 5 ppm of H_2S were introduced into the reactor until the catalyst was completely deactivated.

As the methanation of CO_2 is highly exothermic, large amounts of heat are generated within the fixed bed at chosen conditions. Once the released heat exceeds the heat transport within the fixed bed, a hot spot is formed. In our static experiments, an increase in volume flow and decrease in feed gas dilution, led to an increase in the hot spot temperature (Fig. 1, exemplarily). This trends qualitatively follow the dependence of the released heat of the reaction $\dot{Q}$ on reaction enthalpy $\Delta_r H°$ and CO_2 conversion (eq. 1). At the chosen conditions ($\dot{V}$ ↑ and γ ↑), the reactant mole flow $\dot{n}_{reactant}$ is greatly increased, whereas the conversion of CO_2 X is only affected to a minor extent.

$$\dot{Q} = \dot{n}_{reactant} \cdot \Delta_r H° \cdot X \qquad \text{(eq.1)}$$

The measured temperature profiles over the course of the poisoning experiment is shown in Fig. 2. As can be seen, the reactive zone (hot spot) is located within the first 20 to 30 % of the catalyst bed. As soon as H_2S is introduced into the reactor (TOS = 1500 min), the hot spot begins to migrate through the fixed bed at an approximately constant velocity.

Static and dynamic experiment showed, that thermography is a powerful tool to investigate heat evolution phenomena within a catalytic fixed bed. This study points out some basic principles, which can be observed in static operation. Furthermore, the benefits of the fully resolved temperature profile can be used to monitor dynamic reactions, e.g. *in situ* catalyst deactivation.

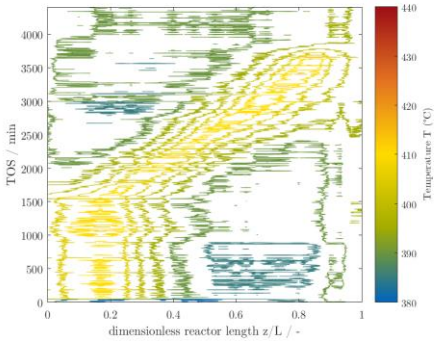

Figure 2: Hot spot movement under aging and deactivation condition. The H_2S feeding starts at a TOS of 1500 min.

Conversion of microalgae oil to biokerosene over WO_3/ZrO_2 supported metal catalysts

Lara Milakovic[a], Yue Liu[b], Eszter Baráth[c], Johannes A. Lercher[d]

[a]lara.milakovic@tum.de, [b]yue.liu@tum.de, [c]eszter.barath@tum.de, [d]johannes.lercher@mytum.de

Introduction

Microalgae is a highly abundant, fast growing, readily cultured biomass resource and is not competing with our food chain. The lipid constitutes up to 70 % of the microalgae dry mass[1] and its transformation into hydrocarbon fuels is considered as an important alternative to petroleum-based fuels.

Diesel like transportation fuel can be produced from microalgae oil (triglycerides, fatty acids) via hydrodeoxygenation[2].Over the past years increasing interest is also gained in the further conversion to hydrocarbons in the kerosene range for the utilization in the aviation sector. This can be implemented by an additional hydrocracking step. In our work, we study the one-step production of kerosene from stearic acid as a model compound for microalgae oil over WO_3/ZrO_2 supported metal catalysts.

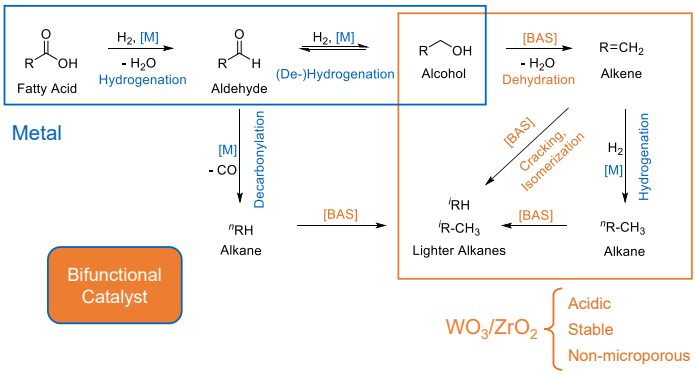

Figure 1: Reaction network of fatty acid conversion

Results

The proposed hydrodeoxygenation and hydrocracking mechanism of a fatty acid is displayed in Figure 1. The reaction network clearly shows the role of a bifunctional catalyst in the conversion process. The metal function catalyzes the hydrogenation of the fatty acid to the aldehyde and further to the alcohol. The acid function then catalyzes the dehydration of the alcohol to an alkene, which in turn is cracked or isomerized. The acid functions of the catalyst are provided by the WO_3/ZrO_2, w by rhodium, p

The tested catalysts showed a successful hydrodeoxygenation of the stearic acid, however, only hydroisomerization but no hydrocracking o the obtained octadecene could be observed.

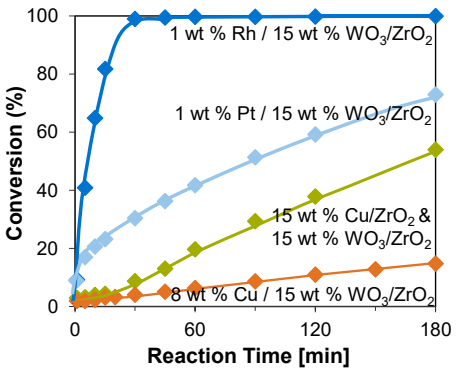

Figure 2: Stearic acid conversion on different WO_3/ZrO_2 supported catalysts

Conclusion

The synthesized WO_3/ZrO_2 supported metal catalysts were capable to catalyze the hydrodeoxygenation of the steric acid. The rhodium catalyst showed the highest activity followed by the platinum and copper (See Figure 2).

Experimental

Catalyst preparation The WO_3/ZrO_2 support was synthesized by incipient wetness impregnation of ZrO_2 with $(NH_4)_{10}(H_2W_{12}O_{42})$ solution, which was then calcined at 1073 K for 4 h. The metal was also incorporated by incipient wetness impregnation of WO_3/ZrO_2 with the corresponding precursor solution (Cu: $Cu(NO_3)_2$, Pt: H_2PtCl_6, Rh: $RhCl_3$). An oxidation at 723 K for 4 h was followed by a reduction at 773 K for 4 h in Hydrogen flow.

Catalytic reactions were conducted in an autoclave (Parr, 300 mL). The reactant and the catalyst were dissolved in 100 mL dodecane. The mixture is heated up to 240 °C, pressurized with H_2 to 40 bar and stirred at 700 rpm for 4 h. In situ sampling of the reaction was analyzed with a GC-MS equipped with a FID.

References

[1] F. B. Metting, J. Ind. Microbiol. 1996 17, 477-489.

[2] B. Peng, X. Yuan, C. Zhao, J. A. Lercher, J. Am. Chem. Soc. 2012, 134, 9400-9405; B. Peng, Y. Yao, C. Zhao, J. A. Lercher, Angew. Chem., Int. Ed. 2012, 51, 2072-2075.

Experimental investigation of carbon deposition on a Ni-YSZ anode in a SOFC cell

Verónica Echeverría[a]

[a]veronicaecheverria8@gmail.com

According to International Energy Agency (IEA) world energy outlook 2017, energy demand will increase by 30% by 2040. The fuel cell allows to transform energy more efficiently, therefore it is a promising prospect for energy production. A solid oxide fuel cell (SOFC) is an all-solid-state type of fuel cell that electrochemically combines a fuel and an oxidant across an ionic conducting oxide electrolyte, with efficiencies as high as 85%, when combined with gas turbine, and low pollutant emissions.

In SOFCs, the conducting species are oxygen ions. Oxygen is supplied air to the porous cathode where it gets absorbed, dissociated and reduced into oxygen ions which are carried to the anode through a solid electrolyte. At the anode, oxygen ions combine with hydrogen from the fuel to produce water. Outside the cell, electrons move from the anode to the cathode through an external circuit, converting chemical energy of the fuel to electrical energy. This type of fuel cell can be operated with a wide range of fuels: carbon-based, hydrocarbons, oxygenates and pure hydrogen. SOFCs allow hydrocarbons reforming, and these can be combined with biomass gasification, which makes SOFCs an advantageous technology for renewable energies. When hydrogen is used as the fuel, only water is a byproduct of the reaction. Yet, there are still some difficulties regarding hydrogen production and storage. When using a carbon containing fuel, other products such as CO, CO2 and C are produced.

When carbon-containing products are formed at the anode, carbon deposition might occur. The most commonly used anode-material is nickel/yttrium-stabilized zirconia (Ni/YSZ). It is highly used due to its excellent electro catalytic effects on the fuel oxidation. Regardless of this, nickel acts as a catalyst for carbon deposition. When a natural gas related fuel is used, Ni/YSZ cermet materials suffer from sulfur poisoning, and carbon deposition caused by the cracking of methane. Carbon deposition occurs on the Ni surface through a dissociative adsorption of hydrocarbons. Several anode materials have been studied to avoid carbon deposition. Nonetheless, Ni/YSZ composite provides the best desired properties, hence it is the most used anode material in SOFCs.

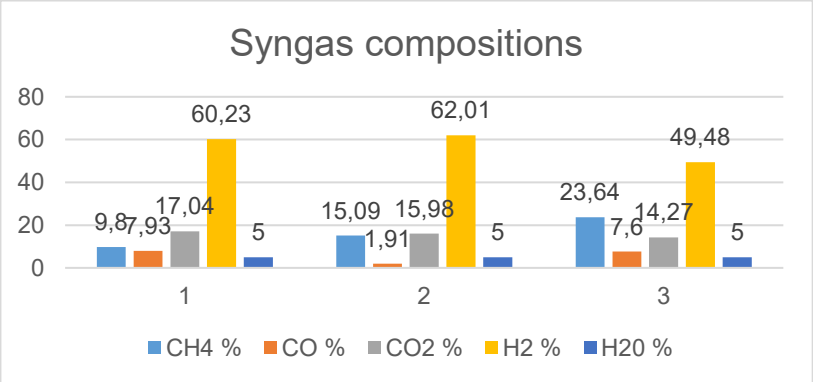

Figure 1. Syngas composition critical for carbon deposits.

Carbon deposition leads to metal dusting-a phenomenon in which metals exposed to carbon supersaturated gas disintegrate. It is of great interest to understand how carbon deposition occurs, as it enhances anode degradation which leads to low cell performance. This work aims to find the time and concentration limit values above which metal dusting begins on an Ni/YSZ anode cermet. For this purpose, a test stand is to be set up in which samples of anode substrate can be exposed to a gas atmosphere critical for carbon deposits at a temperature of 700°C. T. Chen et al. determined critical gas compositions for carbon deposition, which are shown in Figure 1. The samples with the carbon depositions will then be tested for deposited carbon in TGA measurements.

Understanding the mechanism in Ni catalyzed dimerization of butene

Andreas Ehrmaier[a], Yue Liu[b], Stephan Peitz[c], Maricruz Sanchez[d], Ricardo Bermejo DeVal[e], Johannes A.Lercher[f]

[a]andreas.ehrmaier@tum.de, [b]yue.liu@tum.de, [c]stephan.peitz@evonik.com, [d]m.sanchez@tum.de, [e]ricardo.bermejo@tum.de, [f]johannes.lercher@ch.tum.de

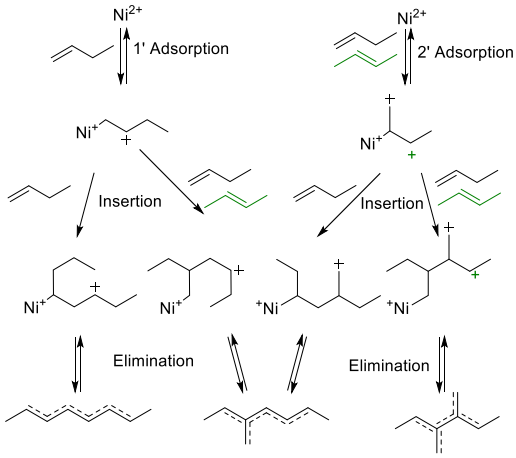

Figure 1: Reaction network of Ni catalyzed butene dimerization.

Butene is a side product from fluid catalytic cracking (FCC), used in the synthesis of linear and monobranched octenes, a crucial step in the synthesis of PVC plasticizers.[1] Currently, butene dimerization is catalyzed with nickel nanoparticles supported on silica-alumina, leading to nanoparticle agglomeration and its deactivation.[2] Thus, the high dispersion of Ni^{2+} in zeolites, compensating two negative charges in the aluminosilicate framework, can enhance the catalytic activity. However, isolated Brønsted acid sites on the support are known to favor a side reaction of the linear dimerization, the formation of branched dimers. These sites can be prohibited in LTA zeolite by the exchange of the protons with co-cations, e.g. Ca^{2+}, increasing the selectivity towards linear octenes. This allows an exclusive study of the reaction pathway happening over the Ni^{2+} sites.

Commercial samples of the zeolite Ca-LTA were exchanged with various amounts of Ni nitrate at 80 °C for 24 h. The prepared catalyst samples were tested in 1-butene oligomerization at 50 bar and 150-180 °C, as well as the formation of surface species upon butene adsorption were studied by infrared spectroscopy.

Dimerization experiments with varied nickel loaded catalysts revealed an increase of activity per Ni upon cation loading, being the 6 % Ni sample the highest in activity. Subsequently, 6 % Ni-Ca-LTA revealed a selectivity towards dimers of above 85 %, with less than 15 % oligomers (mostly trimers) being formed, upon conversions below 40 % (WHSV = 6-240 h^{-1}). Within the dimer fraction, the main products were methylheptene and linear octene, as well as small amounts of dimethylhexene, allowing the exclusion of a Brønsted acid catalyzed pathway.

On the Ni sites, two competitive reactions were found to occur. On the one hand, there is reactant isomerization to 2-butenes, which happens through an adsorption-desorption process of a π-allyl bound butene.
The second, the dimerization, was found to run via a Ni-alkyl-type intermediate. It was found that this first adsorption is necessary to happen at the C_1 position to continue the dimerization route with the adsorption and subsequent insertion of the second butene molecule. The orientation of this second butene molecule in the π-complex controls, whether it is inserted at the C_1 or C_2 position (1'- or 2'-insertion, respectively), and hence, whether methylheptene or octene is formed.
At higher concentrations of 2-butene, the 2'-insertion is favored, enhancing the selectivity to methylheptene.

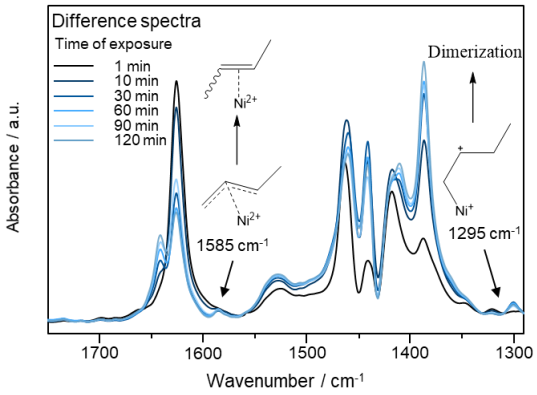

Figure 2: Infrared spectra of surface intermediates for different reaction pathways.

[1] B. Nkosi, F. T. T. Ng, G. L. Rempel, *Applied Catalysis A: General* **1997**, *161*, 153-166.
[2] S. Albrecht, D. Kießling, G. Wendt, D. Maschmeyer, F. Nierlich, *Chemie Ingenieur Technik* **2005**, *77*, 695-709.

Proton- and CO_2-Reduction by Macrocyclic Co(Mabiq)-Complexes

Raphael Lauenstein, Ceren G. Tok, Corinna R. Hess[a]

[a]corinna.hess@tum.de

The production of solar fuels such as hydrogen and the transformation of carbon dioxide to carbon monoxide or organic molecules are gaining in importance in times of rising energy demands and climate change. Promising solutions for the problem of long-term storage of solar energy is the water splitting reaction or the catalytic hydrogen evolution from acidic solutions. For this purpose several transition metal catalysts have been developed. Earth-abudant transition metal catalysts such as Fe, Co and Ni macrocyclic complexes have been extensively investigated as electrocatalysts in the past.

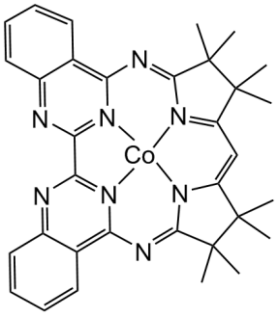

Figure 1: Structure of Co(Mabiq)

Here we will present our studies with the redox-active macrocyclic biquinazoline ligand (Mabiq) coordinating cobalt as the metal center. The ligand stabilises several formal oxidation states of cobalt, namely Co(III), Co(II), Co(I) and Co(0). All these compounds were sucessfully synthesized, isolated and fully characterized by spectroscopic methods. Also their structures were solved by x-ray diffraction. The main focus in this study is the reactivity of these compounds towards proton sources and carbon dioxide.

Novel Second Order Generalized Integrator Frequency Locked Loop for Phase Parameter Detection

Markus Landerer[a], Christoph M. Hackl[b]

[a]markus.landerer@tum.de, [b]christoph.hackl@tum.de

Motivation

In power systems like overhead power lines, the voltage amplitude and frequency should match certain restrictions to ensure a stable operation of the grid. To keep the voltage amplitude and the frequency in the allowed range, it is necessary to detect these quantities online.

Methodology

Usually, the well known *Second Order Generalized Integrator (SOGI)* [1], [2], [3] combined with a *Frequency Locked Loop (FLL)* [4], [5] is used to deal with this task. Unfortunately, a common SOGI has the disadvantage of speed limitation, i.e. the algorithm requires at least a certain time interval to estimate amplitude and phase correctly. Additionally, the FLL leads to a even longer settling time. To minimize the required time interval, this poster proposes a new algorithm which allows detection of amplitude, phase and frequency based on an extended SOGI, called *Modified Second Order Generalized Integrator (MSOGI)*. The MSOGI is able to estimate the parameters within a predefined time interval where the settling time can be specified by pole placement. Hereby, the frequency detection is established via a FLL which is adopted to the MSOGI. In Figure 1, the proposed modified SOGI is shown.

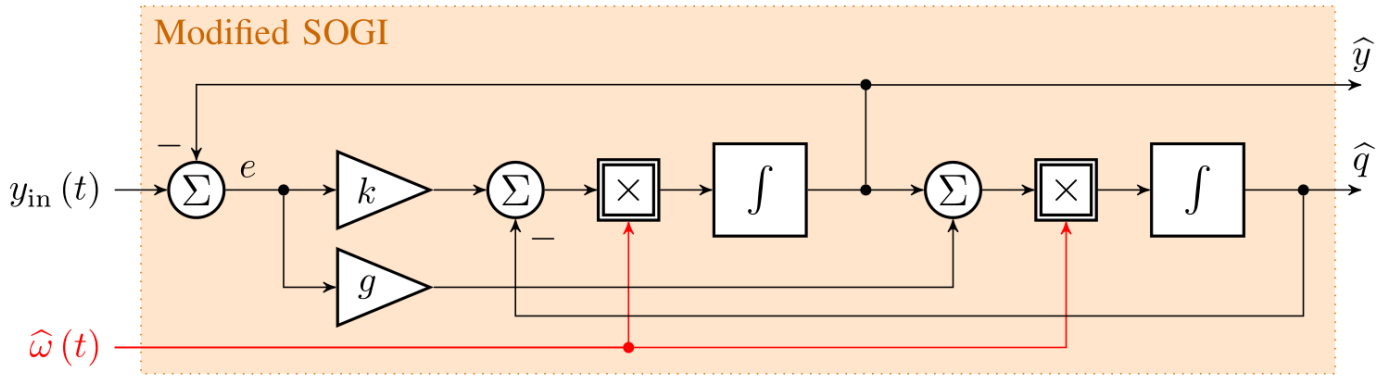

Figure 1: The proposed SOGI algorithm.

Results

Simulation results show that the modified SOGI, in comparison to the common SOGI, is able to estimate the amplitude, phase and frequency accurately and much faster. In combination with the adopted FLL, the over time lag can also be shortened.

References

[1] R. Teodorescu, M. Liserre, and P. Rodriguez, Grid Converters for Photovoltaic and Wind Power Systems. Chichester, United Kingdom: John Wiley \& Sons, Ltd., 2011.

[2] R. Chilipi, N. A. sayari, K. H. A. Hosani, and A. R. Beig, “Adaptive notch filter based multipurpose control scheme for grid-interfaced three-phase four-wire dg inverter,” IEEE Transactions on Industry Applications, vol. PP, no. 99, pp. 1–1, 2017.

[3] G. Fedele, A. Ferrise, and D. Frascino, "Structural properties of the sogi system for parameters estimation of a biased sinusoid," in \textit{2010 9th International Conference on Environment and Electrical Engineering}, pp. 438-441, May 2010.

[4] J. Matams, H. Martin, J. de la Hoz, A. Abusorrah, Y. A. Al-Turki, and M. Al-Hindawi, "A family of gradient descent graid frequency estimators for the sogi filter," \textit{IEEE Transactions on Power Electronics}, vol. PP, no. 99, pp. 1-1, 2017.

[5] K. R. Patil and H. H. Patel, “Modified dual second-order generalised integrator fll for synchronization of a distributed generator to a weak grid,” in 2016 IEEE 16th International Conference on Environment and Electrical Engineering (EEEIC), pp. 1–5, June 2016.

Hydrogen from electrolyzers as an energy carrier for sector coupling in Germany

Kay Bareiß[a], Konrad Schönleber[b]

[a]Kay.Bareiss@tum.de, [b]konrad.schoenleber@tum.de

This study discusses the potential of Hydrogen as an energy carrier for diverse applications. As we believe that sector coupling is a promising method to achieve the climate objectives, hydrogen is used to cover demands of the transportation sector as well as the heating sector. The impact of a partial electrification of the traffic sector in Germany with hydrogen fuel cell vehicles on the energy system is studied using economical optimization. Power-to-heat (P2H) is integrated as a simple competitive technology which benefits from cheap heat-storages in district heating networks. Different scenarios allowing expansion of renewables and electrolyzers, are compared regarding their costs, the integrations of renewable energy and CO_2-emissions. The optimization is carried out for the year 2050 with 80 % CO_2 reduction in the energy system.

Four-leg inverters for unbalanced grid feed-in from Renewable energy sources

Anurag Mohapatra[a], Franz Christange[b]

[a]anurag.mohapatra@tum.de, [b]franz.christange@tum.de

Renewable energy (RE) based Microgrids cannot be assumed as balanced three phase networks. A microgrid has a limited energy pool and thus needs to mitigate network imbalances on an active basis. This control challenge has been tackled through some standard ideas such as split-DC link and delta-star transformers in the past. These methods however have been shown to be sub-optimal and costly.

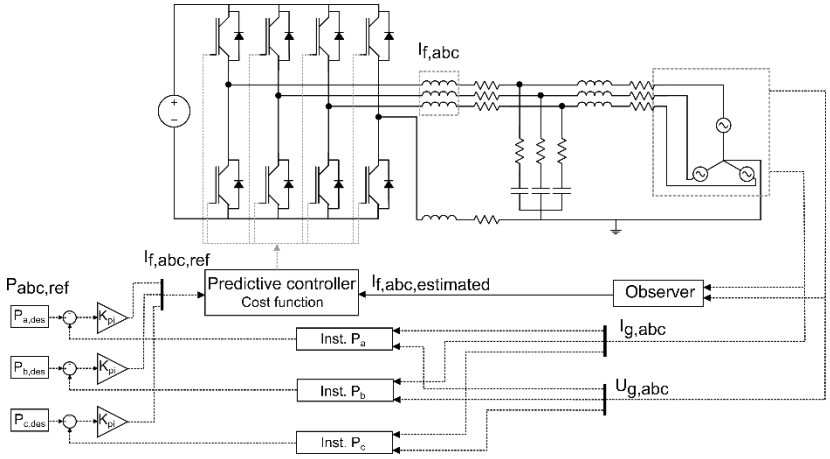

Figure 1: Four-leg inverter, LCL filter, with active power feedback

In this work, unbalanced microgrid feed-in from RE sources using four-leg voltage source inverter with LCL filter has been studied. Four leg inverters handle imbalances robustly, have higher DC voltage utilization and low DC voltage ripple. LCL filters give better harmonic suppression than L filter and also allows for smaller dimensions in hardware which makes them cheaper.

In LCL configuration, the grid current (control output) is not a direct function of the DC switching voltage (control variable). Past approaches have the capacitor and the inductors combined to get an approximate system which behaves like a L filter and thus circumvents the control dilemma. This method is imprecise and not suitable for strict control over the active power being injected into the grid.

In the present work, Fig.1, the active power injected into the grid is measured from values of the sensors and full state observer. This serves as the feedback for the outer control loop which gets an active power reference (as desired) and uses a PI gain to produce a filter current reference for the inner controller. In this loop, the filter current output is directly controlled using a predictive law. By using the multiloop arrangement, this topology can still use LCL filter and precisely control active power injection. The inverter can respond rapidly to fluctuating power references, imbalances and phase failure as seen in Fig. 2. The active power references can themselves be generated from ideas of operational load flexibility and economic incentives, allowing for a dynamic micro grid operation.

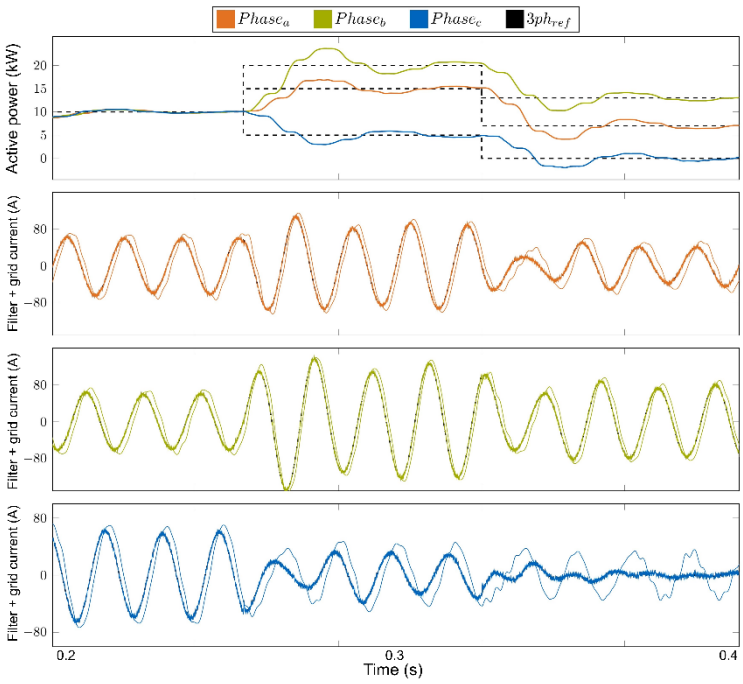

Figure 2: Unbalanced active power reference tracking

Development of an integrated method to optimize the energy supply system of the Campus Garching by using parametric heat-load profiles.

Christoph Matschi [a], Benedikt Schweiger [b], Isabell Nemeth [c]

[a]christoph.matschi@hs-ansbach.de, [b]benedikt.schweiger@tum.de, [c]isabell.nemeth@hs-ansbach.de

Research Approach

In 2015, the German federal government presented the Energy Efficiency Strategy for Buildings: by 2050 the building stock in Germany has to be climate neutral [1]. In order to achieve this goal, the Federal Government specifies as efficiency enhancement potentials in heating, combined heat and power plants as well as heat pumps and district heating networks as actuators. The research project CleanTechCampus picks up the resulting need and aims to develop an integrated transition concept for the Garching Campus, which can be an example on the way to a climate neutral building stock, energy production and in the end an optimized district heating network and an optimized energy supply system, respectively.

Objectives

For an optimized energy strategy of the Campus Garching it is very important to have an optimized energy supply system. For an energy-efficient design of the grids and their components, knowledge about temporally high-resolution load as well as the simultaneity of heat demand is of central importance. For this reason a smart method for creating parametric and transferable load-profiles for non-residential buildings should be developed as base for the development of a smart method to optimize the energy supply system.

Method

In a first step, to optimize the energy supply system using the linear programming model *urbs*, the Campus Garching was divided in eight nodes, whose heat load profiles had the same simplified course. To do these optimizations, load profiles with an hourly resolution are needed. In a second step parametric load-profiles of the buildings of the Campus Garching have been developed, by doing transient calculations to get a better understanding about the thermal dynamic behavior of singular areas of use of a building. These calculations are leading to standardized and parameterized mean heat load-profiles with an hourly resolution. In this case the mean heat load profiles have been developed for a future energy demand scenario. In a third step, to test the method and to gain a deeper insight of the optimization potential of the energy system regarding costs, energy production and CO_2, the different parametric heat load-profiles of step two were used for each node of the district heating network, which leads to an optimized energy supply system.

Prospects

In order to be able to optimize the energy supply system and the power generation in different stages of extension scenarios of the Campus Garching, the method will be applied to different energy demand scenarios to get a more detailed insight into the energy supply of the Campus Garching.

[1] Federal Ministry for Economic Affairs and Energy (BMWi) 18.11.2015: Energy Efficiency Strategy for Buildings

Integrating Prosumer Flexibility in Smart Grids

Michael Kramer, Akhila Jambagi

michael.kramer@tum.de

The trend to electrify the residential heating sector combined with increasing shares of local generation from renewables is an important step on Germany's path to reduce carbon emissions. However, the impact of weather-dependent and price-responsive loads of prosumers may cause additional challenges in the operation of distribution grids. In this context, demand-side management (DSM) is considered a promising strategy to both optimize prosumer scheduling and to mitigate the aggregate's negative impact on the grid.

The presented approach creates simplified resistance and capacitance models to represent the dynamic behaviour of each building's thermal system. The system dynamics account for the available and time-dependent flexibility of the individual buildings to shift their heat pump operation. Finally, the effectiveness of coordinated DSM strategies with respect to the costs of the DSO and prosumers is investigated. An uncoordinated Model Predictive Control strategy (MPC) for each building to minimize energy consumption is compared to a distributed approach (DMPC) to respect both local goals of the prosumers and the global goal of the distribution system operator (DSO) to flatten the aggregate's load profile. DMPC is carried out in a hierarchically distributed way via the Alternating Direction Method of Multipliers. Prosumer dynamics and cost functions are not shared with the DSO to preserve privacy. The model has been further expanded by the integration of a linearized AC power flow model to fully include grid constraints from thermal line ratings and voltage restrictions.

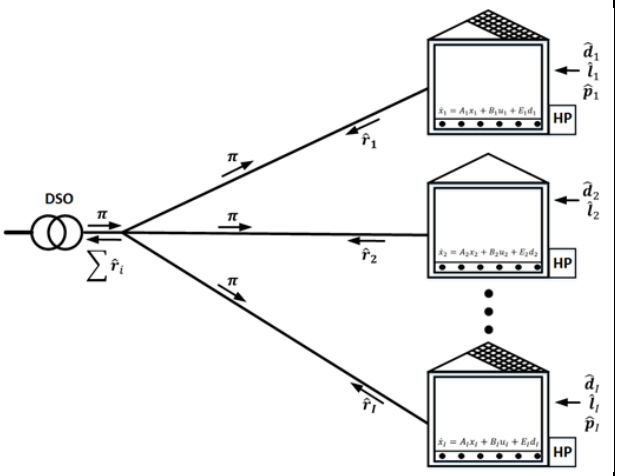

Figure 1: Communication between prosumers and the DSO in the DMPC scheme.

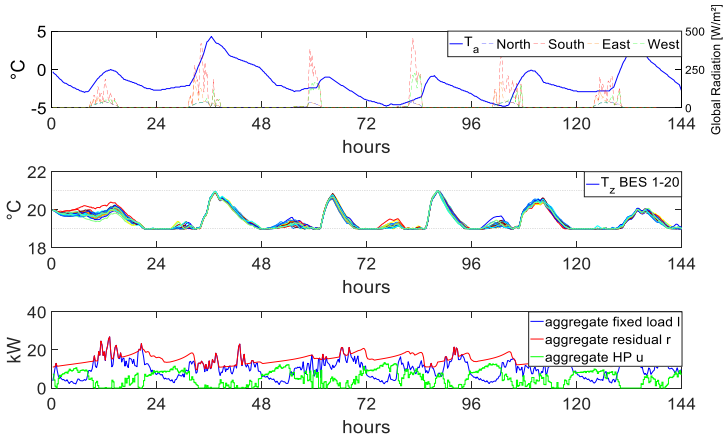

Figure 2: Disturbances, prosumer indoor temperatures and the flattened aggregate load profile (aggregate redsidual r).

The simulation results demonstrate how the aggregate's residual load curve of all prosumers is flattened by load-shifting to avoid overloading at the transformer. The indoor temperatures in subplot 2 of Fig. 2 indicate that each prosumer's comfort range is never violated while shifting the demand of heat pumps towards times preferred by the DSO.

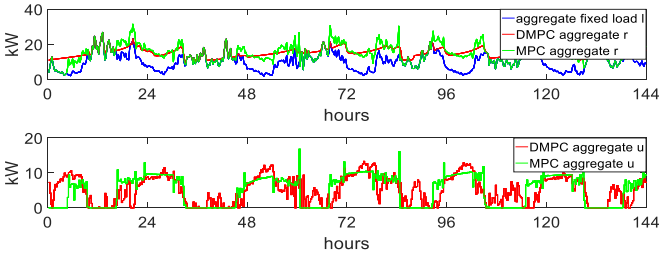

Figure 3: DMPC vs. uncoordinated MPC.

M. Kramer, A. Jambagi, V. Cheng, "Distributed Model Predictive Control for Building Energy Systems in Distribution Grids", in 2017 IEEE PES Innovative Smart Grid Technologies Conference (ISGT), Torino.
M. Kramer, A. Jambagi, V. Cheng, " Bottom-up Modeling of Residential Heating Systems for Demand Side Management in District Energy System Analysis and Distribution Grid Planning", in 15th International Building Simulation Conference 2017, San Francisco.
M. Kramer, A. Jambagi, V. Cheng, "A Model Predictive Control Approach for Demand Side Management of Residential Power to Heat Technologies", in Proc. 2016 IEEE Energy Conference (ENERGYCON), 2016, Leuven.

Optimal planning of battery storage in distribution networks

Akhila Jambagi[a], Michael Kramer[b]

[a]akhila.jambagi@tum.de, [b]michael.kramer@tum.de

There is much indication that energy storage technologies can play an important role in the future energy system. Particularly as the cost of Lithium Ion batteries is reducing by an average of 20% per year for the last 4 years, they are becoming an increasingly viable flexible component in the electricity grid. Out of the many possible applications, in distribution grids they can particularly be used to alleviate grid congestion due to high levels of PV infeed by increasing local self-consumption, as well as reducing grid losses by flattening load peaks. Currently batteries are a relatively expensive component and therefore developing a methodology for optimal planning of the deployment of energy storage is a focus of this work.

A linearized grid representation of voltages and power flows is required for an optimization algorithm, for which the methodology is adapted from [1]. The presented methodology includes the development of an algorithm that performs a cost optimization to identify the optimal sizes and locations of energy storage units in a distribution grid. A case study is performed with a rural network over a period of 8 sample days to represent one year. Load profiles for each node are generated using the in-house residential load profile generator [2], and PV profiles are generated using the HDKR model, the aggregate of the profiles are shown in Figure 1.

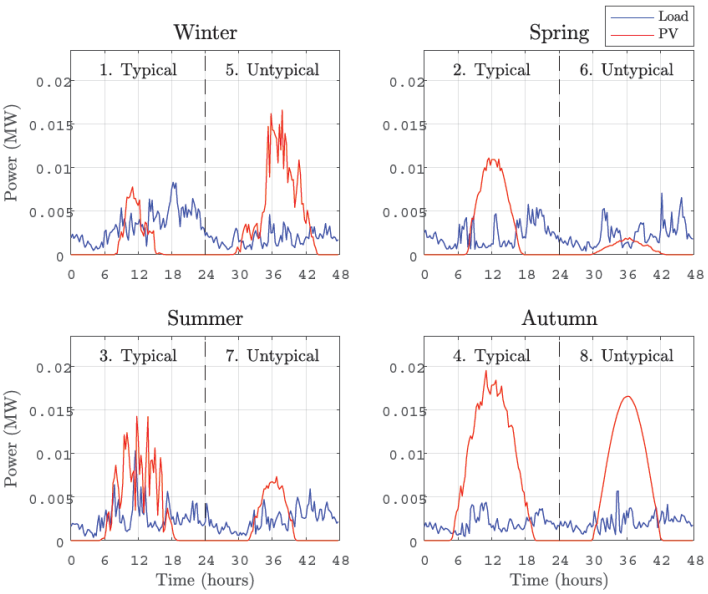

Figure 1: Aggregate Case Study profiles

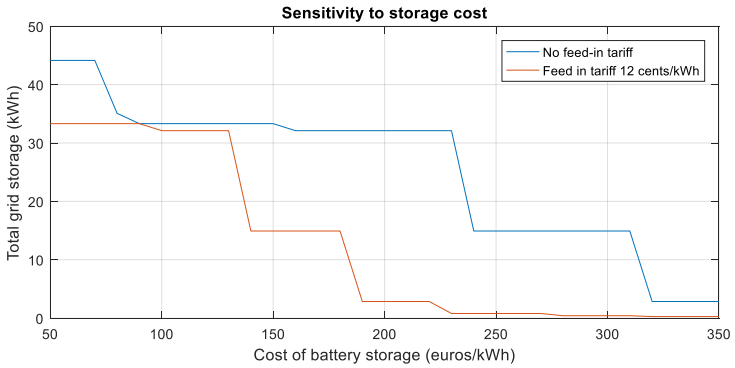

Figure 2: Sensitivity of amount of total storage in case study grid to storage cost

The results show that the optimal amount of battery storage in a network has a very high dependency on the cost parameters of feed-in tariff and price of storage per kWh. This sheds some light on the economic viability of storage, and with current prices it is not yet a viable technology. A sensitivity analysis however shows that with current feed in tariffs of 12cents /kWh, a significant storage will become viable in in the coming years if prices reduce according to current trends.

[1] Yuan, H. ; Li, F. ; Wei, Y. ; Zhu, J. : Novel Linearized Power Flow and Linearized OPF Models for Active Distribution Networks With Application in Distribution LMP. In: IEEE Transactions on Smart Grid 9 (2018).

[2] A. Jambagi, M. Kramer and V. Cheng, "Residential electricity demand modelling: Activity based modelling for a model with high time and spatial resolution," *2015 3rd International Renewable and Sustainable Energy Conference (IRSEC)*, Marrakech, 2015, pp. 1-6.

hynet: A Python-Based Open-Source Optimal Power Flow Framework for Hybrid AC/DC Power Grids

M. Hotz[a], J. Sistermanns, V. Bode, M. Mitterer, C. Wahl, Y. He, W. Utschick[b]

[a]matthias.hotz@tum.de, [b]utschick@tum.de

Optimal power flow (OPF) denotes the problem of identifying the cost-optimal allocation of generation resources (dispatch) and the corresponding state of the power grid to serve a given load, considering a steady-state model of the grid as well as system constraints. The computation of the OPF is central to various tasks, from operational and grid expansion planning to techno-economic studies.

Traditionally, power grids are three-phase alternating current (AC) systems and, correspondingly, OPF tools typically consider a (single-phase equivalent) steady-state AC model. However, due to the recent advances in power electronics, high-voltage direct current (HVDC) systems are increasingly incorporated into existing systems, with applications ranging from point-to-point HVDC systems for long-distance or underwater links to the consideration of multi-terminal voltage source converter (VSC) HVDC systems for the connection of offshore wind farms. These structural changes necessitate new OPF tools that incorporate appropriate models for converters and DC grids to consider these subsystems in the OPF decision-making process.

Besides this need for a more elaborate model, there is also a need for efficient OPF solution methods. The OPF problem constitutes a nonconvex quadratically constrained quadratic program (QCQP), which is often badly conditioned and comprises thousands of optimization variables in case of real-world systems. Recently, there has been a lot of research on convex relaxation of the OPF problem to a semidefinite program (SDP) or a second-order cone program (SOCP), which renders it amenable to polynomial time solution methods. While the relaxation restricts applicability to a certain class of systems, it can significantly improve computational efficiency in those cases.

Based on our previous research on optimal power flow methods, we developed *hynet*, an optimal power flow framework for hybrid AC/DC grids. *hynet* is written in Python, a popular programming language that is freely available, open source, and well suited for scientific computing. *hynet* was designed with a focus on ease of use, while offering different solution methods and providing an adequate modeling depth for proper results. Furthermore, *hynet* introduces a database-driven data format to store infrastructural as well as scenario-related data for hybrid AC/DC grids. Concluding, some key aspects shall be highlighted.

System Model

- AC and DC subgrids
- Transformers, lines, cables:
  - Steady-state π-equivalent model
- Generators, flexible loads, prosumers:
  - Convex piecewise lin. cost function
  - Polyhedral capability region
- Converters:
  - AC/DC, DC/AC, DC/DC, AC/AC
  - Static and dynamic losses
  - Reactive power capability
  - Polyhedral capability region
- Shunt compensators

System Constraints

- Physical limitations:
  - Voltage magnitude
  - Ampacity
  - Injector capability
  - Injector power factor
  - Converter capability
- Stability-related limitations:
  - Voltage angle difference
  - Voltage drop

Solution Methods

- Nonconvex QCQP:
  - IPOPT (via CYIPOPT)
  - PYOMO
- SDP:
  - MOSEK
  - CVXPY
- SOCP:
  - MOSEK
  - CVXPY

hynet will soon be released as open-source software via GitHub.

Influence of the free volume holes probed by positron annihilation lifetime spectroscopy (PALS) on various properties of the proton exchange membrane

Mahmoud M. Gomaa[a] ,Christoph Hugenschmidt[b], Marcel Dickmann[c], Esam E. Abdel-Hady[d], Hamdy F. M. Mohamed[e] and Mohamed O. Abdel-Hamed[f]

[a] mahmoud.gomaa@frm2.tum.de , [b] Christoph.Hugenschmidt@frm2.tum.de , [c] Marcel.Dickmann@frm2.tum.de, [d]esamhady@yahoo.com , [e]hamdy.farghal@mu.edu.eg, [f]mazosman2005@yahoo.com .

Recently, fuel cells are supposed to be a future source of energy due to their capability in many applications, ranging from portable devices to large scale power plants with appropriate fuel cell type. Fuel cells provide a clean power source, but still many challenges remain in further commercializing. One of the challenges of fuel cell production is the components cost, mainly the electrodes and electrolyte. Many studies have been conducted to investigate new, low-cost materials in order to reduce the overall manufacturing costs.

In this study, polyvinyl alcohol (PVA) was cross-linked with sulfosuccinic acid (SSA) in addition to thermal crosslinking at 100 °C to obtain a proton exchange membrane (PEM) using a casting method. Such PEMs are used in different fields of fuel cell applications. Many important properties such as the permeability of gases and small molecules through PEMs are thought to be strongly related to the nano-size holes of the free volume. The size and distribution of the nanoholes in PEMs can be determined using positron annihilation lifetime spectroscopy (PALS), which is a non-destructive and very sensitive technique to determine directly the polymeric material's free volume and the void size distribution. PALS is based on the time difference measurement between positron implantation into the material and the emission of the annihilation radiation.

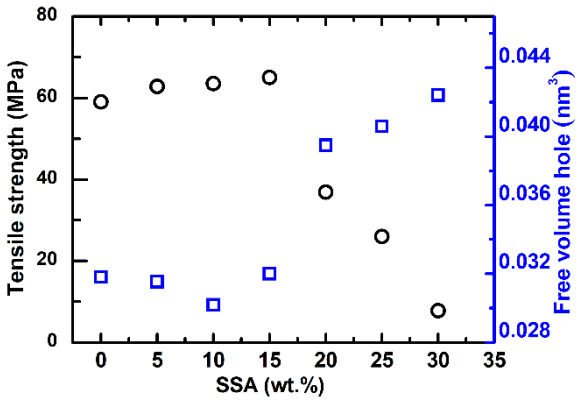

Figure 1: Tensile strength and free volume hole size of PVA/SSA membrane as a function of SSA concentration at room conditions (25 ° C and 30 - 35 % RH).

There is a good correlation between the tensile strength and the free volume hole size as shown in Figure1. A larger free volume reduces the interactions between polymer molecules resulting in a flexible membrane structure with lower tensile strength. This indicates that the mechanical properties of the prepared membranes could be controlled with the free volume size which is shown to agree with the free volume model.

The o-Ps lifetime, which is measured to obtain the size of the hole and the hole size distribution (Fig. 2), was studied at different relative humidity (RH) at room temperature. It was observed that, at low humidity, i.e., below 30 RH%, water molecules begin to fill the intermolecular spaces in the membrane. This leads to a decreasing probability of the positron pick-off annihilation, resulting in a slight decrease in the average value of holes size. On the other side, due to the hydrophilic nature of the PVA, when the humidity is more than 30% RH, plasticizing effect of water leads to hole expansion of the membranes this appeared at increasing the average value of holes size.

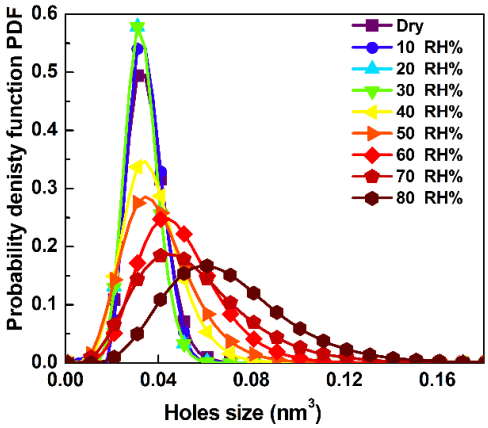

Figure 2: Probability density function (PDF) vs. holes size for PVA/SSA (15 wt.%) membrane at different RH

The free volume properties were investigated by PALS at room conditions and under various relative humidity (RH). The prepared membranes exhibited a strong correlation between water uptake, ionic conductivity, tensile strength and the mean void size.

Active Nanostructured PEM Fuel Cell Oxygen Reduction Reaction Catalysts Produced by Cathodic Corrosion

Johannes Fichtner[a], Sebastian Watzele[b], Batyr Garlyyev[c] and Aliaksandr S. Bandarenka[d]

[a]johannes.fichtner@tum.de, [b]s.watzele@tum.de, [c]ga48yed@mytum.de, [d]bandarenka@ph.tum.de

Automotive industry is undergoing a revolution as consumers are starting to consider electric engines powered by either fuel cells or batteries as competitors to the classical combustion engines. Hence, in the field of fuel cell catalysis, the demand for stable, affordable and easily producible catalysts for the oxygen reduction reaction is stronger than ever. Today's research focusses mainly on the improvement of the well-known bottom up synthesis of Pt nanoparticles and their alloys, which includes multiple-step procedures and high processing efforts.[1,2] Contrary to this, we are reporting a facile way to prepare Pt nanoparticles and alloys (Cu, Ni, Co) with at least 2-fold increased specific activity (~1.4 $mAcm^{-2}$ for 3 nm sized Pt particles at 0.9 V vs. RHE, cf. figure 1) compared to commercial ones, while reducing synthetical complexity and costs by several factors using cathodic corrosion, as described by Marc Koper's group.[3] By alternating application of a high anodic and cathodic potential (>4V vs. Pt pseudo-reference) to a platinum wire, immersed into an alkali-metal cation containing electrolyte, Pt nanoparticles are generated on the surface of the bulk metal and released into the electrolyte subsequently. Moreover, the technique enables size control (by the applied potential window) allowing optimization of the stability and activity. The high increase in activity is most likely caused by the generation of not only conventional convex shaped particles, but rather unique shapes including concavities with high-index facets and improved amount of particularly active sites.[4] Considering the high effort of producing concave shaped particles with similar activity synthetically[5], the facile particle production by cathodic corrosion reveals it's potential to prepare future electrocatalysts.

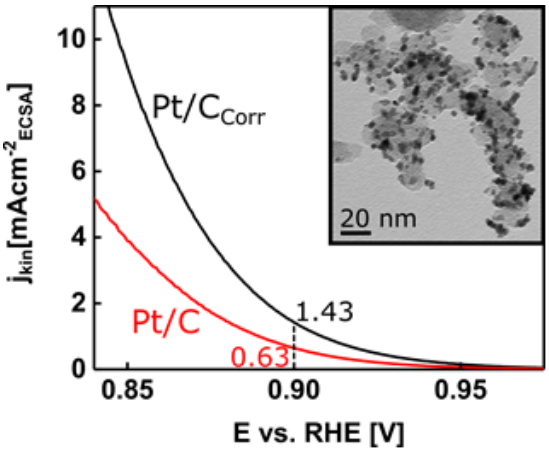

Figure 1: Kinetic current densities of Pt nanoparticles produced by cathodic corrosion (Pt/C_{Corr}) compared to commercial ones (Pt/C, Tanaka TEC10V20E) and transmission electron microscopy image of Pt nanoparticles supported on Vulcan XC 72R (insert).

[1] S.-H. Yu, Doubling up the activity of fuel cell catalysts, National Science Review, 4, 2017, 513–514.
[2] B. D. James, J. M. Huya-Kouadio C. Houchins, D. A. DeSantis, Mass Production Cost Estimation of Direct H_2 PEM Fuel Cell Systems for Transportation Applications: 2016 Update, Strategic Analysis Inc., 3, 2017, 93-98.
[3] A. I. Yanson, P. Rodriguez, N. Garcia-Araez, R. V. Mom, F. D. Tichelaar, M. T. M. Koper, Cathodic Corrosion: A Quick, Clean, and Versatile Method for the Synthesis of Metallic Nanoparticles, Angew. Chem. Int. Ed., 50, 2011, 6346 –6350.
[4] F. Calle-Vallejo, J. Tymoczko, V. Colic, Q. Huy Vu, M. D. Pohl, K. Morgenstern, D. Loffreda, P. Sautet, W. Schuhmann, A. S. Bandarenka, Finding optimal surface sites on heterogeneous catalysts by counting nearest neighbors, Science, 350, 2015, 185-189.
[5] T. Yu, D. Y. Kim, H. Zhang, and Y. Xia, Platinum Concave Nanocubes with High-Index Facets and Their Enhanced Activity for Oxygen Reduction Reaction, Angew. Chem. Int. Ed., 50, 2011, 2773 –2777.

Reconsidering Water Electrolysis: Producing Hydrogen at Cathodes Together with Selective Oxidation of *n*-Butylamine at Anodes

Song Xue[a], Sebastian Watzele, Viktor Čolić, Batyr Garlyyev, Kurt Brandl, and Aliaksandr S. Bandarenka

[a]song.xue@tum.de

Electrocatalysis for the oxygen evolution reaction (OER) is of great interest for improving the effectiveness of water splitting devices. Decreasing the anodic overpotential and simultaneously changing the anodic reaction selectively to produce valuable chemicals instead of O_2 would be a major improvement of the overall cost efficiency. Some amines, when present in aqueous electrolytes, were recently shown to change the selectivity of the anodic process to generate H_2O_2 rather than O_2 on MnO_x at pH 10. This results in unusually high apparent "anodic activities". In this work, industrially relevant OER catalysts, oxyhydroxides of cobalt (CoO_x), nickel-iron ($NiFeO_x$), and nickel (NiO_x) all show more pronounced effects. Moreover, as anodes they also selectively catalyzed the production of *n*-butyronitrile from *n*-butylamine at higher pH as an easily retrievable valuable product (Figure 1). The pH dependence of the activity was investigated at pH values closer those at which alkaline electrolyzers operate. The highest activities were observed for NiO_x thin-film electrodes at pH 12 in the presence of 0.4 m *n*-butylammonium sulfate, without poisoning the active sites of Pt electrocatalysts at the hydrogen evolution electrode. ^{1}H NMR spectroscopy showed that *n*-butylamine is selectively oxidized to *n*-butyronitrile, an organic chemical with numerous applications (Figure 2). However, measurements using rotating ring-disk electrodes also indicated that some H_2O_2 is also generated at the surface of the oxide anodes.

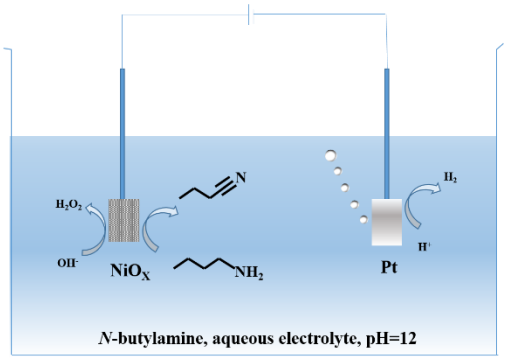

Figure 1: In electrocataltic water splitting devices, decreasing anodic overpotential and simultaneously changing the anodic reaction to produce valuable chemicals instead of O_2 would be a major improvement in overall cost efficiency.

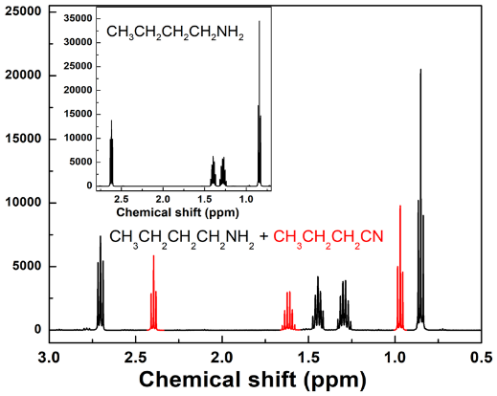

Figure 2: Shows the ^{1}H-NMR spectrums after running the experiment for 48h. Inset of the graph shows the ^{1}H-NMR spectrum before the start of the experiment. Shifts corresponding to the butyronitrile are shown in red color.

*Xue, S.; Watzele, S.; Čolić, V.; Brandl, K.; Garlyyev, B.; Bandarenka, A. S. Reconsidering water electrolysis: producing hydrogen at cathodes together with selective oxidation of n-butylamine at anodes. *ChemSusChem* **2017**, *10*, 4812-4816.

What can electrochemical scanning tunneling microscopy reveal for heterogeneous catalysis?

Y. Liang[a], J.H.K. Pfisterer[b], O. Schneider[c], D. McLaughlin[d], C. Csoklich[e], E. Mitterreiter[f], A.S. Bandarenka[g]

[a]yunchang.liang@tum.de, [b]jonaspfisterer@googlemail.com, [c]oliver_m.schneider@tum.de, [d]david.mclaughlin@tum.de, [e]christoph.csoklich@tum.de, [f]Elmar.Mitterreiter@wsi.tum.de, [g]bandarenka@ph.tum.de

Scanning tunneling microscopy (STM) has been utilized as a sufficient surface topographic tool in the past decades. The events undergoing on the surface or at the interface, especially for heterogeneous catalytic reactions can be locally revealed using tunneling current which depends on several factors (tip-sample distance, surface electronic structure, tunneling medium, etc.)[1, 2]. The catalytic activity of a heterogeneous catalyst is determined by the electronic structure of active centers with optimal adsorption properties for the corresponding reaction intermediates. The knowledge of the properties of the active centers is one of the key factors of fundamental understanding and design of heterogeneous catalyst materials. The "coordination-activity plots" using theoretical calculations predict the geometric structure of optimal active sites[3]. A direct instrumental method capable of locating the catalytic active sites on the sub-nanometer scale under reaction conditions is needed.

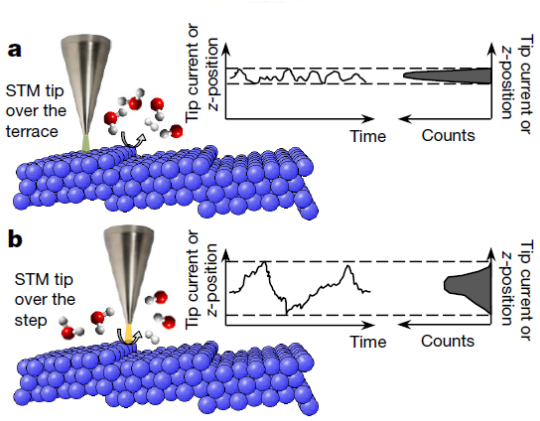

Figure 1: A scheme explaining the concept. Under reaction condition, the tip scans over a non-active site, a, versus an active site, b, the tunneling barrier changes over time. In this scenario, increased tunneling-current noise is likely to appear when the tip is over the active site. Adapted from ref. 4.

Here we demonstrate that during given reactions electrochemical STM can capture 'unexpected' tunneling current disturbances on active centers while scanning over the electrode surfaces, which can locate the active centers[4]. The disturbances are expected to be caused by the catalytic reactions that take place at the active sites, where the relatively stronger disturbances should appear consequently. Hydrogen evolution and oxygen reduction reactions at various model catalyst electrodes in aqueous media involved in the future energy provision.

The proved methodology was applied to investigate other catalytic systems where the activity contributions of different surface sites are not clear, namely oxygen reduction and hydrogen evolution reactions on Pt single crystals in alkaline media[5], and non-metal water-splitting catalysts, transition metal dichalcogenides[6].

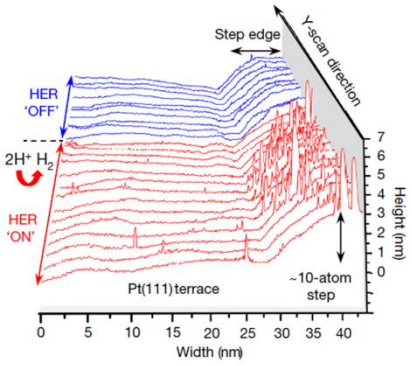

Figure 2: STM line scans obtained over a Pt(111) surface for hydrogen evolution reaction ON and OFF in 0.1 M HClO4. Adapted from ref. 4.

1, Möller, R., Esslinger, A. & Koslowski, B. Appl. Phys. Lett. 55, 2360-2362 (1989).
2, Zambelli, T., Wintterlin, J., Trost, J. & Ertl, G. Science 273, 1688 (1996).
3, F. Calle-Vallejo, J. Tymoczko, V. Colic, Q. H. Vu, M. D. Pohl, K. Morgenstern, D. Loffreda, P. Sautet, W. Schuhmann, & A. S. Bandarenka. Science, 350, 185-189 (2015).
4, J. H. K. Pfisterer, Y. Liang, O. Schneider, & A. S. Bandarenka. Nature, 549, 74. (2017).
5, D. Mclaughlin, Y. Liang, C. Csoklich, A. S. Bandarenka. In preparation.
6, Y. Liang, E. Mitterreiter, C. Csoklich, U. Wurstbauer, A. Holleitner, A. S. Bandarenka. In preparation.

Self-limiting Cu deposition on Pt by hydrogen displacement - first steps towards a scalable nanoparticle synthesis

P. A. Loichet[a], H. A. El-Sayed[b], J. N. Schwämmlein[c], H. A. Gasteiger[d]

[a] paulette.loichet@tum.de,[b] hany.el-sayed@tum.de, [c] jan.schwämmlein@tum.de, [d] hubert.gasteiger@tum.de

The development of highly active electrocatalysts for the anodic and cathodic reactions involved in both electrolyzers and fuel cells has been widely proposed as a strategy to reduce the Pt loading in the membrane electrode assembly (1, 2). Among other Pt alloy catalysts, Cu-Pt(111) near-surface alloys (NSAs) were shown to have a significantly higher activity towards the oxygen reduction reaction (ORR) and the hydrogen evolution reaction (HER) compared to monometallic Pt (3, 4). These NSAs, in particular, have only been prepared as model surfaces on bulk Pt electrodes using electrochemical techniques that involve the use of a potentiostat, forming a structure shown in Fig. 1 (c). However, in order to test their activity and stability in an actual fuel cell or electrolyzer, a scalable method to obtain NSA nanoparticles on a suitable support has to be developed. Hence, our work proposes a new scalable synthesis method for Cu-Pt NSA nanoparticles supported on carbon (Cu-Pt/C) as a catalyst for the ORR and the HER.

First, one monolayer (ML) of Cu is deposited on the Pt surface of a commercially available Pt/C catalyst. In contrast to common copper underpotential deposition (Cu_{upd}) techniques that require potential control to establish a copper monolayer, the method presented here is solely based on the displacement of hydrogen chemisorbed on the Pt surface, and therefore provides an easily scalable synthesis route without the use of a potentiostat. Subsequently, the NSA structure can be formed by annealing of the Cu-Pt/C in H_2 atmosphere. As a proof of concept, experiments were performed on polycrystalline Pt and a thin film of Pt/C in a rotating disk electrode (RDE) setup. Presented in Fig. 1 (a), the open circuit potential (OCP) transients were recorded to monitor the deposition of Cu on Pt from a solution containing Cu ions, while purging H_2 at different concentrations. As a dilute mixture of H_2 enters the system, the OCP of the Pt electrode decreases, thereby promoting the underpotential deposition of Cu. Stripping CVs were then used to quantify the Cu coverage on the Pt surface. For both polycrystalline Pt and Pt/C, copper coverages of essentially 1 ML can be obtained reliably and remain constant over time, suggesting a self-limiting Cu_{upd} process controlled by hydrogen gas rather than by means of potentiostatic control (Fig. 1 (b)). The scale-up of the synthesis for the preparation of larger amounts of catalyst is currently being developed. Preliminary results on the first Cu-Pt NSA nanoparticles synthesis based on this process will also be shown.

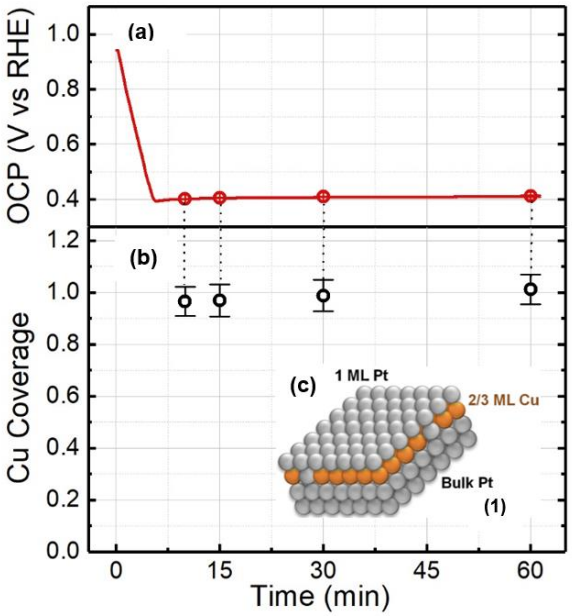

Figure. 1 (a) OCP transient on a Pt/C thin film RDE electrode on a Cu^{+2} solution while purging with H_2. (b) Cu coverage determination at different times. (c) Cu-Pt NSA structure.

References
1.H. A. Gasteiger, S. S. Kocha, B. Sompalli and F. T. Wagner, Applied Catalysis B: Environmental, 56(1-2), 9–35 (2005).
2.M. Carmo, D. L. Fritz, J. Mergel and D. Stolten, International Journal of Hydrogen Energy, 38(12), 4901–4934 (2013).
3.I. E. L. Stephens, A. S. Bondarenko, F. J. Perez-Alonso, F. Calle-Vallejo, L. Bech, T. P. Johansson, A. K. Jepsen, R. Frydendal, B. P. Knudsen, J. Rossmeisl and I. Chorkendorff, Journal of the American Chemical Society, 133(14), 5485–5491 (2011).
4.J. Tymoczko, F. Calle-Vallejo, W. Schuhmann and A. S. Bandarenka, Nature communications, 7, 10990 (2016).

M-N-C materials: cheap electrocatalysts for the Oxygen Reduction Reaction

D. Menga[a], H.A. Gasteiger, T.-P. Fellinger

[a]davide.menga@tum.de

One of the major hindrances to mass commercialization of low-temperature proton-exchange-membrane fuel cells (PEMFCs) is the considerable amount of expensive Pt required, especially at the cathode side, where the oxygen reduction reaction (ORR) takes place.[1]
Metal-nitrogen-doped carbons (M-N-Cs, M = Fe, Co) currently are the most promising platinum-group-metal-free (PGM-free) catalysts and developments in the last ten years have narrowed the gap towards Pt, making them meet the requirements for practical applications.[2-4]
Furthermore, spectroscopic investigations have given strong evidences that the active site for these catalysts is a biomimetic MN_4 feature.[5] Although synthesis protocols have been successfully optimized, obtaining catalysts with increased concentration of such sites is a herculean task. Current methods yield significant amounts of inorganic iron compounds as byproducts and so multiple processing steps are required, making the preparation time-consuming.
Recently, our group introduced a new mild synthetic procedure that decouples the active site formation from the pyrolytic carbonization step.[6] A wet-chemical metal-coordination step is herein employed to form the active site that was previously imprinted into the carbon via carbonization inside a molten Mg^{2+} salt.
Following this work, we now present the synthesis of M-N-Cs catalysts obtained with high carbon yield (up to 70%) starting from cheap precursors. Different molten salts are used allowing to tune the carbon porosity and BET surface area (up to 2756 m^2/g). The resulting active-site imprinted nitrogen doped carbons are then used in the metal-coordination step at low temperature to form the ORR-active MN_4 site (M = Fe, Co). In the presented poster the activity of the materials tested in a rotating disk electrode (RDE) setup will be related to the active site concentration (Figure 1).

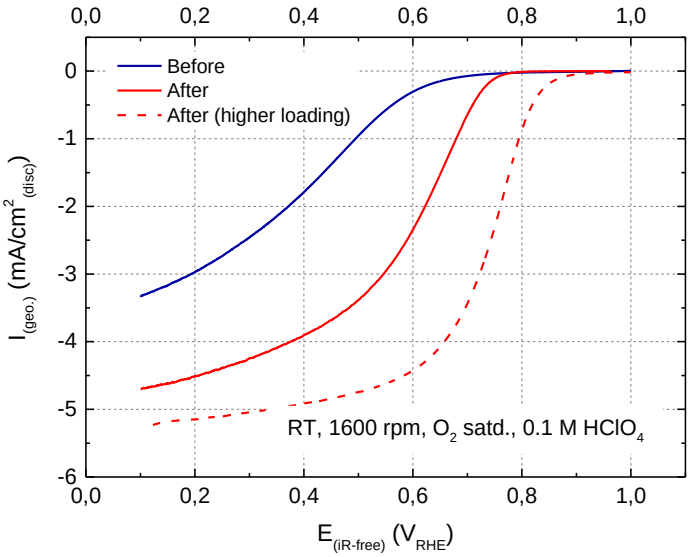

Figure 1: Rotating disc electrode (RDE) measurment of one exemplary sample before and after metal-coordination step

References:
1. A. Kongkanand and M. F. Mathias, *J. Phys. Chem. Lett.*, 2016, 7, 1127-1137.
2. M. Lefèvre, E. Proietti, F. Jaouen and J.-P. Dodelet, *Science*, 2009, 324, 71-74.
3. R. Bashyam and P. Zelenay, *Nature*, 2006, 443, 63.
4. H. A. Gasteiger, S. S. Kocha, B. Sompalli and F. T. Wagner, *Appl. Catal., B*, 2005, 56, 9-35.
5. Q. Jia, N. Ramaswamy, U. Tylus, K. Strickland, J. Li, A. Serov, K. Artyushkova, P. Atanassov, J. Anibal, C. Gumeci, S. C. Barton, M.-T. Sougrati, F. Jaouen, B. Halevi and S. Mukerjee, *Nano Energy*, 2016, 29, 65-82.
6. A. Mehmood, J. Pampel, G. Ali, H. Y. Ha, F. Ruiz-Zepeda and T.-P. Fellinger, *Advanced Energy Materials*, DOI: 10.1002/aenm.201701771, 1701771-n/a.

Origin of Superior Activity of Ru@Pt Core-Shell Nanoparticles towards HOR/HER in Alkaline Media

B. M. Stühmeier[a], J. N Schwämmlein, K. Wagenbauer, H. Dietz, V. Tileli, H. A. El-Sayed, H. A. Gasteiger[b]

[a]bjoern.stuehmeier@tum.de, [b]hubert.gasteiger@tum.de

Unlike in acid, the kinetics of the hydrogen oxidation reaction (HOR) and hydrogen evolution reaction (HER) in alkaline media are slow and therefore require large amounts of platinum, the most commonly used metal for fuel cell applications. Decreasing the required Pt amount can be achieved by using Pt-Ru alloys which in alkaline electrolyte exhibit an exceptionally high HOR activity, compared to Pt/C.[1-2] However, it remains unknown whether this enhancement is due to a bifunctional mechanism involving both Pt and Ru as active sites or an electronic effect of Ru on Pt. In this study,[3] we distinguish between those fundamental differences using Ru@Pt core-shell nanoparticles as a model system (Figure 1).

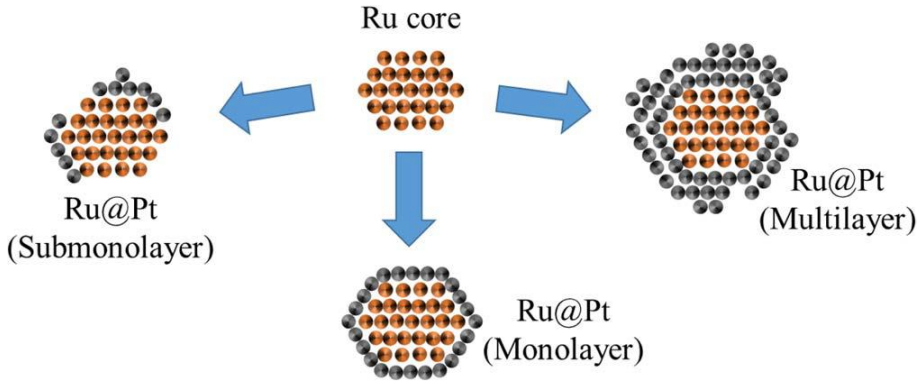

Figure 1: Schematic of Ru@PT core-shell nanoparticles with different Pt-shell thickness on a Ru particle.

Ru@Pt catalysts were prepared from submonolayer to multilayer Pt-coverage. The exposure of Ru on the surface of the catalyst was analyzed by cyclic voltammetry in 0.1 M H_2SO_4, showing that exclusively on Ru@Pt particles with a low Pt-coverage Ru is exposed on the surface. Determining the HOR/HER activity of these catalysts in 0.1 M NaOH revealed that fully Pt-covered Ru is more active than partially covered Ru@Pt nanoparticles. Hence, the participation of Ru as active site in a bifunctional mechanism is of minor importance with respect to the HOR/HER activity compared to its influence on the electronic structure of Pt. Similar to Pt-Ru alloys, the most active Ru@Pt core-shell nanoparticles show a 4 to 5-fold enhancement of the surface-normalized HOR/HER activity compared to Pt/C.

References

1. K. Elbert, J. Hu, Z. Ma, Y. Zhang, G. Chen, W. An, P. Liu, H. S. Isaacs, R. R. Adzic, and J. X. Wang, *ACS Catal.*, **5**, *6764* (2015).
2. S. St. John, R. W. Atkinson, R. R. Unocic, T. A. Zawodzinski, and A. B. Papandrew, *J. Phys. Chem. C*, **11**9, *13481* (2015).
3. J. N. Schwämmlein, B. M. Stühmeier, K. Wagenbauer, H. Dietz, V. Tileli, H. A. Gasteiger, H. A. El-Sayed, *J. Electrochem. Soc.*, **165**, *H229* (2018).

Screening of Transition-Metal-Substituted ZrO_2 on Carbon Black as PGM-free ORR Catalysts for PEMFCs

Kevin Krempl[a], Davide Menga, Pankaj Madkikar, Hubert A. Gasteiger and Michele Piana

[a]kevin.krempl@tum.de

Low-temperature proton-exchange-membrane fuel cells (PEMFCs) are promising energy conversion devices. However, a high amount of scarce and expensive Pt-based catalysts is required at the cathode side to facilitate the oxygen reduction reaction (ORR) and this is viewed as a major hurdle on the way to mass commercialization. Therefore, many efforts have been made to reduce or completely replace platinum in PEMFCs. So far, the best platinum-group-metal (PGM)-free catalysts reported are MC_yN_X (M = Fe/Cu/Co)[1] with activities approaching those of platinum. These catalysts are inexpensive but lack reasonable long-term durability in acidic environment.

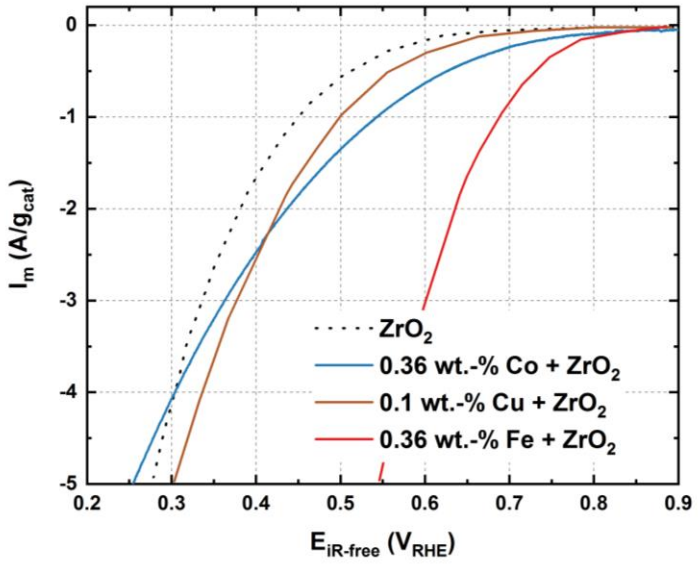

Figure 1: ORR mass activity from thin-film RDE analysis of selected samples of Co+ZrO_2, Cu+ZrO_2, Fe+ZrO_2, and ZrO_2 catalysts supported on graphitized KB.

Approaching the search for active, durable and inexpensive catalysts for PEMFCs, from the stability aspect our group has developed catalysts based on ZrO_2[2][3], a non-reducible and intrinsically stable oxide in acidic environment. Whereas large particles of pure zirconia show no ORR activity, nanoparticles obtained from phthalocyanine zirconium complexes are active catalysts for the ORR. In literature it is further reported that, besides nanoscaling, also doping with aliovalent cations enables the reducibility of zirconia leading to the formation of oxygen vacancies[4], which are hypothesized to be ORR active sites[5][6]. Recent work of our group has shown that Fe-ion doping of zirconia indeed leads to an increased ORR activity and, as shown by DFT+U calculations, also to oxygen vacancies on the surface, hence rationalizing the observed activity increase[7]. Motivated by these findings, further dopants such as Cu- and Co-ions were examined.

The catalysts were prepared by impregnation of soluble metal (Zr/Fe/Co/Cu) phthalocyanines on carbon black (graphitized Ketjenblack) followed by heat treatment. By variation of the dopant loading (0.1-5.0 wt%) and of the heat treatment temperature (700-900°C), the most active samples for each dopant were determined. X-ray diffraction was used to structurally characterize the samples. Furthermore, cyclic voltammetry on thin-film (70-76 $\mu g_{cat}/cm^2$) rotating disc electrode (RDE) was employed to determine the ORR activities of the samples at room temperature in O_2-saturated 0.1 M $HClO_4$ electrolyte at 1600 rpm. Figure 1 shows the increase in mass activity for Fe+ZrO_2, Co+ZrO_2 and Cu+ZrO_2 catalysts compared to pure ZrO_2.

References:

[1] J.-P. Dodelet in *N4-Macrocyclic Metal Complexes* (Eds.: J. Zagal, F. Bedioui, J.-P. Dodelet), Springer New York, **2006**

[2] T. Mittermeier et al., *Journal of The Electrochemical Society*, **2016**, 163 (14), F1543-F1552

[3] P. Madkikar et al., *J. Nanostructure Chem.*, **2017**, 7, 133

[4] A. R. Puigdollers et al., *ACS Catalysis*, **2017**, 7(10), 6493-6513

[5] A. Ishihara et al., *The Journal of Physical Chemistry C*, **2013**, 117, 18837-18844

[6] Y. Ohgi et al., *Journal of The Electrochemical Society*, **2013**, 160, F162-F167

[7] P. Madkikar, D. Menga, G. Harzer, T. Mittermeier, A. Siebel, F. E. Wagner, M. Merz, S. Schuppler, P. Nagel, A.B. Muñoz-García, M. Pavone, H. A. Gasteiger, M. Piana, *manuscript in preparation*

Nanometric $Fe_xZr_{1-x}O_{2-\delta}$ on Carbon Black - A Novel PGM-Free ORR Catalyst for PEMFC

Davide Menga[a], Pankaj Madkikar, Gregor Harzer, Thomas Mittermeier, Armin Siebel, Friedrich E. Wagner, Michael Merz, Stefan Schuppler, Peter Nagel, Ana Belen Muñoz-García,Michele Pavone, Hubert A. Gasteiger and Michele Piana

[a]davide.menga@tum.de

The dependence from Platinum-Group-Metal (PGM) catalysts is one of the major hindrance towards the commercialization of Proton Exchange Membrane Fuel Cells (PEMFCs), due to the limited availability of PGM and their considerable loading required for the Oxygen-Reduction-Reaction (ORR), increasing their cost contribution to the overall system. On the other hand, the challenges for PGM-free ORR catalysts are an activity approaching that of Pt and a long-term operational stability in the strong acidic environment of a PEMFC.

Low-cost FeNC catalysts fulfill the high activity requirement, but they still face degradation issues in acidic environment [1, 2]. On the contrary, pure valve metal oxides as PGM-free ORR catalysts need a significant improvement in ORR activity and H_2O yield but they are very promising in terms of their stability during PEMFC operation.[3, 4]

The aim of this contribution is the combination of the intrinsic high ORR activity of Fe with the stability of valve-metal oxides, via partial substitution of Zr^{4+} with Fe^{3+} in the ZrO_2 structure.[5] As confirmed by theoretical calculation, the formation of a solid solution of oxides of the two aliovalent metals also provides oxygen vacancies or uncoordinated metal sites at the oxide surface, hypothesized to be correlated to an increased ORR activity of valve-metal oxides.[6, 7]

Fe-substituted ZrO_2 was synthesized as described in [8, 9]. XRD and TEM characterizations show that our catalysts consist of nanometric ZrO_2 particles. Mössbauer spectroscopy reveals that the Fe moieties are isolated and in Fe^{3+} electronic configuration at high spin, typical of an oxidic environment. This is confirmed by soft XAS data at the Fe L-edge and XPS data, pointing towards the desired $Fe_xZr_{1-x}O_{2-\delta}$ phase.

Thin-film rotating (ring) disk electrode (R(R)DE) was employed to evaluate the ORR mass activity and H_2O_2 yield of the preferred catalyst $Fe_{0.07}Zr_{0.93}O_{2-\delta}$ as a function of loading. The catalyst mass activity and its Arrhenius analysis in a single PEMFC at ≈0.4 mg_{cat}/cm^2 is compared to the RDE results (Figure 1).[10] The Arrhenius analysis resulted in an ORR activation energy of 16 kJ/mol (RDE) and 18 kJ/mol (PEMFC) at 0.4 V_{RHE}, significantly lower than our best pure-ZrO_2 catalyst reported (21 kJ/mol from RDE and 29 kJ/mol from PEMFC data).[4]

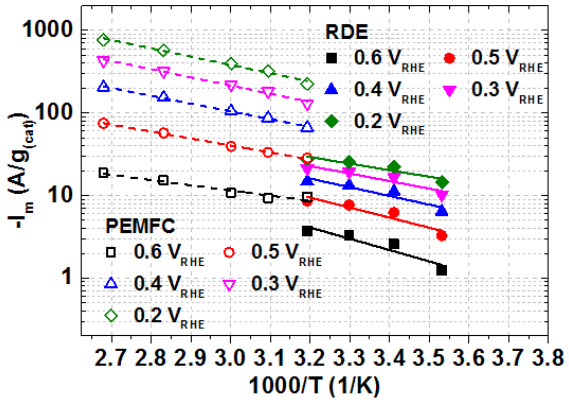

Figure 1: Arrhenius plot of $Fe_{0.07}Zr_{0.93}O_{2-\delta}$ at various potentials from RDE data (0.1 M $HClO_4$, 1600 rpm, O_2 satd.) and PEMFC data (0.383 mg_{cat}/cm^2, 5 cm^2, 400/400 nccm H_2/O_2, 90%

References:

[1] M. Lefèvre, J. P. Dodelet, *ECS Transactions* **2012**, *45(2)*, 35-44.

[2] B. Piela, T. S. Olson, P. Atanassov, P. Zelenay, *Electrochimica Acta* **2010**, *55*, 7615-7621.

[3]A. Ishihara, S. Yin, K. Suito, N. Uehara, Y. Okada, Y. Kohno, K. Matsuzawa, S. Mitsushima, M. Chisaka, Y. Ohgi, M. Matsumoto, H. Imai, K. Ota, *ECS Transactions* **2013**, *58*, 1495-1500.

[4] T. Mittermeier, P. Madkikar, X. Wang, H. A. Gasteiger and M. Piana, *J. Electrochem. Soc.* **2016**, *163*, F1543-F1552.

[5] D. Sangalli, A. Lamperti, E. Cianci, R. Ciprian, M. Perego, A. Debernardi, *Phys. Rev. B* **2013**, *87*, 085206.

[6] A. Ishihara, M. Tamura, Y. Ohgi, M. Matsumoto, K. Matsuzawa, S. Mitsushima, H. Imai, K.-i. Ota, *J. Phys. Chem. C*, **2013**, *117*, 18837–18844.

[7] Y. Ohgi, A. Ishihara, K. Matsuzawa, S. Mitsushima, K.-i. Ota, M. Matsumoto, H. Imai, *J. Electrochem. Soc.* **2013**, *160*, F162-F167.

[8] P. Madkikar, X. Wang, T. Mittermeier, A. H. A. Monteverde Videla, C. Denk, S. Specchia, H. A. Gasteiger, M. Piana, *J. Nanostruct. Chem.* **2017**, *7*, 133-147.

[9] P. Madkikar, T. Mittermeier, H. A. Gasteiger, M. Piana, *J. Electrochem. Soc.* **2017**, *164(7)*, F831- F833.

[10] P. Madkikar, D. Menga, G. Harzer, T. Mittermeier, A. Siebel, F. E. Wagner, M. Merz, S. Schuppler, P. Nagel, A.B. Muñoz-García, M. Pavone, H. A. Gasteiger, M. Piana, *manuscript in preparation*.

Efficiency comparison of control methods for geothermal pump motors

Julian Kullick[a], Christoph M. Hackl[b]

[a]julian.kullick@tum.de, [b]christoph.hackl@tum.de

Motivation

Electric submersible pumps (ESP), which are usually deployed in deep geothermal power applications, are subject to high thermal stress, since being immersed in hot geothermal fluid, while the only way of cooling is to transfer the heat to the hot fluid flowing along the motor casing. As heat is generated by inefficient operation of the pump motor (electric power losses are converted into heat), it is important to maximize the motor efficiency as to reduce the thermal stress and, thus, increase the motor lifetime. Moreover, improving motor efficiency saves cost during normal operation of the geothermal power plants.

Control methods

ESP motors (three-phase AC induction motors) in geothermal power applications are typically controlled by applying a three-phase sinusoidal voltage with a fixed ratio of voltage amplitude and frequency, which is also known as *V/f-control*. This approach is very robust and does not require a speed sensor, making it particularly interesting for applications where the motor is deployed in harsh environments. However, the potential for efficiency improvement is very low and the speed reference is not accurately tracked, since the slip of the asynchronous motor causes a deviation of the motor speed from the electrical frequency.

An alternative might be the widespread industry standard known as *field-oriented control (FOC)*. Unlike V/f-control it allows precise control of the motor currents, torque and speed, respectively. However, measuring or estimating the motor speed is essential for FOC, which is the major drawback. Measurements have shown, though, that compared to V/f-control, FOC is more efficient in most operating points (up to several percent, see Fig. 1) and, hence, could be a viable alternative for the control of ESP motors in geothermal pump systems.

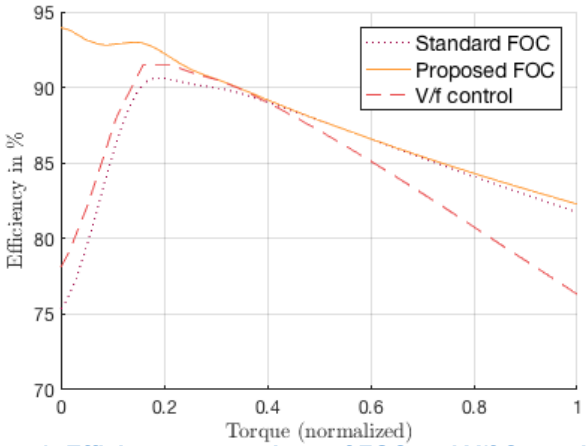

Figure 1: Efficiency comparison of FOC and V/f Control

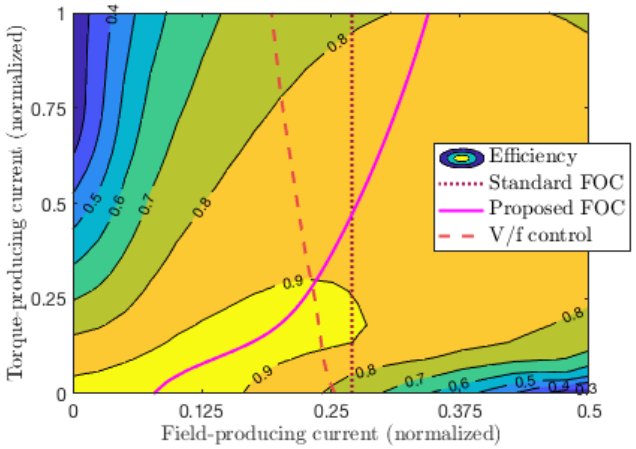

Figure 2: Current reference trajectories over efficiency

FOC improvement

FOC allows to independently control the motor magnetic field and motor torque, by controlling the parallel (d-axis) and perpendicular (q-axis) motor current components with respect to the motor magnetic field. Instead of fixing the magnetic field to a certain value (which is the standard approach), variation of the magnetic field may reduce the overall currents, required to set a certain torque. Measurements have been performed, to find out the optimum current references for a given torque reference to further improve the FOC efficiency. The current reference trajectories for each control strategy are depicted in Fig. 2.

The Potential of Hydrothermal Geothermal Resources for Power Production in Germany

Sebastian Eyerer[a], Christopher Schifflechner[b], Christoph Wieland[c], Hartmut Spliethoff[d]

[a] sebastian.eyerer@tum.de, [b] c.schifflechner@tum.de, [c] wieland@tum.de, [d] spliethoff@tum.de

The German energy market finds itself in a major transition due to the aim of significantly reducing the energy-induced emissions. In order to reach this target, the government aims to increase the amount of electricity produced by renewable resources and has introduced high guaranteed feed-in tariffs for technologies like wind energy, photovoltaics or geothermal energy. During the last years, photovoltaics and wind energy have increased their installed capacity rapidly, while the feed-in tariffs for these technologies reduced significantly at the same time. In contrast to the volatile power generation of photovoltaics and wind power, geothermal energy is a reliable and controllable source for power generation. Despite this large advantage of providing baseload capacity and currently high feed-in tariffs, the geothermal energy sector represents a very small part in the German energy market. Based on the experience gained by the successful installation and operation of the first geothermal power plants during the last years in Germany, the current technical and economic potential of the hydrothermal resources is investigated by a study of the Geothermal-Alliance Bavaria [1].

The analysis of the potential for the deployment of hydrothermal resources in Germany is carried out by an extensive analysis of the existing geothermal power plants. At the time, were the study was made, ten plants with an installed capacity of 41 MW_{el} were in operation. Seven of these plants also provide heat for district heating networks. Their cumulated installed thermal capacity is 142 MW_{th}. Based on the analysis of the existing plants in Germany, a model for the electric net system efficiency as a function of the thermal water temperature at the wellhead is developed.

The economic performance of the plants is investigated by the calculation of the levelized costs of electricity (LCOE) for each plant. Against the background of certain assumptions such as a project lifetime of 25 years, average electricity costs of 23.2 ct/kWh are derived. This is slightly lower than the current feed-in tariff for geothermal projects (25.2 ct/kWh). Based on these results, cost functions are developed, which calculate the LCOE in dependency of the wellhead temperature as well as the geological gradient of the region. The results show that the costs per kWh electricity are decreasing with higher wellhead temperatures in the range between 100 °C and 160 °C. For higher temperatures, the LCOE increase again. This can be explained by the exponential increase of drilling costs with higher drilling depths.

The theoretical potential (the exploitable amount of heat) of the hydrothermal geothermal resources is derived from literature for most of the investigated regions [2–4].

Based on the developed models to evaluate the technical and economic performance, both potentials can be calculated for each of the investigated regions. In summary, the results show that the current technical potential of the hydrothermal geothermal resources in Germany lies around 11.5 PWh_{el}. In addition, approximately 57.5 PWh_{th} could be used for district heating networks, considering the common characteristic of the combined heat and power production of the existing plants. Considering the current market situation, the economic potential amounts to 9.21 PWh_{el}. Arising from the requirement of a sustainable exploitation of the geothermal resources, an exploitation period of 1000 years is applied. By this, an annual technical potential of 11.5 GWh_{el}/a and an economic potential of 9.21 GWh_{el}/a is obtained.

[1] Eyerer S, Schifflechner C, Hofbauer S, Wieland C, Zosseder K, Bauer W et al. Potential der hydrothermalen Geothermie zur Stromerzeugung in Deutschland; 2017.

[2] Pfleiderer S, Götzl G, Bottig M, Brüstle AK, Porpaczy C, Schreilechner M et al. GeoMol - Geologische 3D-Modellierung des österreichischen Molassebeckens und Anwendungen in der Hydrogeologie und Geothermie im Grenzgebiet von Oberösterreich und Bayern. Abhandlungen der Geologischen Bundesanstalt 2016;80.

[3] Agemar T, Alten J-A, Kühne K, Kuder J, Suchi E, Weber Josef and Schulz, Rüdiger. A New Approach to Estimating the Geothermal Potential of Faults in Germany. In: Proceedings of the World Geothermal Congress, Australia, Melbourne; 2015.

[4] Paschen H, Oertel D, Grünwald R. Möglichkeiten geothermischer Stromerzeugung in Deutschland; 2003

Optimization of Organic Rankine Cycle Technology

Fabian Dawo[a], Sebastian Eyerer[b], Christoph Wieland[c], Hartmut Spliethoff[d]

[a] fabian.dawo@tum.de, [b] sebastian.eyerer@tum.de, [c] wieland@tum.de, [d] spliethoff@tum.de

The energy sector can significantly contribute to the mitigation of climate change, especially due to the use of renewable and CO_2-neutral energy sources. In this context, the Organic Rankine Cycle (ORC) is a promising technology focusing on the reduction of energy-induced CO_2 emissions by increasing the share of renewable energy sources for power and heat production. The ORC technology enables low-temperature heat sources for electric power generation and can, thus, be applied to industrial waste heat and renewable energy sources such as solar heat, geothermal brine or biomass combustion. In the case of deep geothermal heat, the thermal water should be utilized with the highest efficiency, especially due to the expensive preparation and operation of the geothermal wells. Therefore, deep geothermal heat is often exploited in combined heat and power (CHP) concepts with heat-driven operation of the power plant. Consequently, the power plant operates in part load most of the time, leading to the need of part-load optimized plants. Over the last years, the optimization of the ORC technology has been enforced, focusing on the ORC plant design, the working fluid selection, the part-load optimization together with combined heat and power (CHP) generation, as well as the optimization of the plant components.

To further investigate these optimization measures, a new ORC plant is being designed and constructed at the Institute for Energy Systems (TUM). This plant incorporates a novel plant design, optimized for geothermal CHP application. It consists of a two-stage extraction expander together with a controllable low-pressure preheater. The aim of this plant design is to increase the utilization of the heat source and the part-load efficiency of the plant. This novel plant architecture has been proven in simulations to overperform the current state-of the art in geothermal ORC-CHP plants [1]. Besides the plant architecture itself, the ORC plant also incorporates a novel condensation concept, which enables the use of approximately 20 % smaller condensers and thus significantly reduce the installation cost. This novel condensation concept has been patented and proven in simulations [2]. A third approach to increase the efficiency of ORC systems is the Trilateral-Flash-Cycle (TFC). The aim of this cycle is to reduce the exergy destruction during heat transfer by heating the working fluid up to its saturation point. The heated fluid then generates power during a flash expansion. Simulations show that the exergy efficiency is 14 % - 29 % higher for the TLC compared to state-of-the-art ORC [3]. However, the isentropic efficiency in the expansion process is assumed to be lower due to the two phase character of the fluid. Upon completion of the new ORC plant, the above-mentioned optimization measures will be experimentally evaluated and compared with simulation data.

Besides the architecture, the new ORC plant is capable to run with a variety of different working fluids. The working fluid selection depending on the application and heat source characteristics is crucial for a good performance. Furthermore, many state-of-the-art working fluids have a significant environmental impact in terms of global warming potential (GWP) or are flammable leading to higher expenses for plant security. A new generation of working fluids, the hydrofluoroolefines, have low GWP values and are not or only mildly flammable and thus overcome these problems. However, their application in existing plants has to be proven. Therefore, the thermophysical properties needs to be very similar to the originally used working fluid. An example is the state-of-the-art refrigerant R245fa and its possible low-GWP alternative R1233zd-E. Both fluids have been tested and compared in terms of plant performance. It can be stated, that this modern fluid can be used as drop-in replacement in existing plants with 7 % higher thermal efficiency. However, the use of this modern fluid reduces the gross power output of the plant by 12 % [4]. Besides R1233zd-E, other modern and low-GWP working fluids will be tested in the new ORC plant upon completion.

[1] Meinel D, Braimakis K, Wieland C, Karellas S, Spliethoff H. Flexible Two-Stage Turbine Bleeding Organic Rankine Cycles (ORCs) for Combined Heat and Power Applications. In: Proceedings of the ECOS; 2016, p. 1–22.

[2] Wieland C, Kohlhepp A, Pili R, Eyerer S, Spliethoff H. Energy Conversion Method and System(EP 16 191 160.7, European Patent Application).

[3] Fischer J. Comparison of trilateral cycles and organic Rankine cycles. Energy 2011;36(10):6208–19.

[4] Eyerer S, Wieland C, Vandersickel A, Spliethoff H. Experimental Study of an ORC (Organic Rankine Cycle) and Analysis of R1233zd-E as a Drop-In Replacement for R245fa for Low Temperature Heat Utilization. Energy 2016;103:660–71.

Production of Smart Sensor Systems for Distributed Sensing by Printing Techniques

Andreas Albrecht[a], Almudena Rivadeneyra[b], José F. Salmerón[c], Marco Bobinger[d], Aniello Falco[e], Paolo Lugli[f], and Markus Becherer[g]

[a]andreas.albrecht@tum.de, [b]almudena.rivadeneyra@tum.de, [c]jfsalmeron@nano.ei.tum.de, [d]marco.bobinger@tum.de, [e]aniello.falco@unibz.it, [f]paolo.lugli@unibz.it, [g]markus.becherer@tum.de

Renewable power plants often require sensors at remote sensing at location where conventional electronics are not desirable. Printing technologies enable electronics directly on any kind of substrate, which are thin, lightweight and even flexible. Printed electronics and sensors can be produced by the right combination of conductive, dielectric, and sensing inks and the production methods.

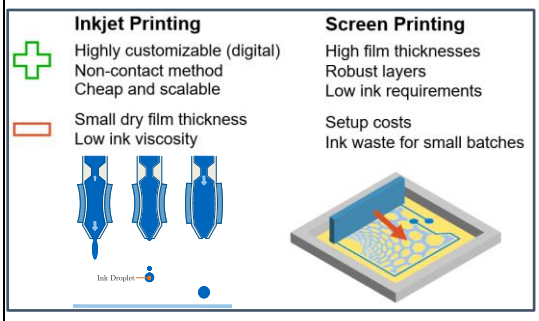

Figure 1: Advantages and disadvantages of inkjet printing and screen printing

We investigate inkjet and screen printing, as well as curing techniques like flash light curing, which employs high-power broad band light pulses to specifically heat deposited films on temperature-sensitive substrates like plastics.

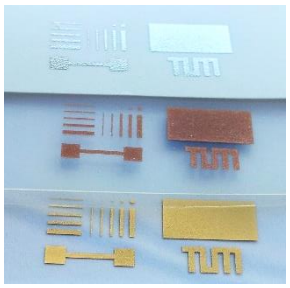

Figure 2: Inkjet-printed patterns on paper and PET

We developed deposition processes for silver, gold, copper, graphite, and conductive polymers to create conductive patterns. We can print well-defined, continuous, and conductive wires on flexible and on stretchable substrates for sensor electrodes and antennas. In combination with dielectric and semiconducting pastes, sensors for temperature, humidity, pressure, strain, gases, and chemical parameters were produced directly on the same substrate using printing techniques. Examples are shown in Figure 4. The wires on a stretchable film can recover from strains above 300 % after thousands of stretching cycles. Printed pressure sensors can measure forces across more than five orders of magnitude. The combination of printed electronics with conventional surface mount devices results in hybrid sensor systems consisting of one or more sensors with the sensing electronics and the communication platform.

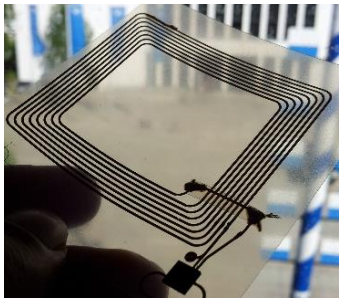

Figure 3: Inkjeted NFC tag on PET film with SMD components

In comparison to traditional electronics manufacturing, the production process is much simpler: Only a small number of additive process steps reduce chemical waste reduced to a minimum, and the electronics can be produced directly on the substrate where they are needed. This enables lightweight and smart devices on surfaces where conventional electronics are hard to integrate. This enables distributed, smart sensor systems in renewable and conventional power plants at the ideal location for sensing the desired parameters.

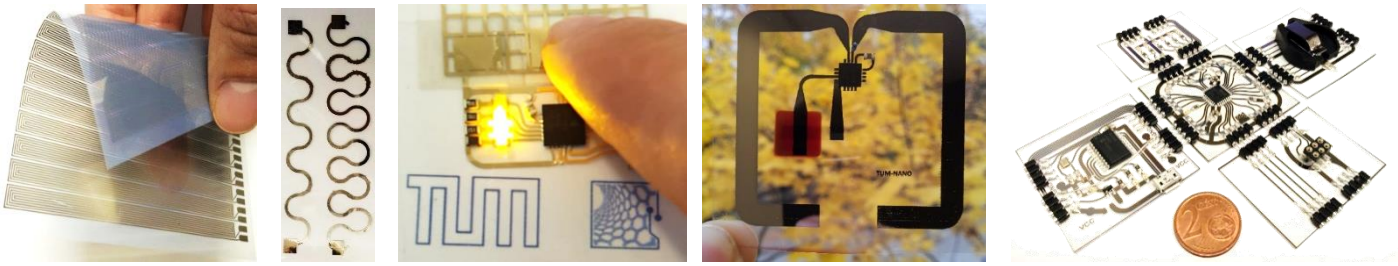

Figure 4: Selected applications from left to right: Thin and long electrode structures for a tamper-evident film; Conductive wires on a stretchable silicone film; Inkjet- and screen printed force sensor tag with assembled LED indicators; Inkjet-printed UHF tag with organic photo-diode; Printed modular circuit board with assembled surface mount components

Model-Based Optimization of Refrigeration Systems

Joerg Bentz[a], Christian Schweigler[b]

[a]joerg.bentz@hm.edu, [b]christian.schweigler@hm.edu

Refrigeration systems are among the most important power consumers. They use about 14% of the total electrical power in Germany. In refrigeration systems several individual devices interact, which leads to a high number of degrees of freedom in their mode of operation. Several interdependencies occur when chillers are operated in conjunction with heat rejection units. Identification of an optimal setting of the process variables is essential for finding the most efficient point of operation resulting in a reduction of the power consumption. A mathematical optimization procedure is needed to find the best solution. Depending on the complexity and type of the objective, different optimization procedures can be used. The process starts with modeling of the operating characteristics of all system components in sufficient quality. For the purpose of validation, the simulation data are updated by operational data which reflect the current status of the technical installation. Finally, by mathematical regression a polynomial representation of the operating characteristics is found which can be used for the optimization procedure. The modeling workflow is shown in figure 1.

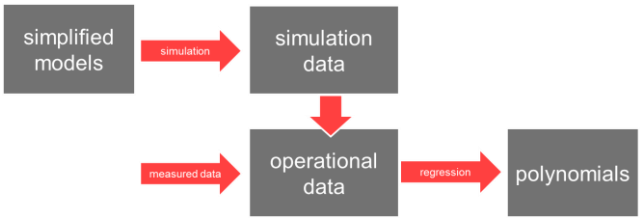

Figure 1: Optimization Workflow

In search of suitable modeling methods for the refrigeration machinery, two relevant fundamentally different model approaches were investigated. A detailed semi-empirical physical model contrasts with a highly simplified and generalized model. In the semi-empirical physical model, the most important components, such as the compressor or the heat rejection unit, are modeled based on empirically collected data. These are incorporated into a reduced model that includes the basic physical relationships. This achieves a comparatively high accuracy of the model with limited modeling effort. The simplistic model, on the other hand, consists only of basic relationships that map the characteristics of the system components with simplified equations.

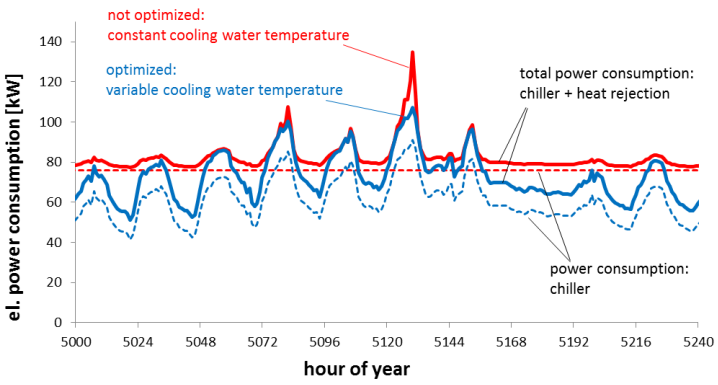

Figure 2: Example of Optimization Results

For optimum operation of the system, the cooling water temperature and the volume flows of the water circuits represent the decisive degrees of freedom. These parameters can be influenced by the drives of the cooling tower fan and the circulating pumps. In response to the setting of the cooling tower, the power input for the compressor of the refrigeration cycle has to be adjusted accordingly. Optimization criterion is the overall electric consumption. See figure 2.

In order to address different types of refrigeration systems, modular models with a high degree of flexibility and sufficient accuracy are necessary. Complexity of the models shall be low in order to avoid narrowing of the choice of optimization algorithms and to reduce computational effort. These modular models are unique in the field of operational optimization of refrigeration machinery and can be used in many applications in this field.

One of the goals of our future research deals with scenarios in which several chillers or heat rejection plants are used in a modular installation with on/off operation of single components is taken into account. In this case the optimization algorithm must be selected specifically. Thus, starting from a quadratic or nonlinear optimization, a mixed-integer quadratic optimization problem (MIQP) is obtained, inducing a further increase of the complexity.

Smart Rural Electrification - Integrating Smart-Grid Solutions into Rural Energy Systems in India

Anna-Kaarina Seppälä[a]

[a]anna.seppaelae@tum.de

The government of India recently declared the country fully electrified but in reality, over 240 million of its citizens still live without access to electricity despite substantial efforts to connect them to the grid. Bad power quality and low willingness to pay play a definite role as, even though those living below the poverty line are guaranteed free connections, villagers often decide to opt out of energy services rather than paying monthly minimum fees for insufficient power supply with frequent interruptions.

Figure 1: Nepalese woman with her mobile phone

As a result of lack of energy, conventional fuels such as firewood, kerosene and dung are widely used in India with averse health and environmental effects. Even households with grid connection report substantial expenditure on such back-up fuels due to constant power cuts.

Small renewable off-grid systems could greatly improve the situation by providing relatively cheap, flexible and reliable power to rural communities. To this end, they have to be adequately designed and operated to assure constant power supply under normal and sub-optimal conditions. This problematic is very similar to that now experienced in industrialised countries in the wake of the energy transition, but governed by stricter financial and technological constraints.

The purpose of this project is to explore the possibilities of integrating smart-grid technologies such as efficient energy management, demand response and communication in the rural electrification scenario. The main focus is on open-source tools and low-cost implementation in order to provide a solution that is accessible for the rural, low-income target group. Robust, computationally cheap algorithms with plug-and-play characteristics are preferred.

Hybrid nanomaterials for environmental sensing applications

Josef Mock[a], Alina Lyuleeva[b], Marc Kloberg[c], Ebru Üzer[d], Marco Bobinger[e] and Markus Becherer[f]

[a]josef.mock@tum.de, [b]alina.lyuleeva@tum.de, [c]marc.kloberg@makro.ch.tum.de, [d]ebru.uezer@mytum.de, [e]marco.bobinger@tum.de, [f]markus.becherer@tum.de

Nanomaterials attracted much attention during the last decades. Various two-dimensional (2D) as well as one-dimensional (1D) materials have been presented since. We present fabrication and characterization techniques for environment sensing applications using novel nanomaterials. As an example, we utilize 2D silicon and 1D SnIP to build first nanoelectronic devices.

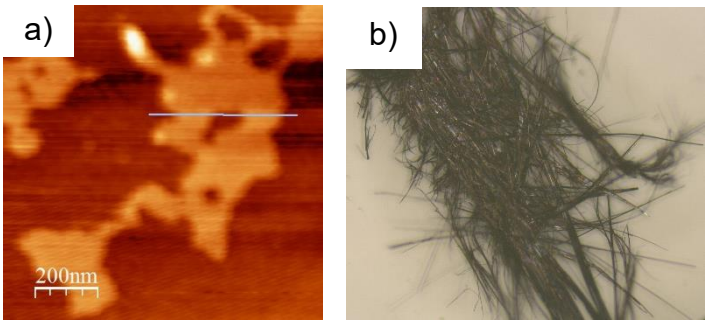

Figure 1: a) Atomic force microscope (AFM) image of a functionalized silicon nanosheet. b) Light microscope image of bundled SnIPs.

Pure 2D silicon is called silicene and is expected to exhibit similar properties to those of graphene. We use functionalized silicon nanosheets (SiNSs) in order to enhance the material properties. The SiNSs are synthesized via chemical exfoliation from calcium disilicide ($CaSi_2$) and functionalized with a variety of different molecules. Another material under investigation is SnIP, an inorganic double helical material made of a helical P^- chain and a second helical SnI^+ chain with opposite chirality. Figure 1 a) displays an AFM image of SiNSs and b) shows a microscope image of bundled SnIPs.

For the fabrication of electronic sensing devices, several aspects have to be considered: *e.g.*, nanomaterials' deposition and the use of their mechanical, electric and photonic properties. Possible applications for nanomaterial-based sensors are health care (*e.g.*, biosensors and fluidics), safety (*e.g.*, detection of CO) and environmental monitoring (*e.g.*, pH value and humidity measurement). Figure 2 schematically displays the different fabrication steps of electronic sensing devices. In Figure 2 a), the material deposition on pre-patterned structures is demonstrated, while in b) the oxidation is shown. Nanomaterials usually exhibit a high surface-to-volume ratio and therefore, they are prone to oxidation. In order to protect the nanomaterial from oxidation, several approaches are possible. Figure 2 c) shows the deposition of a passivation layer using materials like metal oxides or polymers, which already exist for different applications in industry. Other approaches are a homogenous blend formation of the nanomaterial with for example poly(3-hexylthiophene) (P3HT) or a hybrid materials' synthesis with functional groups on the surface. After fabrication, the sensing devices are characterized under controlled environment conditions, *e.g.* temperature and humidity.

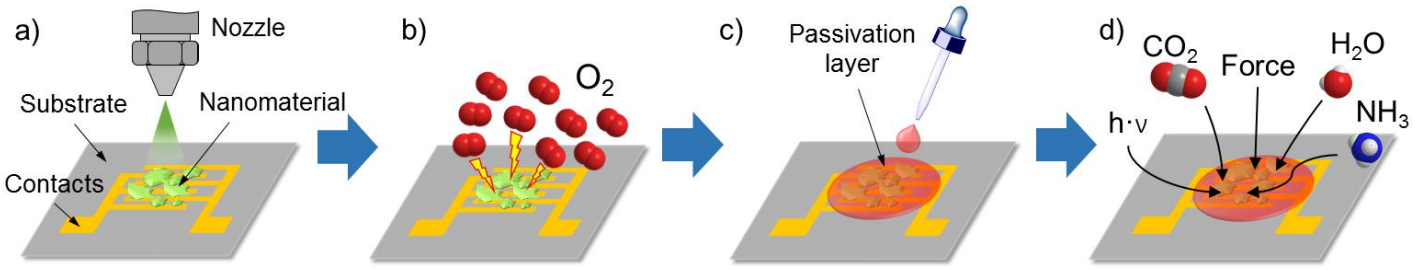

Figure 2: Schematic workflow of the fabrication of nanoelectronic sensors. a) Deposition of the nanomaterial on pre-patterned structure. b) Illustration of possible oxidation of non-protected nanomaterial. c) Passivation deposition to prevent oxidation. d) Environment sensing possibilities for different physical quantities.

Printed films of conjugated polymers and small acceptor molecules

Kerstin Wienhold[a], Peter Müller-Buschbaum[b],

[a]kerstin.wienhold@ph.tum.de, [b]muellerb@ph.tum.de

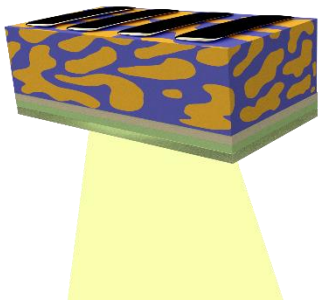

Figure 1: Device Structure of an Organic Solar Cell

Organic photovoltaics (Figure 1) are a promising alternative to conventional silicon solar cells as they offer several potential advantages e.g. low weight, high mechanical flexibility and low-cost production. Resent research focuses on identifying new high-efficiency polymers and acceptor molecules to reach high power conversion efficiencies (PCEs).

To date, a PCE of 13% could be obtained with a PBDB-T-SF: IT-4F based organic solar cell device [1]. The fluorinated conjugated polymer PBDB-T-SF acts as a donor whereas the fluorinated small molecule IT-4F acts as an electron acceptor. Both molecules are promising for photovoltaic applications as they show higher absorption coefficients, higher efficiency in exciton separation and charge transport as well as enhanced chemical stability as compared with their non-fluorinated counterparts. [1]

However, before commercialization, the solar cell performance must be optimized and an up-scale of the thin layer deposition is necessary. Printing of the individual layers of the solar cells can overcome the up-scale challenge.

Characterization techniques such as UV/Vis spectroscopy (Figure 2), photoluminescence and scattering methods such as GISAXS and GIWAXS are applied to get a deeper insight into the composition and morphology of the active layer of the printed films with the aim to further improve the solar cell efficiencies.

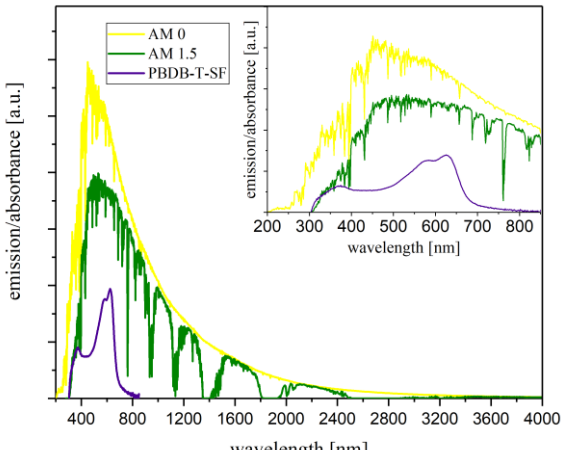

Figure 2: Absorbance of PBDB-T-SF and Solar Spectra

References:

[1] W. Zhao, S. Li, H. Yao, S. Zhang, Y. Zhang, B. Yang, J. Hou J. Am. Chem. Soc. **139**, 7148-7151 (2017)

Morphology and optoelectronic properties tuning of ZnO/P3HT/P3HT-b-PEO hybrid films via spray deposition method

Kun Wang[a], Lorenz Bießmann, Matthias Schwartzkopf, Stephan V. Roth, Peter Müller-Buschbaum[b]
[a]kun.wang@ph.tum.de, [b]muellerb@ph.tum.de

Hybrid solar cells, a combination of conventional inorganic and organic photovoltaic systems, offer outstanding potential due to their minor investment compared to inorganic solar cells and higher stability compared to organic solar cells. In this kind of solar cells, nanostructured inorganic metal oxides with tunable morphologies are of great importance. Among the inorganic metal oxides, ZnO has been widely explored due to its outstanding electrical and optical properties and rich variety of morphologies. To date, many different routes towards ZnO nanostructures have been reported, such as hydrothermal synthesis, metal–organic chemical vapor deposition and others, of which the sol-gel process is one of the most widely used methods in solar cells due to the production of a homogeneous material and fabrication of ceramic coatings from solutions by wet chemical means. However, the structures obtained by the conventional sol-gel process are limited, regarding both morphologies and structure sizes. A possible way to improve the film structure is to introduce amphiphilic block copolymers into the sol-gel process. The hydrophilic and hydrophobic polymer blocks of amphiphilic block copolymers are covalently bound, which could modify the interface of ZnO. Unlike the traditional diblock copolymer, in the present approach we make use of a new functional block copolymer P3HT-b-PEO, in which P3HT acts as hole transport material and light absorber, while PEO serves as a template for ZnO synthesis. The initial solution is subsequently spray coated to obtain the hybrid film. Scanning electron microscopy (SEM) and grazing-incidence small-angle X-ray scattering (GISAXS) measurements reveal a significant change in the morphology of the hybrid films during deposition. Figure 1 illustrates the difference of the sprayed hybrid films with and without the diblock copolymer P3HT-b-PEO and a scheme of the GISAXS measurement. Optoelectronic properties illustrate the improved charge separation and charge transfer process. Both, the amount of the diblock copolymer and the annealing temperature play an important role to tune the morphology and the optoelectronic properties. Thus, the presented simple, reagents- and energy-saving fabrication method provides a promising approach for a large scale preparation of bulk heterojunction P3HT:ZnO films on flexible substrates.

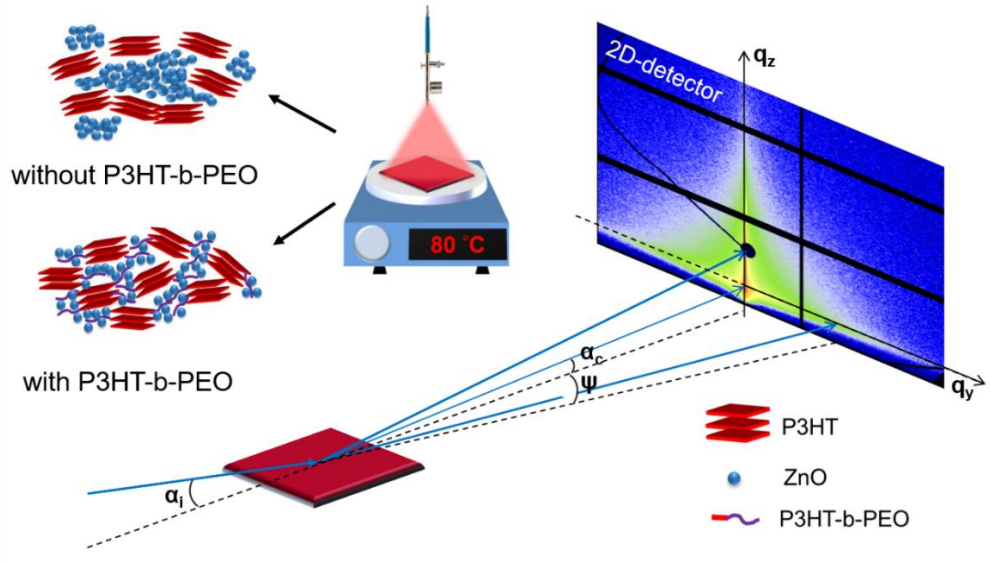

Figure 1: Schematic representation of the sprayed films with and without the diblock copolymer P3HT-b-PEO and the GISAXS measurement.

Cost-effective fabrication techniques for organic solar cells

Marius Loch[a], Andreas Albrecht, Marco Bobinger, Florin Loghin, Markus Becherer, Almudena Rivadeneyra-Torres

[a]marius.loch@tum.de

Organic solar cells are a promising candidate for a future of ubiquitous, low-cost solar power harvesting. While this promise is founded on easily scalable, large-area solution processing techniques, most of the scientific research community a) uses small-scale deposition methods convenient for the lab, b) works in an inert nitrogen or argon atmosphere inside a glovebox and c) deposits the electrodes by physical vapour deposition in vacuum. These three issues are not compatible with real large scale production. In this work, we compare different fabrication techniques like spray coating, screen printing, and inkjet printing to commonly employed spin coating. The challenges of the three techniques and the requirements of the different layers involved in the solar cell (opaque and transparent electrodes, blocking layer and light absorbing layer) are discussed towards fully solution-processed devices.

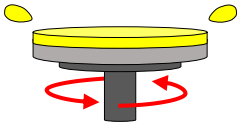

Spin coating

Spray Coating

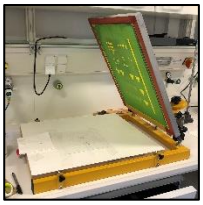

Screen printing

Inkjet printing

Figure 1: Different solution-based fabrication techniques

One of the two electrodes needs to be transparent, to let light into the device. The go-to-material indium tin oxide (ITO), contains rare and pricey indium, is brittle and requires high annealing temperatures thus unsuitable for flexible foil substrates and cannot be processed from solution. A proposed alternative are spray-coated silver nanowire (AgNW) networks, which combine the high conductivity with high transmittance and can be processed from solution.

Spray coating of polymer layers for the blocking layer (PEDOT:PSS) and the light absorbing layer (P3HT:PCBM) is proposed to overcome the scale limitations of spin coating, but requires careful tuning of the spray parameters to get the desired film thickness and overcome film roughness introduced by drying of single droples.

Eventually spray coating and screen printing of silver nano particles (AgNP) are evaluated for solution-processed top electrodes. While film morphology is less critical for the metal layers and nanoparticles tend to be more forgiving in the film formation, working on top of the sensitive organic layer is delicate and also puts limitations on possible after-treatments required to make highly conductive AgNP films (sintering).

We present different working devices for each for the proposed fabrication techniques.

Figure 2: Solar cells with silver electrodes made from (left to right) spray coating, screen printing and evaporation.

Printed high-transparent blocking layers for photovoltaic applications

Xinyu Jiang[a], Wei Cao, Peter Müller-Buschbaum[b]
[a]xinyu.jiang@ph.tum.de, [b]muellerb@ph.tum.de

Bulk heterojunction (BHJ) polymer solar cells have gained significant improvements via novel organic synthesis and easy fabrication methods, especially their potential roll to roll processing and large-area processing ability on low cost makes conjugated polymer-based organic solar cells very attractive as a cost-effective solution to today's energy-shortage problem. Figure.1 shows a typical device configurations of BHJ solar cells. When the light is absorbed in the active layer, the electrons and holes are not directly created. Instead, excitons are formed, which need to be dissociated. The conductive polymer poly(3, 4-ethylene dioxythiophene) (PEDOT) doped with poly(styrene sulfonate) (PSS) is frequently used as hole blocking layer for BHJ solar cells, for its' high transparency in the visible range, high mechanical flexibility, excellent thermal stability and can be fabricated through conventional solution processing. Moreover, PEDOT: PSS films can be easily nano-structured to enhance the localized light intensity to the active layer and generate more power.

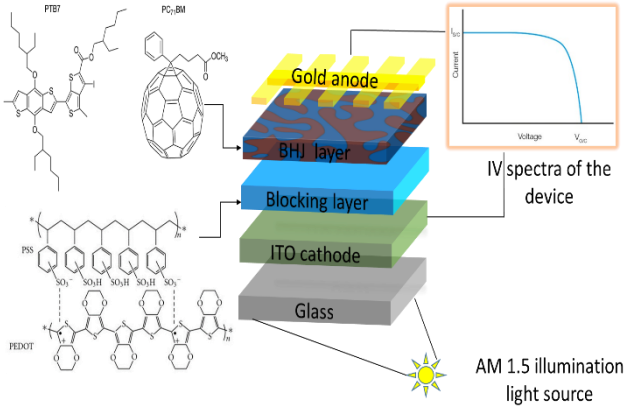

Figure 1: Device structure of a typical BHJ solar cell

Printing techniques allow for up-scaling to industrial-oriented scales which is not the case for laboratory techniques like spin coating. Thus, roll-to-roll processing on flexible substrates is the goal of production techniques for organic solar cells. Several methods of printing techniques can be used to reach this goal, such as slot-die coating, screen printing or flexographic printing. Especially slot-die coating, is a very cost-effective production technique that offers the possibility of large scale manufacturing and custom designed pattern coating. Figure 2 shows the printing set-up in our lab. We focus on fabricating a large-scale hole blocking layer for BHJ polymer solar cells with slot die printing technique. In such a BHJ polymer solar cell, the morphology plays an important role for device efficiency. Different factors can influence the morphology of active layer. For example, the morphology of the underlying layer can influence the nanostructure of the active layer. Therefore, the preparation of uniform PEDOT:PSS thin electrodes with the printing technique is the first step for large scale production for BHJ solar cells.

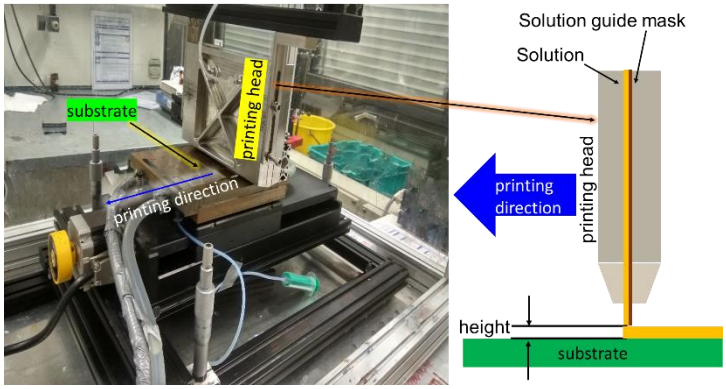

Figure 2: Printing set-up in the lab

In the present work, we study printed transparent PEDOT:PSS thin film with respect to morphology and optical properties when different heating-treatments are introduced for the substrates. The different morphologies were characterized and an optimal preparation protocol was established. Furthermore, for a better understanding of the relationship between temperature and morphology of PEDOT:PSS thin films, the films were probed with optical microscopy, UV-vis spectroscopy, scanning electron microscopy (SEM), atomic force microscopy (AFM), X-ray reflectometry and grazing incidence small/wide angel X-ray scattering (GIWAXS/GISAXS).

Thermal treatment on Quantum Dot Solid for Photovoltaics

Wei Chen[a], Peter Müller-Buschbaum[b]

[a]wei.chen@ph.tum.de, [b]muellerb@ph.tum.de

Colloidal quantum dots (CQDs) have attracted many attentions for various electronic applications, like light emitting diodes, photodetectors, photovoltaics etc. due to their unique intrinsic properties, like tunable energy band-gap and stability against ambient circumstance. Comparing with cadmium chalcogenides CQDs, the lead chalcogenides CQDs reveal much weaker exciton binding energy because of the smaller effective electron mass, which is beneficial for the extraction of electrons and therefore suitable for being utilized in photovoltaics (PV) rather than light-emitting diodes.

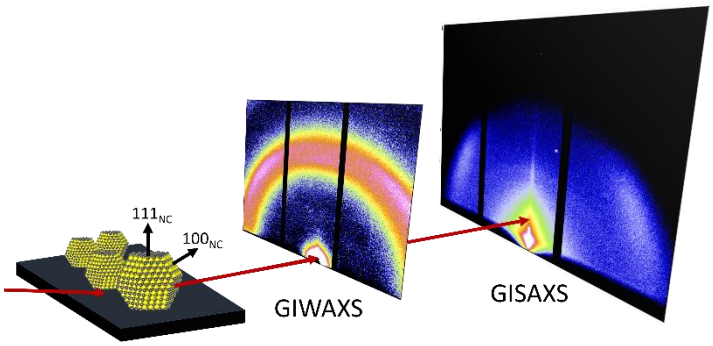

Figure 1: GIWAXS and GISAXS measurements on CQDs' array solids. red arrows: incident and reflcted x-ray

Size-monodisperse CQDs are normally obtained from a hot-ions injection method in solution. The long-chain organic ligands, like oleic acid chains, are necessary to be employed as surface surfactants to prevent the CQD's aggregation during the fabrication process, purification process and long-time storage afterwards. In order to realize and improve the charge transportation among CQDs' array, the distance between each CQD is required to be decreased reaching a certain value homogeneously. The long chain ligands are always removed during the ligand exchange process and film deposition. Thus, the wavefunction of as generated excitons could have larger overlap and better couple for forming energy transport tunnels.

Additionally, the functional CQDs' array films are normally deposited by one of various solution processes, like spin-coating, spay-coating or dip coating in room conditions. The obtained CQDs films by one of these methods inevitably reveal a porous structure, which may result in disordered film structure and bring in a large number of trap states. The thermal treatment is a regular method in organic PV device fabrication for annealing of crystalline polymers but rarely used in CQDs films for fabricating related devices. In this work, we proceed the thermal treatments on CQD films with different temperatures. We used grazing incidence small angle / wide angle x-ray scattering (GISAXS/ GIWAXS) to investigate the inner structure of thermal treated CQD films, including the superlattice structure, inter dot spacing and the nano-crystals orientations. We also used pump-probe transient absorption (TA) spectroscopy to observe the order of energy distribution and qualitatively evaluate the yield of generated excitons.

Our results indicate that, the structure order of the films depends on the annealing temperature. The crystal orientation rearrangement behavior is observed with temperature increasing. The thermally treated films tend to generate more excitons but also revealed a broader energy distribution.

Development of a physical model for polymeric solar thermal flat-plate collectors

Mathias Ehrenwirth[a], Wilfried Zörner[b], Vicky Cheng[c]

[a]Mathias.Ehrenwirth@thi.de, [b]Wilfried.Zoerner@thi.de, [c]Vicky.Cheng@tum.de

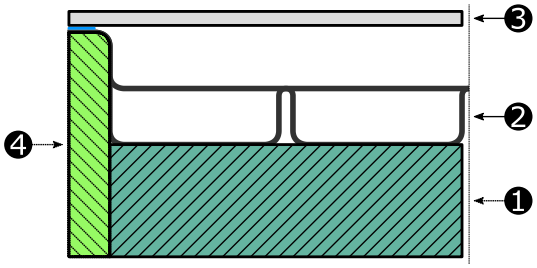

Figure 1: Setup of a polymeric solar thermal flat-plate collector (PFPC).

Solar thermal polymeric flat-plate collectors (PFPCs) allow for cost-effective solar thermal systems, both in terms of investment and operating costs. To balance the drawbacks of polymeric materials such as low pressure and temperature resistance, PFPCs must be integrated into appropriate systems, e.g. drain back systems (DBS). A typical setup of a PFPC is shown in Figure 1. To minimize the (back)side heat losses of PFPCs, an insulation (1 / 4), e.g. made of polystyrene or glass wool, is mounted to the (back)side of the polymeric absorber (1). Transparent covers (3), typically made of glass or PMMA, reduce the frontside heat losses. The design and material properties of these components (such as thickness, heat conduction, absorptance, reflectance, etc.) provoke a conflict between the technical and economical efficiency of a PFPC. On the one hand, low material thicknesses yield reduced material costs. The resulting lower weight (especially of the frontside cover) can positively contribute to the installation costs. However, the solar thermal efficiency will suffer from insufficient insulation properties in case of reduced insulation thicknesses. On the other side, over-dimensioned material thicknesses yield an overheating of the polymeric absorber, which negatively affects to the lifetime of PFPCs. An appropriate design is therefore essential for both cost-effective and durable PFPCs.

To shorten development times and to identify reasonable configurations, a physical model of a PFPC was developed. The model is divided into multiple layers, where each layer (c.f. Figure 2, highlighted areas) represents one physical component of the PFPC (e.g. glazing, absorber, insulation). Each layer is further subdivided into several nodes (capacitors), which are connected by thermal resistors (RC-model). The resistors enable the heat transfer mechanisms in- and outside the PFPC, e.g. radiative heat transfer between the glazing and the absorber, convective heat transfer inside the absorber or conduction through the backside insulation. The capacitors represent the thermal masses of each component. The purpose of the model is to predict the temperature increase between collector in- (T_{In}) and outlet (T_{Out}) based on external boundary conditions such as incident irradiation I or ambient temperature T_{Amb}.

The model was setup with *MATLAB / Simscape* and validated with experimental results from four different PFPCs, which differ regarding their size, material and setup. Comparing the experimental results with numerical data indicates a high correlation of the developed physical model and measurement results. In a subsequent step, the developed collector model will be used to identify appropriate parameters for PFPCs where experimental data is lacking. In addition, this model provides information regarding the operating temperatures of all components and is therefore a useful contribution to the development of cost-effective solar thermal systems.

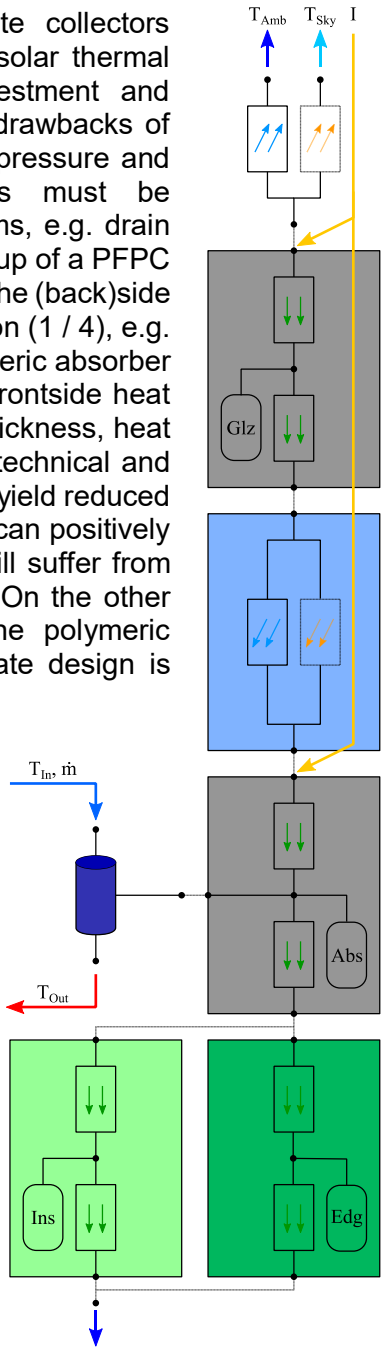

Figure 2: Setup of the physical collector model. = Conduction, = Convection, = Radiation.

On the impact of the colloidal nature of hybrid perovskite precursors on thin film microstructure

Shambhavi Pratap[a], Johannes Schlipf[b], Peter Müller-Buschbaum[c]

[a]shambhavi.pratap@ph.tum.de, [b]johannes.schlipf@ph.tum.de, [c]muellerb@ph.tum.de

Thin films based on crystalline hybrid organic-inorganic lead halide perovskites are processed by spin coating from precursor solutions of the organic and inorganic counterparts within suitably polar, organic solvent systems (DMSO, DMF, GBL). Resultant films display a range of microstructures including grain sizes, crystal strains, preferential orientations and remarkably, vivid hierarchical surface morphologies. By compositional engineering of the precursor chemistry, it is possible to tune the final film composition, as well as alter film morphology.

Colloidal nature of perovskite precursor solutions used for film fabrication is suggested, and phenomena such as glass-transitions, Marangoni flows, crystal twinning, and growth instabilities are explored in order to explain diffusion-limited self-organization of thin films. Microstructures are further demonstrated to be tunable by control of the colloidal chemistry of the precursor solution as well as the drying of the thin film. The significance of such a finding would suggest that perovskite films could possibly possess 'soft' properties, implying there exists a delicate balance between entropic and enthalpic contributions towards the free energy of the dynamically changing system, which needs to be regulated for controlling film morphology; which has been established as a crucial prerequisite for improving solar cell performances.

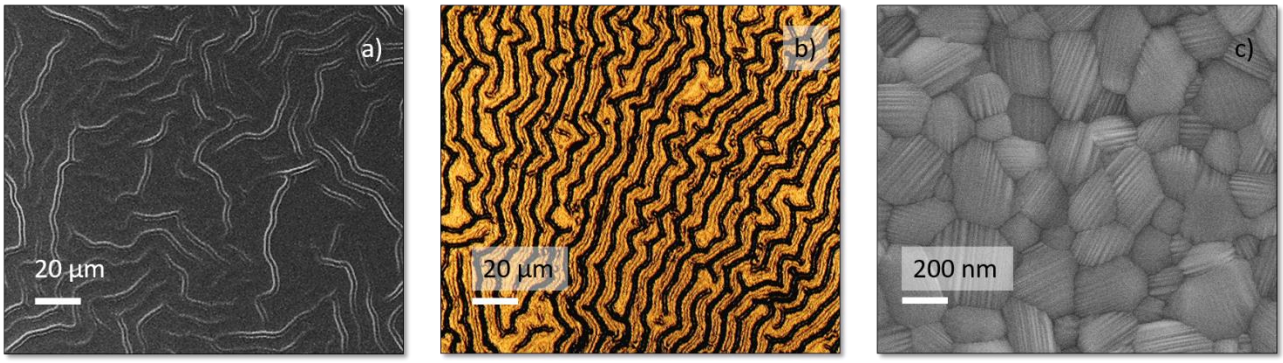

Figure 1. Microstructure exhibited within thin films, in the form of wrinkles (SEM, Fig. 1 a), buckles (OM, Fig. 1b), and crystallographic twinning (SEM, Fig. 1c) within crystalline perovskite films with varying compositions

Directional, hierarchical films via spray coating

J. Heger[a], P. Müller-Buschbaum[b]

[a]julian.heger@ph.tum.de, [b]muellerb@ph.tum.de

Since the beginning of industrial age, humanity has an exponential growing demand of energy supply. The use of fossil fuels is not only restricted to a very limited amount of resources, it further also enhances climatic changes and has a strong impact on nature. Therefore, supplying clean, safe and renewable energy is an essential task. For the benefit of this, it is of reasonable interest to enable energy consumers satisfying their own demand based on renewable energy sources. Towards this self-sufficient and “green” energy supply, the possibility of large scaled and cheap roll to roll solar cell fabrication based on organic materials is an important step. With the potential of flexible, semi-transparent properties these solar cells open new paths of design and application, for example integrated in architecture, clothing and all day accessories. Enhancement of these solar cell’s lifetime and efficiency is a key challenge, for which it is necessary to understand and control the morphology and formation of the solar cell layers during the deposition process.

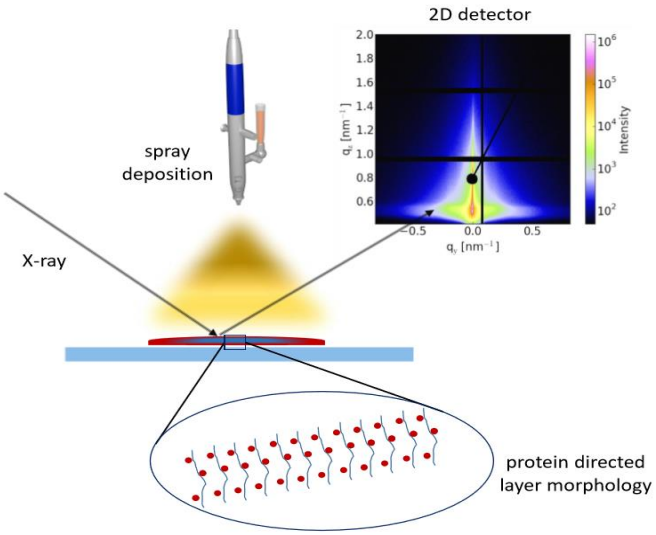

We focus on providing spray coating (see figure) as a roll to roll compatibility technique in order to investigate directional, functional material deposition. We address metal-biopolymer composite films as a new class of materials, which has high potential in a green energy scenario. For example, protein nanofibrils offer a way of templated structuring and directed material synthesis [1]. It is the aim to install hierarchical nanostructures by mixing metal and polymeric colloids. In situ GISAXS and GIWAXS measurements will display the complex morphology evolution during the spray coating process (see figure) [2]. The resulting directional optical and electrical properties will be characterized by methods such as ellipsometry and conductivity measurements.

References

[1] G. Wei, et al.: *“Self-assembling peptide and protein amyloids: from structure to tailored function in nanotechnology”*, Chem.Soc.Rev., 46, 4661 (2017)

[2] S. V. Roth: *“A deep look into the spray coating process in real-time—the crucial role of x-rays”*, J. Phys.: Condens. Matter 28, 403003 (2016)

Morphology phase diagram of printed titania films assisted a sol-gel technique

Nian Li[a], Lorenz Bießmann, Peter Müller-Buschbaum[b]

[a]nian.li@ph.tum.de, [b]muellerb@ph.tum.de

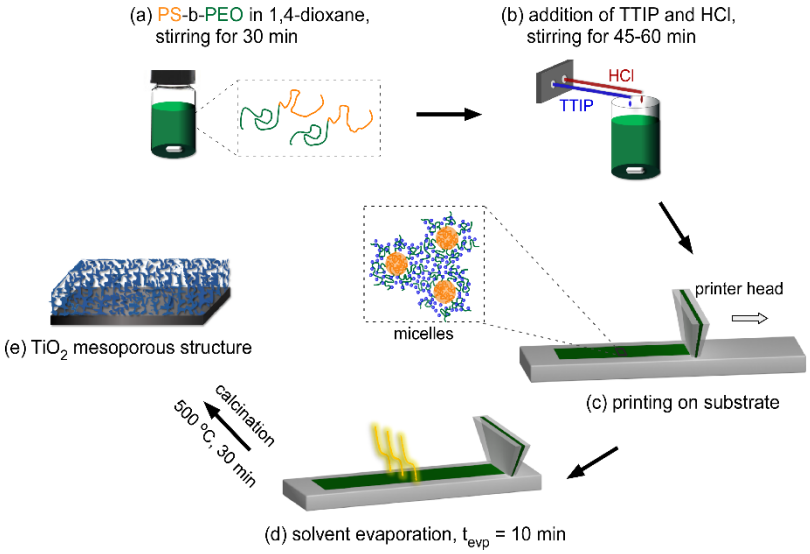

Figure 1: Schematic illustration of printing titania films based on a block copolymer assisted sol-gel synthesis process using titania precursor

Nanostructured titania (TiO_2) thin films are promising candidates for a wide range of applications, such as photocatalysis, sensors, and especially in photovoltaics. For example, the crystalline anatase titania with network, as an electron-conducting layer, has attracted considerable attention in hybrid solar cells, because it has a larger surface area, accessibility of the inner surface, and suitable morphology. Until now, several methods for the preparation of titania thin films, such as spin coating, solution casting, doctor blading or dip coating, are extensively used in laboratory scale. While for an industrial scale, printing is a simple and low-cost technique and available in large quantities for producing titania films. The sol-gel process combined with amphiphilic block copolymer templates is a promising route to tune the morphology of titania films.

In the present work, titanium tetra isopropoxide (TTIP) is used as precursor and diblock copolymer polystyrene-block-polyethylene oxide (PS-b-PEO) as the structure-directing template. The amphiphilic block copolymer PS-b-PEO undergoes phase separation and self-assembly due to a good-bad pair solvent, namely 1,4-dioxane and hydrochloric acid (HCl). By adjusting the weight fraction of 1,4-dioxane, HCl and TTIP, the titania films with different morphologies, containing foam-like structure, nanowire aggregates, collapsed vesicles and nanogranules, are obtained after evaporation and calcination processes. The surface morphology of the titania film is probed via scanning electron microscopy (SEM) and optical microscopy (OM), and the inner morphology is detected by grazing incidence small-angle X-ray scattering (GISAXS). The crystallinity of anatase titania is proved by X-ray diffraction (XRD) and transmission electron microscopy (TEM) upon calcination of the nanocomposite films at 450 °C in air.

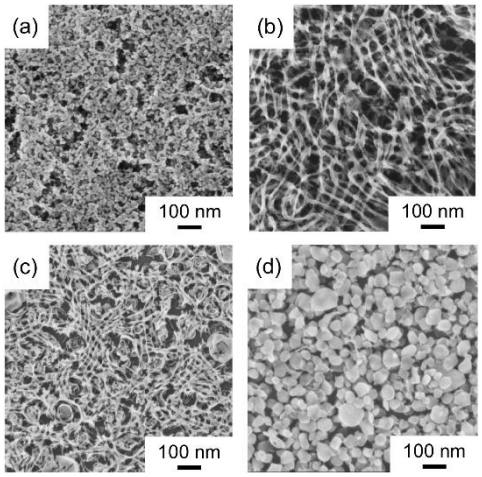

Figure 2: SEM images of different TiO_2 morphologies after calcinating the printed films

Next Generation Hybrid Solar Cells Based on Heavy Element Containing Small Molecules and High-Performance Polymer PTB7-th

Raphael Märkl[a], Nuri Hohn[b], Prof. Dr. Peter Müller-Buschbaum[c]

[a]raphael.maerkl@ph.tum.de, [b]nuri.hohn@ph.tum.de, [c]muellerb@ph.tum.de

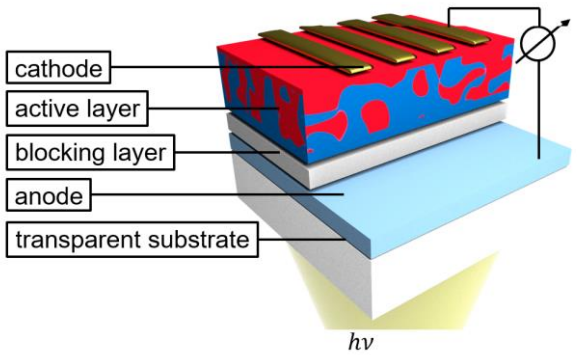

Figure 1: Principle of a hybrid solar cell with hole conducting material (blue) and electron conducting material (red)

With an ever growing world population and increasing global wealth, the search for an abundant source of sustainable energy is paramount to satisfy the large energy demand. As fossil fuels have proven to be non-sustainable and nuclear power faces many political challenges, renewable energy sources emerge as the most promising candidate for sustainable energy generation. Nowadays, a considerable share of industrial energy generation is based on photovoltaics. Challenges are imposed in the form of optimization of power generation efficiency, lifetime and high production expenses. Versatility in the field of solar energy generation could be further increased through the introduction of certain characteristics such as transparency and light-weight devices. These new characteristics represent a main pillar to ensure economical competitiveness and the role of photovoltaics as a major energy supplier for future generations.
The above-mentioned, future-shaping properties of next-generation solar cells can potentially be achieved through an inorganic-organic hybrid photovoltaics (HPV) approach. Inorganic solar cells already exhibit good efficiency and are widely used but are rather expensive, rigid and heavy. Organic photovoltaic devices on the other hand can be created on flexible and/or transparent substrates and are potentially produced at low cost. Their low efficiency and long-term instability unfortunately limit their economical competitiveness. HPV therefore offers a solution to extract the best properties of both technologies.

Essential for a functioning HPV device is efficient charge separation at the interface between inorganic and organic material. High surface-to-volume ratio inorganic matrices increase the effective interface and thereby bear the potential to increase charge separation efficiencies. An inorganic structure must therefore be infiltrated by a organic hole-conducting material. Mesoporous titania thin films, which are synthesized in a bottom-up sol-gel process, are investigated within this frame.[1] Furthermore, titania contributes outstanding properties such as being a wide-bandgap semiconductor and good electron mobility.
On the organic part, the high-efficiency, hole-conducting polymer **PTB7-th** is infiltrated into titania films to form the active layer of the photovoltaic device. Additionally, a novel, heavy element containing polymer molecule (**Phen-Te-BPinPh)** has been synthesized and properties with regard to photovoltaic applications are characterized. To further enhance the solar cell performance, **Phen-Te-BPinPh** could be implemented either by backfilling into a layered setup between the **PTB7-th** and the mesoporous TiO_2 layer or as a dopant into the **PTB7-th**. It is expected that the heavy element enhances the exciton lifetime, thereby increasing exciton diffusion length and reducing the recombination rate. As a result, photo conversion efficiencies are expected to reach new benchmarks in the field of hybrid photovoltaics.

[1] L. Song, W. Wang, V. Körstgens, D. M. González, Y. Yao, N. K. Minar, J. M. Feckl, K. Peters, T. Bein, D. Fattakhova-Rohlfing, G. Santoro, S. V. Roth and P. Müller-Buschbaum, *Adv. Funct. Mater.*, 2016, **26**(10), 1498.

Printed fullerene-free thin films for photovoltaic applications

Rodrigo Delgado[a], Sebastian Grott, Peter Müller-Buschbaum[b]

[a]rodrigo.delgado@ph.tum.de, [b]muellerb@ph.tum.de

In the past decades, organic photovoltaics (OPVs) have attracted considerable attention owing to their remarkable characteristics, such as light weight, flexibility, easy processability, potential low-cost fabrication and high throughput. Fabrication techniques include spin-coating, doctor-blading, spray casting and roll-to-roll printing. Among these, the scalability of printing processes makes them attractive for industrial fabrication methods.

Solution processed bulk heterojunction (BHJ) solar cells have been the most widely used method to build OPVs. In this type of solar cell, donor and acceptor are mixed and deposited together in one step to build up the active layer, which make them good candidates for printing techniques. In an ideal BHJ solar cell, the intermixing of donor and acceptor is a comb-like structure offering a high interfacial area. This is desired as the exciton diffusion length is about 10 nm. Hence, a donor-acceptor interface must be reached to separate the exciton before it recombines and so extract the charges, generating external current. Nevertheless, the morphology of the active layer is far from ideal and the efficiency lower than the theoretically possible, due to enlarged diffusion lengths which result in higher recombination rates.

Fullerene materials have been so far the main choice of acceptor material combined with polymeric semiconductors as donors. In this work the fullerene-free blend poly(benzodithiophene-benzotriazole) (**PBDBT**):3,9-bis(2-methylene-(3-(1,1-dicyanomethylene)-indanone)-5,5,11,11-tetrakis(4-hexylphenyl)-dithienol[2,3-d:2',3'-d]-s-indaceno[1,2-b:5,6-b']dithiophene (**ITIC**) is investigated. This mixture has shown outstanding power conversion efficiencies (PCE) in spin-coated devices [1], and hence it is promising a material system for printing coating techniques.

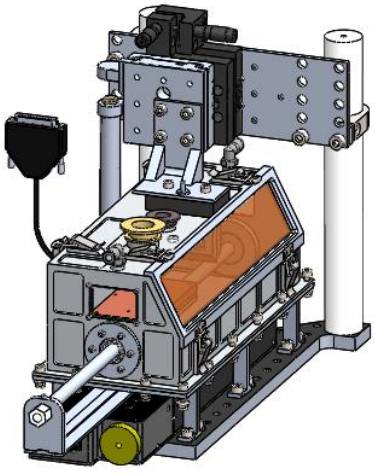

Figure 2: 3D model of the printer setup for *in situ* studies on printed films

The work presented consist in the design and fabrication of a printing setup capable to deposit the active layer for photovoltaic applications following the design introduced by Pröller et al [2]. The design of this printer can simulate the conditions that might be encountered during industrial processing. Thus, the printer is capable to print under various atmospheric conditions and offers the possibility to perform *in situ* studies on the active layer´s inner morphology using advanced scattering techniques, like grazing incidence small angle X-ray scattering (GISAXS) and grazing incidence wide angle X-ray scattering (GIWAXS). Due to the fact that the final morphology depends on the film deposition´s conditions the parameters have to be studied. For this goal, two different strategies are carried out: evaluate the printing conditions itself (substrate temperature, solution flow rate and coating speed) and study the material properties (such as weight ratio of the polymers and concentration). The differences on the active's layer thickness and absorption spectra are then used to obtain the optimal parameters for printing this mixture. The information can be correlated with the usually obtained photoelectrical properties, giving full characteristics of the printed solar cells. Hence, understanding the formation process of the active layer and its morphology in comparison to data obtained using lab-scale deposition techniques is of high interest.

References

[1] Wenchao Zhao et al., Adv. Mater. 28 (2016): 4734-4739
[2] Stephan Pröller et al., *Adv. Energy Mater.* 6 (2016):1501580

Ge9-xSix-ZINTL Clusters as Wet Chemical Precursors for Mesoporous Ge1-xSix-Films

M. A. Giebel, M. A. Narreto, C. Jensen, N. Amer, D. Böhm, F. Hegmann†, T. F. Fässler*

†hegmann@ualberta.ca, *thomas.faessler@lrz.tu-muenchen.de

Hybrid solar cells combine the unique properties of inorganic semiconductors and organic polymers which result in low production costs and flexibility.[1] However, routes to periodic porous materials are scarce. Oxidative decomposition of ZINTL clusters in presence of a specific template leads to homogenous thin films. So far, we succeeded in preparing germanium films with inverse opal morphology and a well-defined pore size in the range of 300 nm using solutions of the intermetallic compound K4Ge9 which contains nine-atomic clusters.[2]
Also, we succeeded in showing the use of these materials as an anode material in Li-ion batteries.[3] Moreover, we used Si-Ge mixed ZINTL clusters to prepare periodic porous silicon-germanium morphologies as well as Si ZINTL clusters to prepare silicon films with inverse opal structures.

Herein we present studies of these GexSi1-x-films (x = 0, 0.25, 0.5, 0.75, 1) that highlight carrier dynamics in these materials using Time Resolved Terahertz Spectroscopy (TRTS). Furthermore, this is monitored in means of temperature as well as fluence (incoming laser power per sample area) dependency. Finally, we compare the data for inverse opal structured Ge films with data on unstructured flat Ge sheets.

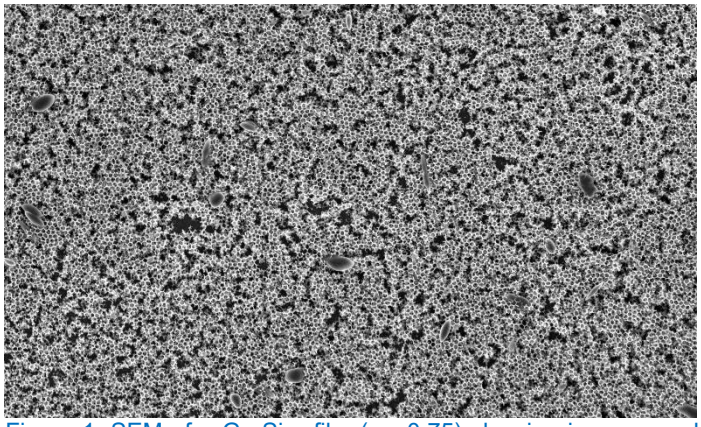

Figure 1: SEM of a Ge_xSi_{1-x}-film (x = 0.75) showing inverse opal structured material throughout a large area.

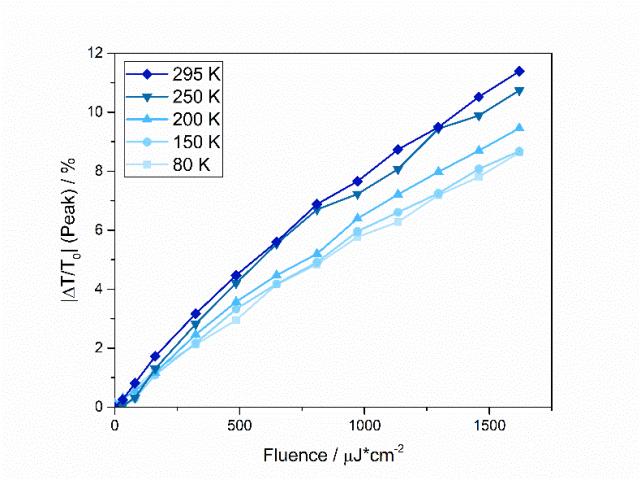

Figure 2. TRTS of a Ge_xSi_{1-x}-film (x = 0.75). Temperature as well as fluence dependency of peak signal. ΔT: change in transmittance

[1] S. Günes, N. S. Sariciftci, Inorg. Chim. Acta 2008, 361, 581-588.
[2] M. M. Bentlohner, M. Waibel, P. Zeller, K. Sarkar, P. Müller-Buschbaum, D. Fattakhova-Rohlfing, T. F. Fässler, Angew. Chem. Int. Ed. 2016, 55, 2441-2445. DOI: 10.1002/anie.201508246.
[3] S. Geier, R. Jung, K. Peters, H. A. Gasteiger, D. Fattakhova-Rohlfing, T. F. Fässler, Sustainable Energy Fuels 2018,
2, 85-90

A low temperature route towards hierarchically structured titania films for thin hybrid solar cells

Lin Song[a], Amr Abdelsamie, Christoph J. Schaffer, Volker Körstgens, Weijia Wang, Nicola Hüsing, Paolo Lugli, Sigrid. Bernstorff, Peter Müller-Buschbaum[b]

[a]lin.song@ph.tum.de, [b]muellerb@ph.tum.de

Fabricating titania based solar cells at low temperature has an energy-efficient significance and a potential for flexible photovoltaic devices, since most of photovoltaic devices with titania require high-temperature calcination. Moreover, dye-free hybrid solar cells are a novel photovoltaic device, which lower production costs and avoid problems related with dye bleaching. Therefore, dye-free hybrid solar cells are a promising alternative for current dye-sensitized solar cells technology.

Although many efforts have been made for boosting the photovoltaic performance of the dye-free hybrid solar cells, to date, most power conversion efficiencies (PCE) are generally less than 1 % even with high-temperature sintered TiO2 films. In order to improve light harvesting in the active layer of the hybrid solar cell, we superimpose superstructures (micro-scale) on mesoporous titania films in the present work. The mesoporous titania films could be achieved via various routes, among which the sol-gel synthesis in combination with block copolymer assisted templating is very promising. In this approach, the morphologies of titania are controllable (ranging from form-like structure to worm-like aggregates by adjusting the reactant ratio in the sol-gel chemistry) and the mesopores can be tuned through the micro-phase separation of diblock copolymer induced by a so-called good-poor solvent pair. However, sol-gel process normally results in amorphous TiO_2 rather than the crystalline phase which is more desirable for the photovoltaic application. Therefore, we use a special titania precursor, ethylene glycol-modified titanate (EGMT), which could crystallize TiO_2 during sol-gel process. Afterwards, the resulted film is patterned by nano-imprint lithography (NIL) to achieve superstructures. In this study, we use a PDMS master for nano-imprinting. It features nano-pillars with size of 200×200 nm^2 and lattice period of 400 nm as sketched in Figure 1. In the end, a low-temperature route, UV irradiation, is chosen to remove polymer template to obtain mesopores. The surface and inner morphologies of the hierarchical titania film are probed by scanning electron microscopy (SEM) and grazing incidence small-angle x-ray scattering (GISAXS) techniques, respectively. The result shows the NIL does not impact titania nanostructures and mesopores.

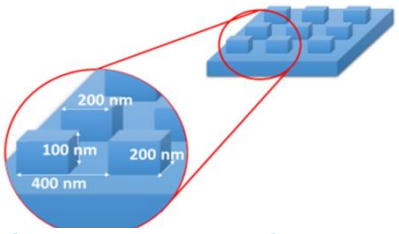

Figure 1: PDMS master for NIL

The achieved hierarchical titania films then are backfilled with P3HT (exciton generator and p-type conductor).to fulfill the active layer. The P3HT solution is dripped on top of titania films and subsequently spin-coated. Next, the samples were post-annealed in nitrogen atmosphere. The surface and inner morphologies of the active layer are investigated with SEM and GISAXS measurements, respectively. The result indicates that P3HT could only infiltrate large pore efficiently. The efficacy of light harvesting is characterized by UV-Vis absorption spectra, which suggests that the active layer with the hierarchical titania film can absorb more light.
Finally, we produce dye-free solar cells based on the hierarchical titania film at low temperature. From the current-voltage characteristics, the device with superstructured features exhibits better photovoltaic performance (Figure 2).

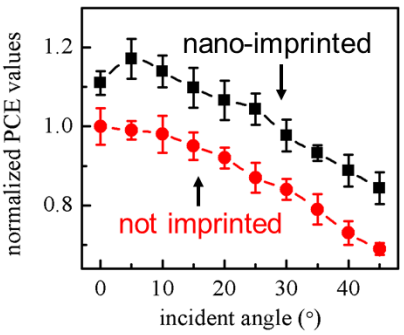

Figure 2: angular dependent PCE

Time-resolved structural analysis of perovskite formation in mesoscopic perovskite solar cells

Oliver Filonik[a], Margret E. Thordardottir, Jenny Lebert, Stephan Pröller, Sebastian Weiß, Jia H. Lew, Anish Priyadarshi, Philippe Fontaine, Peter Müller-Buschbaum, Nripan Mathews, Eva M. Herzig[b]

[a]oliver.filonik@tum.de, [b]eva.herzig@uni-bayreuth.de

Organometal halide perovskite based solar cells have emerged as the fastest-advancing photovoltaic technology to date, reaching certified power conversion efficiencies of up to 22.7%. Along their unprecedented gain in efficiency, the possibility to process the photoactive materials out of solution allows for industrial large scale fabrication techniques like blade coating, ink jet printing and screen printing. One major challenge related to the upscaling from lab scale devices is the need for stable device architectures.

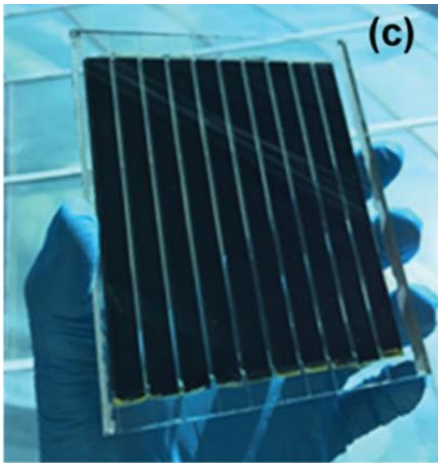

Figure 2: Photograph of a perovskite solar cell module fabricated by ERIAN, NTU. [1]

A novel solar architecture that yields high stability is based on a screen printed mesoporous triple layer out of Titania, Zirconia and Carbon. The photoactive perovskite is infiltrated by solution casting of a precursor solution and subsequent crystallization within the porous scaffold. Our project partners at Nanyang Technological University (NTU) have reported their progress in upscaling this device structure to module sizes with photoactive areas of 70 cm², seen in Figure 1. [1] Together, we have also investigated the moisture tolerance of other perovskite devices [2].

To be able to systematically optimize the device performance, we want to improve our understanding of the perovskite crystal formation. In the Herzig Group, we therefore investigate the influence of processing conditions on the crystallization process with time-resolved characterization methods in order to identify optimal processing protocols. With the generated knowledge, we aim to tune the crystallization process and corresponding device performance.

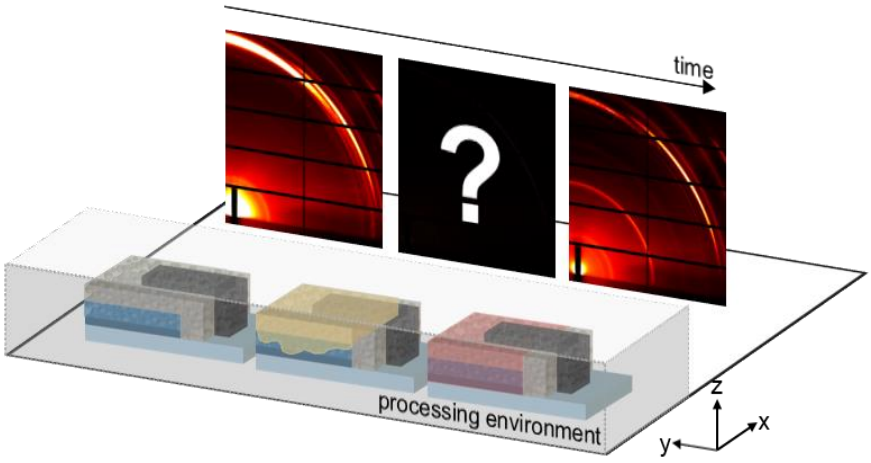

Figure 1: Utilizing time-resolved grazing incidence wide angle X-ray scattering to follow the perovskite formation under controlled processing conditions.

In this project, we present the systematic investigation of the influence of the processing environments on the perovskite formation inside the mesoscopic scaffold by time-resolved grazing incidence wide angle X-ray scattering (Figure 2). Based on our experimental results, we are able to elucidate the impact of solvent environment on the crystallization process, directly related to the device performance. We further highlight the need for controlled processing conditions to ensure reliable device fabrication.

References:

[1] A. Priyadarshi, L.J. Haur, P. Murray, D. Fu, S. Kulkarni, G. Xing, T. C. Sum, N. Mathews* and S. G. Mhaisalkar *Energy Environmental Science, (2016),* **9***, 3687-3692*.

[2] T. M. Koh, V. Shanmugam, X. Guo, S. S. Lim, O. Filonik, E. M. Herzig, P. Müller-Buschbaum, V. Swamy, S. T. Chien, S. G. Mhaisalkar, and N. Mathews, Journal of Materials Chemistry A (2018) **6,** 2122.

In-situ R-SoXS study on a solvent annealing process on OPV materials

Mihael Coric[a], Isvar Cordova, Gregory Su, Feng Liu, Cheng Wang, Eva M. Herzig[b]

[a]mihael.coric@tum.de, [b]eva.herzig@uni-bayreuth.de

In recent years the use of X-rays for investigations on the morphology of polymeric thin films in photovoltaics has increased significantly. X-rays are a suitable tool to investigate morphological changes in polymer films. Generally hard X-rays around 8 keV are used to probe organic photovoltaic samples in grazing incidence geometry. One major issue at this energy regime is that organic materials scatter very similarly. This fact arises due to very similar electron densities within this material class.

Reducing the X-ray energy to absorption edges of certain elements contained within the examined materials can result in drastic changes in the absorption as well as in the dispersion behavior of the materials, offering a much higher contrast compared to hard X-rays. A very powerful and well established tool to exploit these advantages, is Resonant Soft X-ray Scattering at the carbon edge (R-SoXS). Over the past decades it has become a very powerful technique in the analysis of structure and morphology determination in organic thin films, commonly used in organic photovoltaics applications. One drawback of this technique is that it requires the sample to be in a high vacuum, since absorption and scattering is too strong in air.

This, so far, only enables measurements of static samples. However, in regards to the examination of structure formation processes, in-situ studies are essential to achieve a better understanding of the formation processes taking place in thin films.

In this work we present a method using the well-known R-SoXS method in combination with a setup that enables us to execute in-situ studies under a steady flow of vapor inside the vacuum chamber. We will show that it is possible to track changes in the morphology of organic thin film materials for the application in photovoltaics during a solvent annealing process. As a complementary technique, we use in-situ UV-Vis measurements, enabling us to gain a better understanding of the structure and formation processes involved during the solvent annealing process.

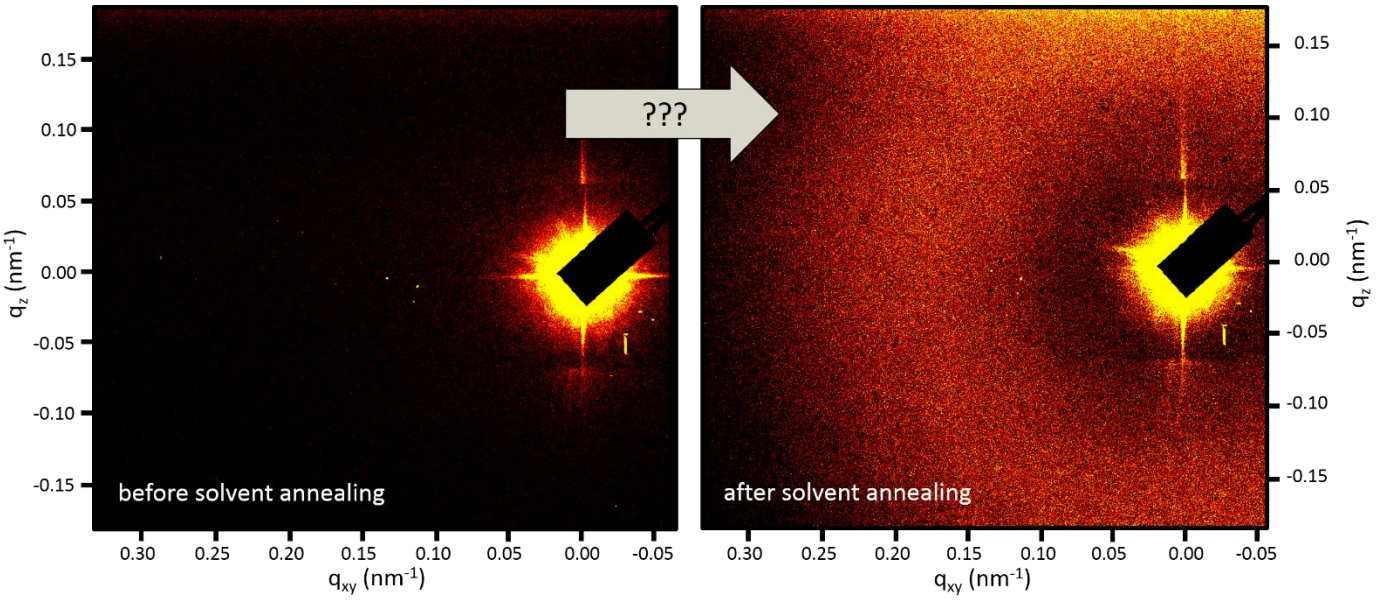

Investigating spray casting as a deposition technique of polymer thin films for large scale photovoltaic applications

Debamitra Chakraborty[a], Sebastian Grott[b], Peter Müller-Buschbaum[c]

[a]debamitra.chakraborty@ph.tum.de, [b]sebastian.grott@ph.tum.de, [c]muellerb@ph.tum.de

Bulk-heterojunction (BHJ) organic solar cells (OSC) have emerged as a promising alternative for conventional inorganic based solar cells over the past few years reaching power conversion efficiencies exceeding 11% [1]. OSC exhibit the potential to be light-weight, flexible and semi-transparent which makes them ideal candidates for a variety of applications. They can be processed using much simpler and low-cost techniques because conductive polymers can be deposited out of solutions. The organic solar cell systems consisting of poly(3-hexylthiophene) (P3HT) as electron-donor and [6,6]-phehyl-C61 butyric acid methyl ester (PCBM) as electron-acceptor have been studied extensively in recent years [2-3]. However, the application of the polymer-based solar cells is still limited. One of the main reason is that the most common scientific method for the preparation of OSC out of solution is spin coating, which is difficult to be scaled up for a large-scale industrial production. The possibility to process this kind of solar cells out of solution offers the chance to apply industrial up scalable methods like inkjet printing, roll-to-roll printing, doctor blading, or spray coating. The advantage of the spray coating method is the usage of small amounts of materials in a dilute solution for large-area deposition and thereby minimize the amount of material discarded during deposition as compared to spin coating. However, there are several drawbacks of this processing technique, like, bare control on the inner morphology. Furthermore, by spray casting, it is not only difficult to control the inner morphology but also difficult to achieve an overall good homogeneity of sprayed films which results in a higher surface roughness.

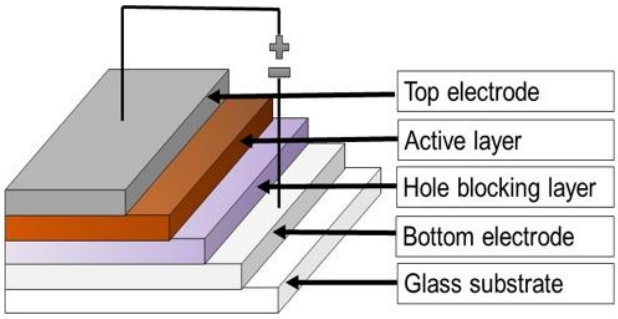

Figure 1: Solar cell in standard geometry

In this study, we focus on achieving a homogeneous layer thickness using spray casting. The deposition conditions of the P3HT:PCBM film was optimized to minimize the surface roughness by controlling various spray parameters like flow rate, nozzle to substrate distance etc. To further enhance the film surface homogeneity, the samples were treated with thermal annealing. Moreover, we investigated thin films of different mixtures of conjugated polymers forming organic bulk hetero-junctions, which were processed by both spin coating or spray casting to investigate the influence of the two different processing techniques on the film‘s morphology and photophysical properties.

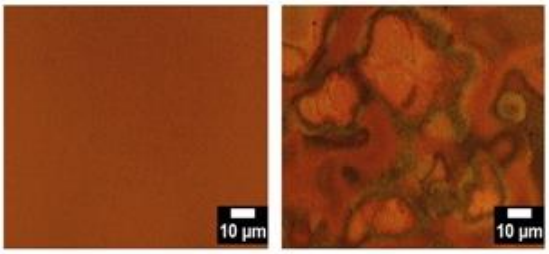

Figure 2: Surface Morphology of Spin and Spray coated samples

[1] W. Zhao, D. Qian, M. Hernández, S. Zhang, S. Li, O. Inganäs, F. Gao, J. Hou, *Adv. Mater.* **28**, 4734-4739 (2016).
[2] J. Cui, Á. Rodríguez-Rodríguez, M. Hernandez, M. C. García-Gutierrez, A. Nogales, M. Castillejo, D. Moseguí González, P. Müller Buschbaum, T. A. Ezquerra, E. Rebollar, *Appl. Mater. Interfaces* **8**, 31894-31901 (2016).
[3] C. Girotto, B. P. Rand, J. Genoe, P. Heremans, *Sol. Energy Mater. Sol. Cells* **93**, 454-458 (2009).

Investigation of novel material systems for increasing the efficiency of organic solar cells

Christian Weindl[a], Franziska C. Löhrer[b], Peter Müller-Buschbaum[c]

[a]christian.weindl@ph.tum.de, [b]franziska.loehrer@ph.tum.de, [c]muellerb@ph.tum.de

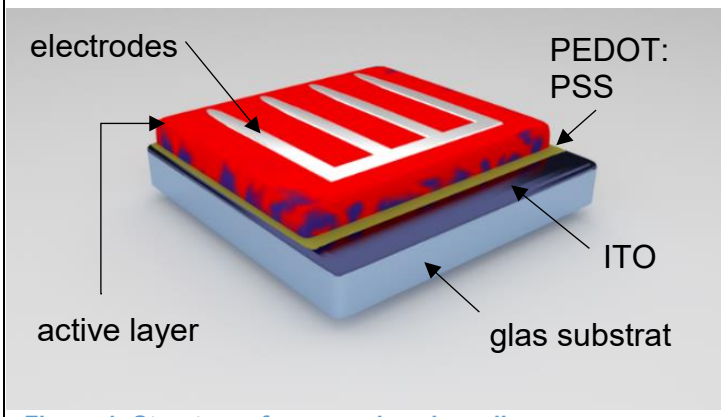

Figure 1: Structure of an organic solar cell

In the last decade, interest in organic photovoltaics has increased strongly with enhanced performance values. Even though organic solar cells cannot compete with conventional solar cells in terms of efficiency and long-term stability yet, they have reached the point of industrial application due to a range of unrivalled advantages. Apart from their light weight and their highly tunable optical and mechanical properties, organic solar cells can be produced in an easy and cheap, solution-based way which offers the possibility of mass production via roll-to-roll processing. Their advantages play a particular role in areas not accessible to conventional solar cells, such as curved, flexible or transparent surfaces as well as mobile devices. In our work, we investigate novel material systems used to increase the performance of organic solar cells in terms of efficiency as well as long-term stability. Here, we present insights into the correlation of optical and morphological properties of polymer-based organic photovoltaics by combining real-space imaging and optical spectroscopy.

For years, carbon nanostructures have played a prominent role in case of electrochemical energy storage. Especially carbon nano onion films as a conductive additive for supercapacitors can be implemented to improve electrical characteristics. These onions with an almost spherical shape consist of several enclosed fullerene-like carbon shells. Amongst various ways to synthesize these onions, the most commonly used technique is the graphitization of nano diamonds at temperatures above 1000 °C. [1] These high temperatures lead to a high degree of sp2-hybridization and thereby, result in comparatively high electrical conductivity values, a large surface area and nanoscopic size. [2] However, not much is yet known about the synthesis and morphology of thin films with implemented carbon onions. Therefore, we aim to investigate the influence of different processing pathways on the structural and optoelectronic properties of these films. In first studies, we optimize processing parameters such as the type of solvent, concentration and spin coating velocity in order to avoid generating discontinuous or inhomogeneous films.

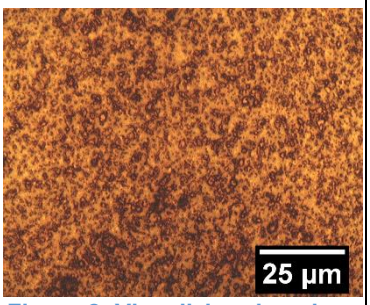

Figure 2: Visualizing domains with an optical microscope

[1] M. Zeiger, N. Jäckel, V. N. Mochalin, V. Presser, J. Mater. Chem. A, 2016, **4**, 3172-3196
[2] M. Zeiger, N. Jäckel, D. Weingarth, V. Presser, Carbon, 2015, **94** , 507-517

Printing technology of organic solar cells

Benjamin Predeschly [a], Sebastian Grott [b], Peter Müller-Buschbaum [c]

[a]benjamin.predeschly@ph.tum.de, [b]sebastian.grott@ph.tum.de, [c]muellerb@ph.tum.de

Global warming caused by air-polluting combustion engines and continually increasing energy consumption all around the globe has been giving rise to finding new methods of converting energy. Consequently, the focus has been shifted to discovering and making use of renewable resources that don't harm the environment and are of non-limited occurrence. One of these resources, namely the sunlight, can be harvested by photovoltaics, converting energy from the sun into electrical energy, which is arguably the most important and practicable form of energy available on earth.

A very promising technology of photovoltaics is based on organic materials. These solar cells exhibit advantages in comparison to inorganic photovoltaics, which are light weight, potential transparency, low-cost processing (less energy consumption and manufacturing costs) and lower energy payback time. In the last decades, great effort has been made by intense investigation in this research area. It continues to be an important and future-compliant branch of research. In this context it is essential to ensure the competitiveness of the organic solar cell by improving and simplifying its fabrication process as well as increasing its reliability, lifetime and efficiency. [1] Responsible and of prime importance for this is the morphology of the solution-based bulk heterojunction in organic solar cells, which is why the inner structure has to be analyzed and improved in the production process continually. Therefore, advanced scattering techniques, like grazing incident small angle scattering (GISAXS) and grazing incident wide angle scattering (GIWAXS) are applied to probe the inner morphology of organic active layers. [2]

Figure 1: Laboratory printing setup [4]

An organic solar cell in lab scale is prepared by the widely used spin coating method. Other methods which are suitable for industrial application are spray coating or the printing procedure. They have got the advantage of a large-scale production, especially the roll-to-roll printing, which is a low-cost manufacturing process and it's one of the most promising methods to process organic solar cells on large surfaces. [3]

Further investigations of this print technology of organic materials on foils are carried out in these studies. With the printing technology the fabrication process and the properties of organic solar cells are intended to be optimized. Furthermore, photoelectric characteristics as well as spectroscopic investigations will be carried out to get a full view on the properties of printed organic solar cells.

References

[1] W.Wang, C.J.Schaffer, L.Song, V.Körstgens, S.Pröller, E.Dwi Indari, T.Wang, A.Abdelsamie, S.Bernstorff, P.Müller-Buschbaum; *J. Mater. Chem. A 3*, 8324-8331 (2015).
[2] A.Hexemer, P.Müller-Buschbaum; *IUCrJ 2*, 106-125 (2015).
[3] C.J.Schaffer, J.Schlipf, E.Dwi Indari, B.Su, S.Bernstorff, P.Müller-Buschbaum; *ACS Appl. Mater. Interfaces 7*, 21347-21355 (2015).
[4] S.Pröller; *Doctoral dissertation*, 78 (2018).

Live fast, die young – understanding degradation processes in high-efficiency organic photovoltaics

Franziska C. Löhrer[a], C. Senfter, P. Müller-Buschbaum[b]

[a]franziska.loehrer@ph.tum.de, [b]muellerb@ph.tum.de

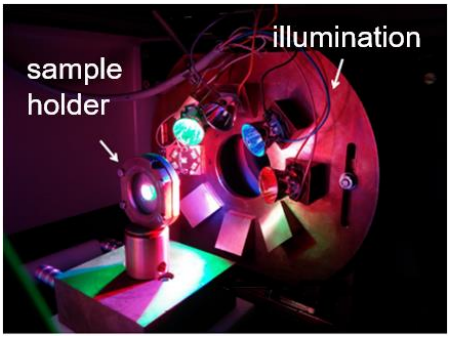

Figure 1: Illumination setup used to induce aging in photoactive thin films

With a growing population and an increasing living standard, the world's demand for sustainable energy is rising. Alternative energy sources such as solar, wind or hydropower already contribute significantly to the energy landscape in Germany with around 36.2 % of the overall produced electricity for 2017 [1]. However, they are typically limited to static, large-scale applications. Organic photovoltaics (OPV) have received high attention in recent years as an interesting alternative to conventional solar cells. Using polymer films as active material for energy conversion has a variety of potential advantages. Photoactive polymers can be synthesized from low-cost, abundant precursor materials and enable the formation of thin, light-weight and flexible films with tunable color. The devices can be produced via roll-to-roll processing, an easily up-scalable and thereby low-cost production technique. Due to these advantages, OPV devices could be integrated into a wide range of applications, combining functionality with design in fields as diverse as mobility, architecture or clothing.

Recent research efforts focus on enhancing the photovoltaic performance in order to make organic solar cells feasible for industrial purposes. This has led to the development of low band-gap materials with reported power conversion efficiencies nearing 12 %. [2] However, especially high-efficiency polymers are sensitive to various degradation processes, which strongly decrease their lifetime in comparison to commercially available inorganic photovoltaics. Several issues concerning the optimal thin film morphology and architecture will need to be addressed to make organic solar cells a potential candidate for mass market applications. Our work takes a deeper look at these aging processes of photoactive materials used in OPV devices.

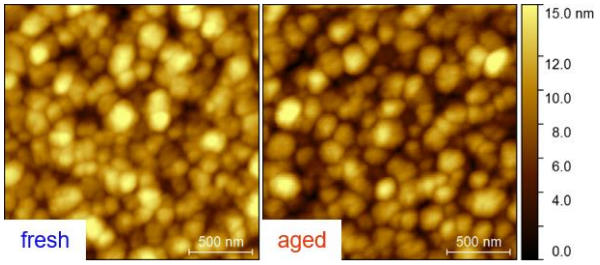

Figure 2: Microscopy images of a freshly prepared vs. an aged polymer film

We follow the chemical and physical changes occurring in low bandgap polymers during light-induced aging and test ways to eliminate typical degradation pathways. The thin film morphology is investigated using real-space imaging as well as X-ray scattering techniques. Optical and IR spectroscopy methods give insights into the chemical changes inside the polymer.

References

[1] Quartalsbericht 04/2017, Umweltbundesamt, AGEE-Stat.
[2] J. Zhao, et al., Nat. Energy 1, 15027 (2016)

Challenging Silicon: Perovskite-Based Photovoltaics

Lennart Reb[a], Peter Müller-Buschbaum[b]

[a]lennart.reb@tum.de, [b]muellerb@ph.tum.de

Sunlight is one of the most promising clean and renewable energy sources to supply the continuously growing global power demand. Today, silicon-based photovoltaics (PVs) convert sunlight into electric power, exceeding efficiencies of 20 per cent. However, their resource- and energy-intensive and therefore cost-intensive production drives the search for novel materials, which might eventually substitute silicon-based PVs.

One particularly promising novel material is hybrid organic-inorganic halide perovskite $CH_3NH_3PbX_3$ (X=I,Br,Cl). In contrast to silicon, the absorption characteristic of perovskite is highly tunable, so it can also efficiently absorb the more energetic part of the solar spectrum. More importantly, solution-based fabrication techniques of thin film perovskite solar cells are low-cost and offer therefore a tremendous advantage over silicon based PVs, while exerting similar efficiencies. Since the use of flexible substrates is possible, thin film devices will find an application in new fields, as e.g. windows, where conventional silicon is unfeasible.

However, on the way towards commercial perovskite-based PVs it is necessary to overcome challenges: perovskite shows a poor long-term stability; in particular, it is known to be sensitive to moisture, which seems to primarily drive the degradation of the crystal structure. Some of the typically used organic contact layers, which enclose the photo-active perovskite layer, also show long-term degradation in natural environments. Mastering these challenges, in particular the long-term stability of perovskite and its contact layers is a key objective to open a wide range for future applications for perovskite-based, potentially solution-processed, and therefore low-cost PVs.

In this project, we will analyze the degradation of thin film perovskite and organic donor and acceptor contact layers caused by moisture. In detail, we will probe the moisture-induced morphological changes in a selection of typically employed contact layer materials as well as in mixed halide perovskite including different amounts of chlorine or bromine with several methods, such as ultra-violet/visible spectroscopy, scanning electron microscopy (SEM), photoluminiscence (PL) spectroscopy, and X-ray diffraction (XRD) techniques. This enables us to characterize the degradation rate of the different compounds, which in turn will provide us a better understanding of the dominant degradation processes – essential for the selection of suitable materials for perovskite PVs with an improved long-term stability. Designs with a promising stability will be subjected to *in-situ* measurements (as shown schematically on the right), to directly assess the nano-morphological changes which drive the degradation of perovskite PVs [1].

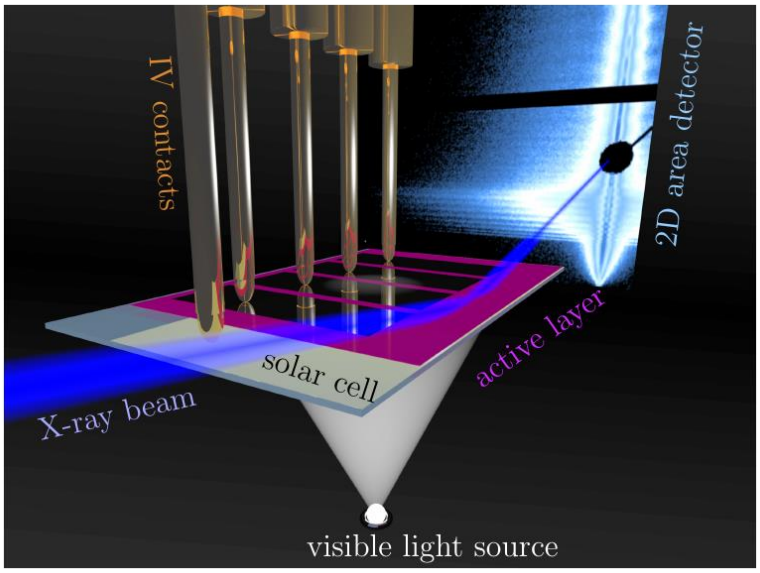

[1]: Schaffer, C. J., Palumbiny, C. M., Niedermeier, M. A., Jendrzejewski, C. , Santoro, G. , Roth, S. V. and Müller-Buschbaum, P. (2013), A Direct Evidence of Morphological Degradation on a Nanometer Scale in Polymer Solar Cells. Adv. Mater., 25: 6760-6764.

Influence of SnIP nanoparticles on organic thin films for photovoltaic applications

Sebastian Grott[a], Claudia Ott, Nuri Hohn, Senlin Xia, Kun Wang, Tom Nilges, Peter Müller-Buschbaum[b]

[a]sebastian.grott@ph.tum.de, [b]muellerb@ph.tum.de

In the last decades, the influence of the global warming caused by the extensive usage of fossil fuel combustion has become increasingly discussed. Furthermore, the limitation of gas, oil and coal resources has led to increasing interest in renewable energies to tackle the evolving energy demand. Thereby photovoltaics are a promising candidate for future energy provision, as the energy delivered by the sunlight is converted into electricity. This technology has the potential to cover the world's energy consumption.

In this context organic photovoltaics (OPV) devices are a promising technology, owing many advantages compared to the conventional semiconductor-based solar cells, like light weight, flexibility and semi-transparency. Furthermore, organic photovoltaics offer the possibility to be produced at low-cost, due to the processing out of solutions, which allows large scale manufacturing techniques like roll-to-roll printing or spray casting. These properties open a wide field of applications.

Recent research efforts focused on the photovoltaic performance to make solar cells attractive for industrial purposes. This results in the development of new compounds for the preparation of organic photovoltaics with power conversion efficiencies surpassing 11%. [1] However, OPVs still exhibit efficiency losses and lower lifetimes in comparison to conventional inorganic photovoltaic devices. To make organic photovoltaics competitive for mass market applications, several issues have to be investigated.
Thus, the inner morphology of the organic thin films applied in organic solar cells is one of the key aspects concerning the charge carrier separation and thereby the power conversion efficiency. Furthermore, a promising approach to enhance the efficiency of organic photovoltaic devices seems to be the doping of the bulk heterojunction active layer with inorganic nanoparticles. Recently, the most widely investigated bulk hetero junction donor-acceptor system of P3HT:PCBM was doped with iron oxide nanoparticles, resulting in an increase of the efficiency of these solar cells. [2]

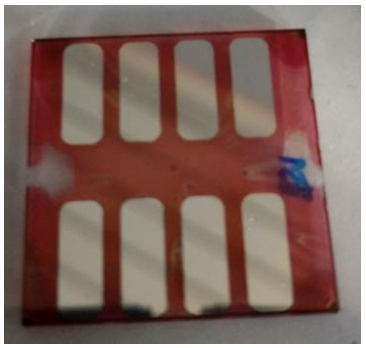

Figure 1: Photograph of an organic solar cell.

Based on such approach, our work takes a deeper look at the effect of inorganic SnIP nanoparticles [3] on the electrical characteristics of organic solar cells, depending on different concentrations of the nanoparticles, investigated via current density-voltage measurements. Furthermore, we study the influence of the incorporated inorganic compounds on the crystallinity and the inner morphology of the active polymer layer, using advanced scattering techniques, like grazing incidence small angle X-ray scattering (GISAXS) and grazing incidence wide angle X-ray scattering (GIWAXS). [4] Additionally, we want to gain further insight in the correlation of inner morphology and photoelectric characteristics of organic solar cells. Complementary UV-Vis spectroscopy and photoluminescence measurements are carried out in these studies.

References

[1] W. Zhao, et al., Adv. Mater., 28, 4734 (2016).
[2] D. M. González, et al., Adv. Energy Mater. 5, 1401770 (2015).
[3] D. Pfister, et al., Adv. Mater., 28, 9783 (2016).
[4] A. Hexemer, et al., IUCrJ, 2, 106 (2015).

Cellulose-based conducting nanocomposite films via spray deposition with *in situ* GISAXS

Volker Körstgens[a], Felix Martin, Calvin Brett, Daniel Söderberg, Stephan V. Roth, Peter Müller-Buschbaum[b]

[a]volker.koerstgens@ph.tum.de, [b]muellerb@ph.tum.de

In the emerging field of printable electronics there is a growing demand for transparent, flexible conductive materials. Cellulose-based substrates are a promising sustainable alternative to fully synthetic polymers [1]. We present the fabrication of conducting composite films of cellulose nanofibers (CNF) and poly(3,4-ethylenedioxythiophene)-poly(styrenesulfonate) (PEDOT:PSS). CNF of high surface charge are produced with TEMPO (2,2,6,6-tetramethylpiperidine-1-oxyl radical)-mediated oxidation [2] and mixed with PEDOT:PSS in aqueous dispersion. Composite films are produced with a spray deposition followed in situ with GISAXS with sub-second time resolution. GIWAXS applied to the final films was used for the investigation of crystallinity in the composite. Different CNF/PEDOT:PSS ratios and the influence of the additive glycerol were investigated. The changes of the morphology and the influence on electric conductivity with the introduction of a compositional gradient are discussed. As the synchrotron-based investigation allowed for a high temporal resolution of 0.1 s, insights into the very first stages of the deposition process were obtained. From the overall situ study improvements for the spray deposition procedure are derived that allow for a better control of the morphology of the conducting films.

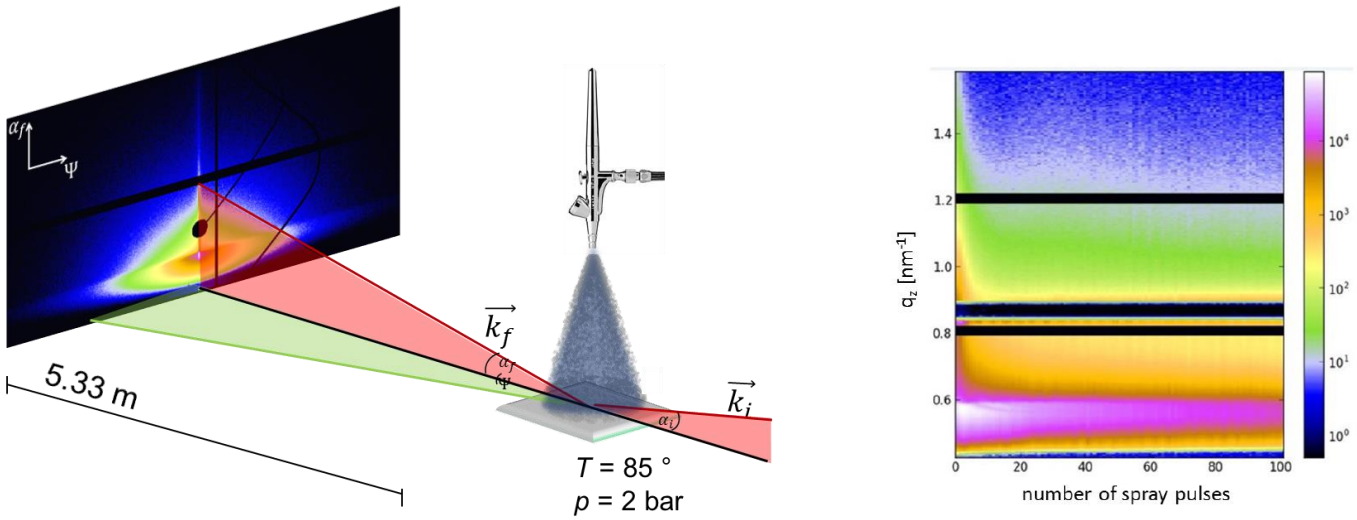

Figure 1: spray deposition set-up with *in situ* GISAXS and composite image of vertical cuts of 2D detector images

One of the advantages of the polyelectrolyte complex PEDOT:PSS is its processability as an aqueous dispersion. The complex structure with its non-conductive PSS part although makes it necessary to use additives like glycerol or a post-treatment with ethylene glycole in order to reach high conductivities. The increase in conductivity can be explained by a change of morphology in the meso- and the nanoscale [3]. The *in situ* investigation of the CNF/PEDOT:PSS composites are consistent with the application of glycerol as a plasticizer allowing for morphological changes especially with elevated temperatures as used with the spray deposition process.

[1] Zhu et al., Chem. Rev. 116, 9305-9374 (2016)
[2] Isogai et al., Nanoscale 3, 71-85 (2011)
[3] Palumbiny et al., J. Phys. Chem. C 118, 13598-13606 (2015)

Biogas power plants for deterministic power generation

Katharina Bär[a], Abdessamad Saidi [b], Wilfried Zörner[c], Christoph Hackl[d]

[a]Katharina.Baer@thi.de, [b]Abdessamad.Saidi@thi.de, [c]Wilfried.Zoerner@thi.de, [d]Christoph.Hackl@tum.de

Due to the expansion of renewable but fluctuating power generation from wind and solar energy, the demand for advanced energy system management is steadily increasing. To meet the resulting challenges and ensure future electricity grid stability, controllable power suppliers are required. Apart from solid biomass, biogas represents the only energy source that shows high storage capacities among the renewable energies.

Within the present research project, the technical and economic potential of flexible biogas power plants to contribute to grid stability via flexible power generation is determined. In this context, flexible plant operation signifies energy production, considering the needs of the energy markets as well as the requirements of electricity and heat grids. The main objective of the research project is to adapt the present control systems of a biogas power plant to meet the requirements of the future electricity grid. To be able to optimize a biogas power plant within a regional electricity grid including further renewable variable energy producers, the interactive operation of biogas and photovoltaic (PV) power plants at one grid connection point has to be investigated and simulated.

Analyzing each component to improve the interaction of the whole system is crucial to understand the system behavior and to obtain valid simulation results. The main focus of the research project is on the development of a predictive control system, which is supposed to respond to short-term fluctuations in photovoltaic (PV) power generation within seconds. The predictive control system will take further components and aspects, such as the capacity limits of the local power grid and time-varying weather conditions (Figure 1) into account. To generate valid concepts for the flexible electricity production via biogas power plants, considering all components of the energy system, the development of optimization algorithms represents a further main aspect of the research project.

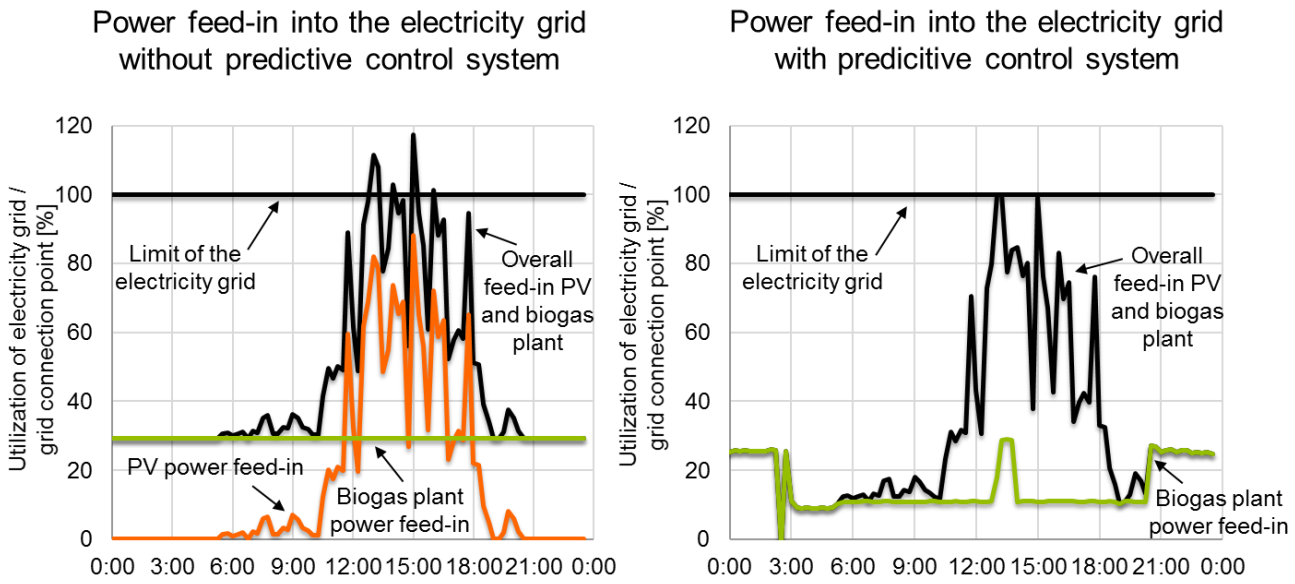

Figure 1 Flexible power generation of the biogas power plant with a predictive control system

With this predictive control system, an increase of the overall energy feed-in of the biogas and PV power plant into the electricity grid can be achieved simultaneously to the improvement of the security and reliability of the electricity grid.

Network Design and Yield Optimisation of Solar District Heating Systems for Urban Applications

Daniel Beckenbauer[a], Wilfried Zörner[b], Vicky Cheng[c]

[a]Daniel.Beckenbauer@thi.de, [b]Wilfried.Zoerner@thi.de, [c]Vicky.Cheng@tum.de

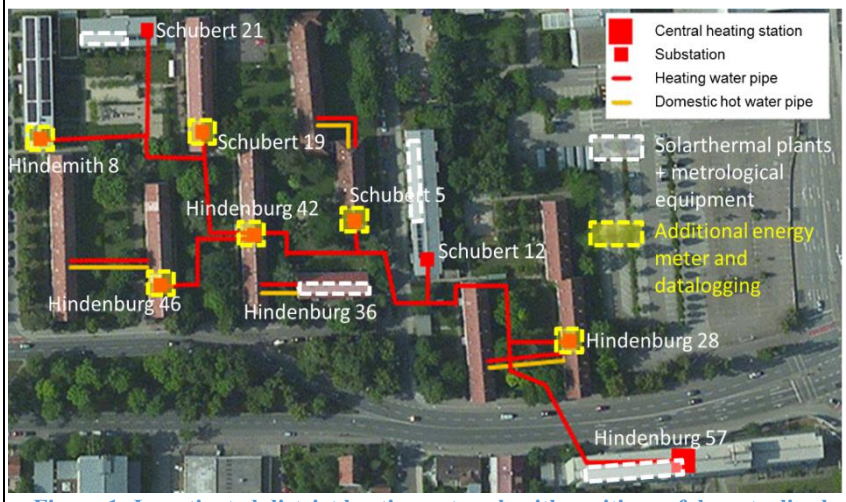

Figure 1: Investigated district heating network with positions of decentralized solar thermal plants

Multi-storey residential buildings provide high potential for solar-assisted local district heating. Current research projects focus on the utilisation of large seasonal storages to achieve a solar fraction of above 50 %. However, for retrofitting densely built-up urban areas, the feasibility of solar district heating is often restricted by the limited space available for collector arrays and heat storages. Moreover, high storage capacities come with high investment and heat production costs. These drawbacks impede the applications of seasonal storage concepts in existing urban areas and hinder the dissemination of large solar-thermal systems.

This project aims to tackle these challenges by investigating a novel solar district heating design based on distributed solar collector arrays and thermal heat storages in multi-storey residential buildings with bi-directional heat distribution capability and the intelligent interaction of these components. The study will examine the network design and yield optimisation of such a system in various urban contexts. Within the project, a real district heating network in Ingolstadt was equipped with decentralised solar thermal plants (Figure 1). These plants provide either a local use of the solar gains for domestic hot water preheating, a pure feed in to the return pipe of the district heating network or a combination of the aforementioned options.

The comprehensive metrological data acquired during one year of operation served as a basis for the validation of the simulation model, which was originally used to design this system. Subsequently, modified components were derived, enabling the simulation of a reversed flow behaviour in the district heating system model for the investigation of a return-supply feed-in strategy (Figure 2). The purpose of these components is a realistic reproduction of heat losses, transport delays and thermal capacities of the pipes, which mainly influence the operation and efficiency of the complete network. Based on the modified model, a simulation-based comparison of different hydraulic integration schemes was performed for multiple numbers and sizes of decentralised solar thermal plants and different types of residential buildings. Recommendations for the design and dimensioning of similar retrofitting projects can be derived from the simulation results regarding fossil energy savings and heat production costs.

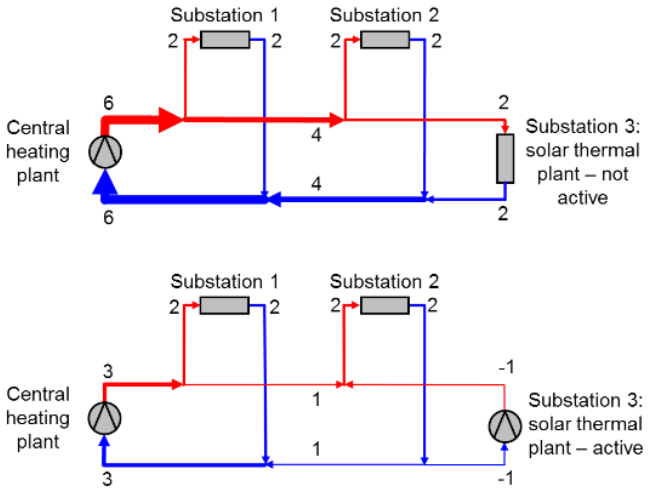

Figure 2: Change in flow rates during pure central supply (top) and decentralized feed-in (bottom)

Operational Volatility and Synergistic Value in Vertically Integrated Energy Systems

Gunther Glenk[a], Stefan Reichelstein[b]

[a]gunther.glenk@tum.de, [b]reichelstein@stanford.edu

We examine the magnitude of synergistic effects in vertically integrated energy systems that arise when the external market for an intermediate input (electricity) is imperfect and the two subsystems are subject to operational volatility in terms of price and output fluctuations. Our study is motivated by the rapidly changing economics of renewable energy. As has been widely reported, the cost of generating electricity at wind and solar photovoltaic installations has been falling dramatically, a trend that has been accompanied by a corresponding increase in the share of renewable power. Yet, the intermittent nature of wind and solar photovoltaics presents new challenges in balancing electricity supply and demand in real-time. One potential remedy is to divert surplus energy from renewable power sources to the production of energy storing products like hydrogen.

Our main question in this study is whether investment in a facility that combines renewable energy with Power-to-Gas (PtG) production has *synergistic value*. Our criterion for such synergies is that the net present value (NPV) of the vertically integrated system exceeds the sum of the optimized NPVs of the two stand-alone facilities that would buy or sell electricity only on the external market. If either or both energy systems have negative NPVs on their own, the presence of a synergistic value must entail operational synergies that more than compensate for the cost of capacity investments, which would be excessive if the individual systems were to operate in stand-alone mode. In the presence of such synergistic values, our analysis also characterizes the relative optimal size of the two capacity investments. We refer to the lowest hydrogen price at which the vertically integrated system achieves a synergistic value the break-even price for hydrogen.

We apply this framework to current settings in Germany and Texas for systems that combine wind energy with Power-to-Gas (PtG) facilities for hydrogen production. In the context of Texas, it turns out that neither electricity production from wind power nor hydrogen production from PtG facilities will be profitable on its own in the current market environment. Yet, provided the capacity of the two subsystems is sized optimally in relative terms, the attendant synergistic gain from a vertically integrated system more than compensates for the stand-alone losses of the subsystems.

The final part of our analysis seek project likely improvements in economics of combined en systems that integrate wind pc with hydrogen production. Sev factors are likely to contribute more robust synergistic values ir future. These include sustained p reductions for both wind turbines PtG facilities as well as gre operational volatility in terms fluctuating market prices electricity. Overall, our project indicate that even relative to the benchmark of the low hydrogen prices associated with large-scale industrial supply, synergistic value for the integrated systems will widely emerge in both Texas and Germany within a decade (Figure 1). These projections take into account that the public support for wind energy, e.g., the production tax credit available in the U.S., is scheduled to be phased out in the coming years.

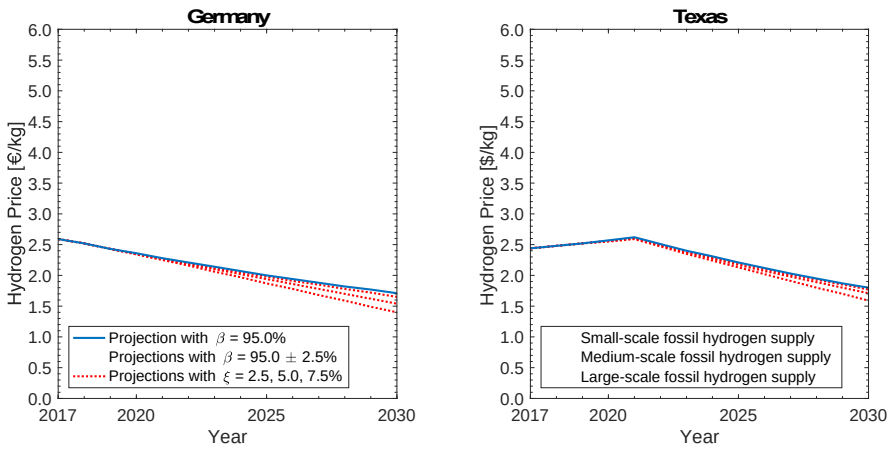

Figure 1: Trajectory of future hydrogen break-even prices.

Potential of the oxygenate fuel oxymethylene ether: emission-neutral and particulate-free diesel engines

Patrick Dworschak[a], Dr.-Ing. Martin Härtl[b], Prof. Dr.-Ing. Georg Wachtmeister[c]

[a]dworschak@lvk.mw.tum.de, [b]haertl@lvk.mw.tum.de, [c]wachtmeister@lvk.mw.tum.de

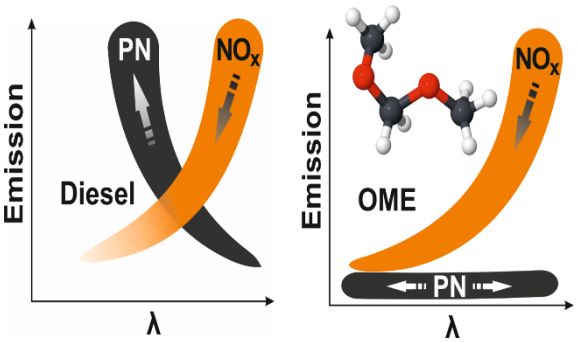

Figure 1: NO_X-PN trade-off for diesel (left) and soot-free combusting OME (right)

Current efforts to reduce the use of fossil resources towards a CO_2-neutral energy and transport scenario 2050 involve the search for suitable energy platforms and corresponding synthetic fuels. Primary requirements for synthetic fuels are in hierarchical sequence: CO_2-neutrality, availability of energy on a sustainable basis, low impact on environment, economic efficiency, and functionality. Suitable fuels will have to be qualified in terms of long-term stability, low toxicity, good material compatibility, adequate evaporation, ignition behavior, and other material specific properties. This qualification needs to be defined for each fuel in corresponding standardization.

Diesel engines require a fuel with good ignitability and a high flash point, which makes it possible to maintain a reliable infrastructure and allow safe handling. Various experiments with the C1 substance-class of oxymethylene ethers (OME_n, CH_3-O-(CH_2-O)$_n$-CH_3) as fuel for diesel engines have shown a beneficial emission behavior. In 2011 MAN Truck&Bus tested a blend of diesel fuel, 7 % biodiesel and 20 % OME_n with chain lengths of n=3, 4 in a heavy-duty diesel engine and reported significant reductions of PM, soot, and PN compared to diesel fuel. Neat and blended OME_n with n=2,3,4,5,6 was tested by Pellegrini and co-workers starting in 2012 on a light-duty engine and displayed substantial improvements of the soot behavior and effective reduction of NO_X by utilizing new potential of ECU calibration and high EGR.

OME_1 was found to be the most effective fuel for soot-less combustion in a screening of various ether substances. Engine testing on a heavy-duty diesel engine was performed and both OME_1 and OME_n of n>1 revealing positive effects on gaseous and particle emissions, especially on particulate number (PN, Figure 1). Corresponding work with similar findings was performed at the universities of Dresden, Aachen, and Darmstadt, the latter addressing the possibility to run a diesel engine at stoichiometric A/F ratio without soot emissions and hence allowing the use of a three-way-catalyst (TWC). Experiments in a constant volume combustion chamber of Barro et al. at the university of Zürich proved the reduction of soot to be an effect evident in the complete course of combustion and thus not only associated with an improved oxidation behavior, but also with the inhibition of soot formation.

The aim of this poster is to document the latest experimental results of OME-combustion in a diesel engine at the Institute of Internal Combustion Engines. The utilization of exhaust gas recirculation (EGR) leads to highly reduced NO_X-emissions while particulate matter output at ambient level is realized due to the low-soot combustion of OME.

Gaseous emission components are measured with an AVL-FTIR system before and after an oxidation catalyst (DOC). Particulate emissions are measured using a Horiba MEXA-2300 SPCS particle counter and an AVL Microsoot Sensor (Figure 2).

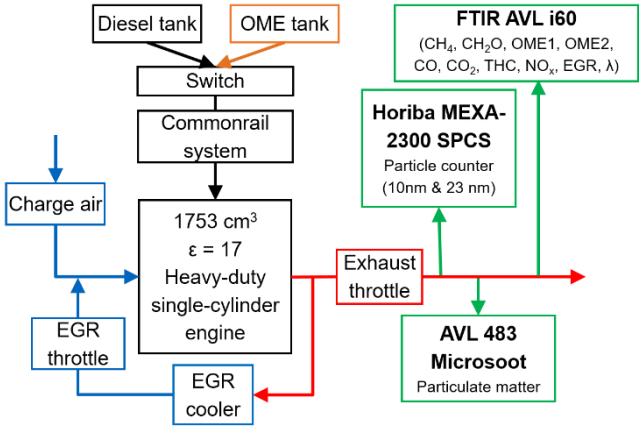

Figure 2: Engine test bench

Biomass-fired Boilers with Utilization of Condensing Heat by Means of a Sorption Heat Pump

Tina Hermann, Julian Geier-Pippig, Christian Schweigler

tina.hermann@hm.edu

Extracting heat from hot flue gas leads to a significant increase in boiler efficiency. By utilization of condensing technology, the flue gas is cooled down below the dew point of the contained water vapor and allows recovering the latent heat in addition to the sensible heat.

In conventional systems, the flue gas is cooled down and condensed by heat exchangers that transfer heat to the return flow of the district heating network. The cooling and condensation is thereby limited to a temperature around 50 °C. The integration of an absorption heat pump (AHP) allows cooling of the flue gas down to temperatures around 25 °C and serves for upgrading the low grade heat for further utilization in conventional heating systems. Therefore, the fuel utilization rate can be increased up to 20 %, depending on the water content of the biomass fuel.

Within the research project the integration of an AHP into the heating system of a woodchips fired biomass boiler is investigated. The development aims at biomass boilers with outputs above 50 kW.
The single components of the AHP are designed regarding an optimized thermo-hydraulic integration into the heating system. For generating the required driving heat for the heat pump at about 90 °C, heat extraction from the boiler is modified accordingly. The heat of condensation of the flue gas is released below 55 °C and is directly transferred to the evaporator of the AHP. To ensure a reliable operation, the sorption cycle is realized by natural circulation of sorbent between Generator and Absorber.

The poster presents the increasing fuel utilization rate, the hydraulic concept for the integration of biomass boiler, heat pump and heat supply to the district heating network as well as the conceptual design of the main components of the AHP.

Multitier Reference Model for Energy System Operation - Digitalization and Interoperability

Franz Christange[a], Thomas Hamacher[b]

[a]franz.christange@tum.de, [b]thomas.hamacher@tum.de

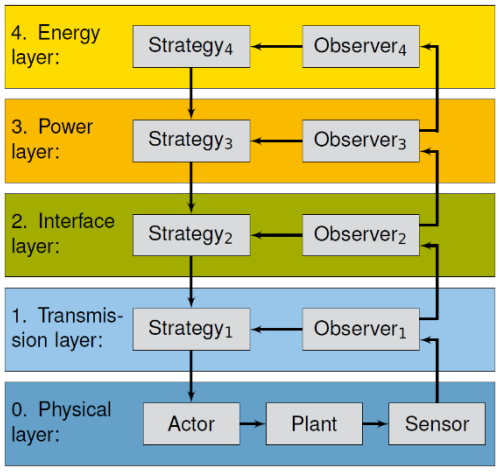

Figure 1: Energy system in five layers

Conventional communication and computation systems and the electricity system rank among the highest innovations of the 20th century. While communication and computation systems have already taken the next step from analogue to digital systems in the end of the 20th century, the transition of the electricity system is imminent. The functionality and complexity of communication systems escalated by its digitalization. We state that one major brick to handle the emerged challenges was the well-known open systems interconnection (OSI) Model, a multitier reference model which standardizes the communication functionality without specifying the underlying technology. Its aim is to enable the interoperability of diverse communication systems with standard protocols.

A similar requirement emerges from the transition to future digitalized energy systems. The number of different appliances in the electricity system increases continuously which means an escalating complexity through the requirement of cooperation of diverse technologies. We propose this multitier reference model for energy system operation to enable the interoperability of the emerging diverse appliances and technologies without endangering the reliability of electricity system operation. This reference model partitions the energy system into five layers (Fig. 1). Each device in the electricity system can only interact with other devices on the same layer with the joint goal to fulfill the layer's specific goal. Each layer contains a strategy which interacts top-down through setting specified references. The observer of each layer abstracts bottom-up measurement data specifically for each corresponding layer's strategy. This leads to a decoupling of the five layers such that each layer's strategy can operate independent of the other layer's specific implementations and technologies. The abstraction of each layer only requires its underlying layer's specific task to be accomplished, which leads to the depiction as the cascaded control loop in Fig. 2.

The bottom layer, called physical layer, comprises the real appliances and facilities of the energy system. It is characterized by field quantities like electrical and magnetic fields and charge flow densities. The transmission layer comprises the fast dynamical interactions of instantaneous voltages and currents. It converts waveform references mathematically into machine commands for the actor to be controlled. The interface layer abstracts the transmission layer's processes to transform the dynamics of instantaneous voltages and currents into a dynamical process of fixed sinusoidal oscillations. Consequently, the dynamical processes get decelerated to keep the sinusoidal shape. The powerflow layer focuses on the actual active and reactive power flow in the available infrastructure, for instance it considers each phase individually. It is faced with limited transmission capabilities and its goal to reduce transmission losses. The energy layer mainly meets the constraints of conservation of energy. It mainly optimizes and coordinates the required energy generation to supply the energy consumption and the occurring losses.

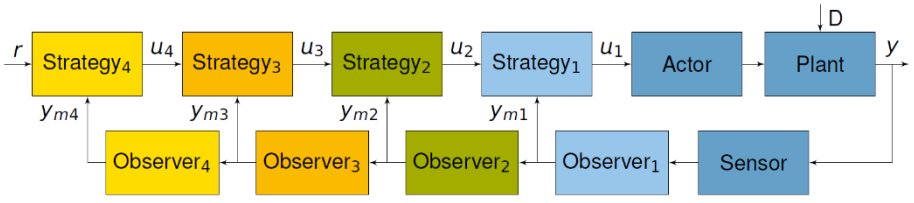

Figure 2: Energy system dynamics as cascaded control loop

Hybrid thermoelectric films based on PEDOT:PSS

Nitin Saxena[a], Anton Greppmair, Mihael Čorić, Jan Wernecke, Mika Pflüger, Michael Krumrey[b], Eva M. Herzig[c], Martin S. Brandt[d], Peter Müller-Buschbaum[e]

[a]nitin.saxena@ph.tum.de, [b]michael.krumrey@ptb.de, [c]eva.herzig@ph.tum.de, [d]martin.brandt@wsi.tum.de, [e]muellerb@ph.tum.de

The usage of fossil fuels has led to increased levels of greenhouse gases, which in turn result in devastating meteorological phenomena. Indications of this imminent change in global climate have, over the past years, been responsible for an increased interest in techniques for power generation based on renewable energies.
Solar cells possess the ability to convert visible solar radiation into electrical power. While they are already highly efficient and have been implemented in daily life, it is also feasible to think of alternative ways of harvesting energy. Heat is lost in almost all processes which occur in daily life, which is evident looking at the heat production in the human body or in combustion engines in cars. It is desirable to transform this low-quality form of energy into high-quality energy in the form of electrical power.
Thermoelectric materials are able to generate an electrical voltage upon application of a temperature gradient along the material. The gradient leads to a flow of charge carriers from the hot to the cold side and therefore to an imbalance in the charge distribution. The occurring thermovoltage or Seebeck coefficient (S), along with electrical (σ) and thermal conductivity (κ) can be put into the following equation for the temperature-dependent figure of merit ZT, which directly correlates to the energy conversion efficiency at a given average temperature: $ZT= (\sigma S^2/\kappa)T$.
Although inorganic thermoelectrics based on elements such as Te, Se, Pb, Bi, As, etc., exhibit high values for ZT, the price, low abundance, potential toxicity and environmental concerns regarding the raw materials have impeded the large-scale application for heat conversion.

Using the electrically conducting polymer blend PEDOT:PSS, we want to overcome the limitations of inorganic thermoelectrics, by making use of the high abundance of raw materials, facile solution-based processing and lowered toxicity. In literature, many different procedures for improving the electrical conductivity, usually by treating thin films with high-boiling solvents or other chemical agents, have been shown [1].
In our approach, we wish to tune the thermoelectric parameters, especially the thermal conductivity, by means of nanostructuring using inorganic nanoparticles. While maintaining a high electrical conductivity it should reduce the thermal conductivity through phonon scattering. We are able to fully characterize the polymer films regarding their thermoelectric properties, by using standard techniques for determination of S and σ and IR thermography for determination of κ. This enables the calculation of ZT values for PEDOT:PSS thin films. In addition, we performed resonant tender x-ray scattering (R-TeXS) experiments on the PEDOT:PSS/Si-NP composite films using synchrotron radiation energies close to the sulfur K-edge. Using the contrast variation capabilities of this technique, we are able to devise a structural model and attempt to correlate this with the thermoelectric properties of the composite films [2].

References

[1] H. Shi, C. Liu, Q. Jiang, J. Xu, Adv. Electron. Mater. 1, 1500017 (2015).
[2] N. Saxena, A. Greppmair, M. Coric, J. Wernecke, M. Pflüger, M. Krumrey, E. M. Herzig, M. S. Brandt, P. Müller-Buschbaum 3, 1700181 (2017)

Thermal and Mechanical Energy Harvesting based on PVDF

Marco Bobinger[a], Stefan Hinterleuthner[b], Marius Loch[c], Andreas Albrecht[d], Florin Loghin[e], Josef Mock[f], Almudena Rivadeneyra-Torres[g], Markus Becherer[h], Sherif Keddis[i], Norbert Schwesinger[j] and Paolo Lugli[k]

marco.bobinger@tum.de[a], stefan.hinterleuthner@mytum.de[b], marius.loch@tum.de[c], andreas.albrecht@tum.de[d], florin.loghin@tum.de[e], josef.mock@tum.de[f], almudena.rivadeneyra@tum.de[g], markus.becherer@tum.de[h], sherif.keddis@tum.de[i], schwesinger@tum.de[j] and paolo.lugli@unibz.it[k]

We report on the fabrication and characterization of energy harvesters based on the piezo- and pyroelectric material polyvinylidene fluoride (PVDF). Potential energy sources for the harvesters are for instance the hot exhaust system in cars or any source of mechanical vibration that occurs in e.g. large machine halls.

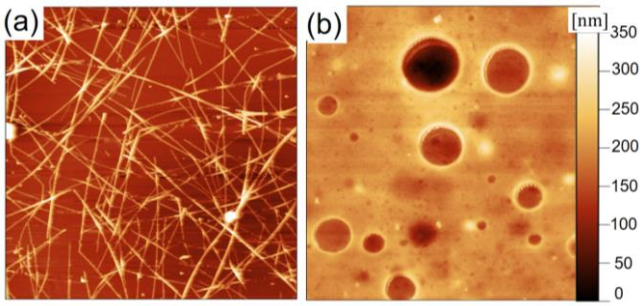

Figure 1. Atomic Force Microscope (AFM) images for (a) AgNWs and (b) PEDOT:PSS.

For the top and bottom electrodes that contact the 40 µm thick PVDF-foil, spray-coated and transparent electrodes (TEs) are utilized. As illustrated in Fig. 1, the TE films are made of (a) silver nanowires (AgNWs), (b) poly(3,4-ethylenedioxythiophene) polystyrene sulfonate (PEDOT:PSS) or a composite of these two materials. The transparency is required for the pyro-effect to allow the heat source, i.e. a conventional light bulb, to penetrate the electrode material and rapidly heat up the PVDF-foil. In principal, any source that induces a time-varying temperature in the PVDF foil can be exploited to harvest energy.

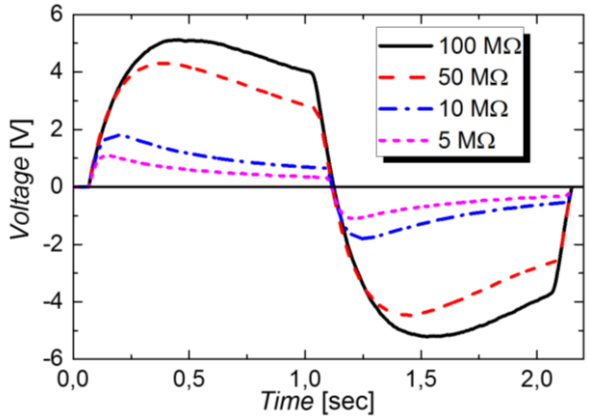

Figure 2. Transient voltage response for a PVDF-based energy harvester that is subjected to heating and connected to different ohmic load resistors.

The fabricated harvesters are characterized with regard to their voltage and current output as well as their optimum load resistances, as exemplarily depicted in Fig. 2 for the transient voltage response of a PVDF foil. The foil is subjected to the light of a conventional light bulb and the generated voltage is delivered to different load resistors. The presented energy harvesters can for instance be used to power smart as well as autonomous electronics, whose power consumptions are visualized in Fig. 3 (a). Attributed to the power output of the presented prototypes that can easily be up-scaled and lie in the sub-µW range, a promising application is to power a Wireless Sensor Node (WSN). Schematics for a WSN along with a power-management IC are shown in Fig. 3 (b) and (c).

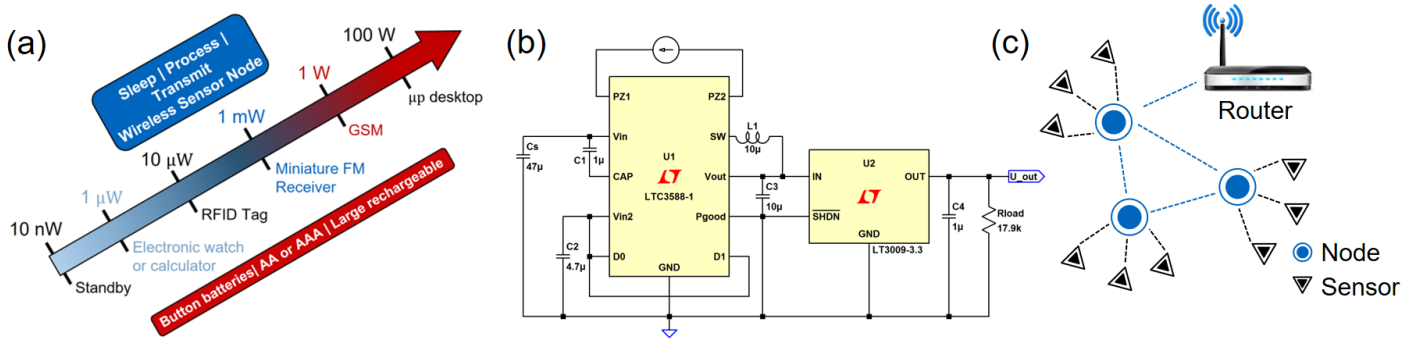

Figure 3. (a) Power consumption for a selection of smart electronic devices. (b) Sketch for a low-power management IC. (c) Schematic for a WSN.

Composites of laser ablated titanium dioxide and a water soluble polythiophene for energy transition

Jiabin Gui[a], Volker Körstgens[b], Klara Stallhofer,
Hristo Iglev, Reinhard Kienberger, Peter Müller-Buschbaum[c]

[a]jiabin.gui@ph.tum.de, [b]volker.koerstgens@ph.tum.de, [c]muellerb@ph.tum.de

Hybrid solar cells (HSCs) are feasible with an active layer consisting of laser-ablated titanium dioxide and a water-soluble polythiophene P3P6T [1]. HSCs combine organic and inorganic materials. Organic semiconductors have very high absorption coefficients, which allow very thin films to be used, whilst still absorbing a sufficient portion of the solar spectrum. Low cost manufacturing techniques, as well as light weight, implies that organic semiconductors have the potential to make a significant impact on the PV market. On the other hand, inorganic acceptor materials are more environmentally stable than organic materials, with high conductivity. Regarding the environmental impact hybrid solar cells which can be processed from aqueous solutions are of special interest. Furthermore the composite TiO_2/P3P6T investigated concerning its possible application in the field of thermoelectric materials, which convert heat directly into electricity, beneficial for recovering the wasted heat. The laser-ablation process is used in our work to functionalize the titania nanoparticles in order to achieve a good mixture and connection to the corresponding polymer. Laser ablation in liquids is also a convenient technique to structure nanomaterials, which additionally requires only a low energy demand. While the structure or the built-up of certain materials, compounds or alloys can be changed, the irradiation can also be used to change the size, shape and composition of already existing and suspended nanoparticles. When a focused laser beam hits a particle, the high energy density produces a strong ionization, resulting in a local plasma plume. The plasma plume has a spherical shape, with a high temperature and high pressure zone in the center. Due to the short duration of the laser pulse and medium as water, the plasma plume is instantly quenched again and the next pulse produces a new plasma plume.

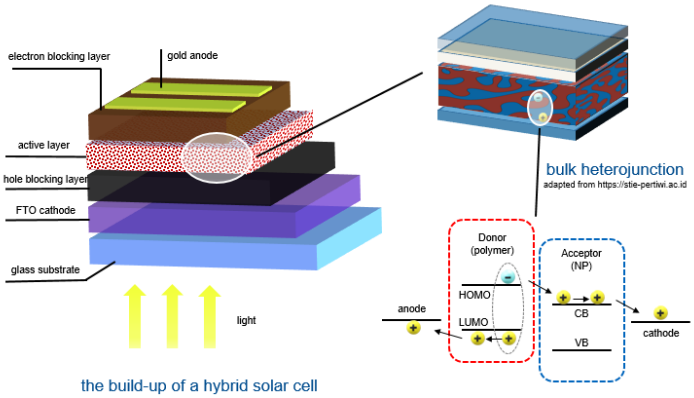

Figure 1: Principle of a hybrid solar cell

Spray coating as deposition technique is used due to its low cost, scalability and ability for layer-by-layer deposition. As a rapid, solution-based process technology finds itself a broad range of applications, including energy-saving applications, photovoltaics, and energy storage devices.

In our work, titanium dioxide particles are processed with laser ablation in water. Then mixed with P3P6T, TiO_2/P3P6T was spray coated on glass and silicon substrates. Films have been characterized with optical and spectroscopic methods as well as with x-ray characterization techniques. To further investigate the thermoelectric properties, Seebeck coefficient and electrical conductivity are discussed.

[1] Körstgens V, et al., Nanoscale, 2015, 7(7): 2900-2904

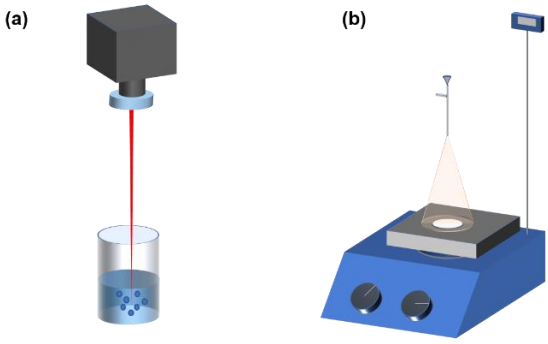

Figure 2: (a) Laser ablation (b) Spray coating

Modular test rig design for a pulsating heat pipe

Lukas Dirnberger[a], Felix Schily[b], Wolfgang Polifke[c]

[b]schily@tfd.mw.tum.de.de

The emergence of more compact designs with high power density, especially in micro electronics, has created a demand for an efficient heat transfer device, i.e. a device that can transfer large amounts of heat over long distances requiring merely a small temperature difference. This demand is met to some extent by conventional heat pipes. However, the complex inner structure and size restrictions limit their performance and applicability. The *pulsating heat pipe* has the prospect to overcome some of the limitations, i.e. it enables smaller geometries, cheaper manufacturing and easier system integration. As the conventional heat pipe, the pulsating heat pipe is a passive device and does not require auxiliary systems, such as a pump.

A pulsating heat pipe is a thin, wound tube, filled with a working fluid (often water or refrigerants) in two-phase state. Typically about half the volume is filled with liquid and the rest is occupied by the vapor of the working fluid. The diameter of the tube is sufficiently small that the working fluid forms bubbles and liquid slugs in the tube due to surface tension. Every other bend of the tube is in the evaporator section, whereas the others are in the condenser section. When heat is provided via the evaporator, some of the liquid evaporates and leads to growth of the bubble present. The bubble pushes the adjacent liquid slugs and bubbles in the direction of the condenser, where the bubbles are compressed. The temperature difference caused by the compression can then be used for heat rejection by condensation. The kinetic energy in the heat pipe is not completely absorbed by the cooling and therefore the pulsating heat pipe can enter a self-excited oscillating state with very high effective heat transfer rates. Despite experimental and also numerical studies, it is presently poorly understood, under which conditions an oscillation is amplified and maintained permanently.

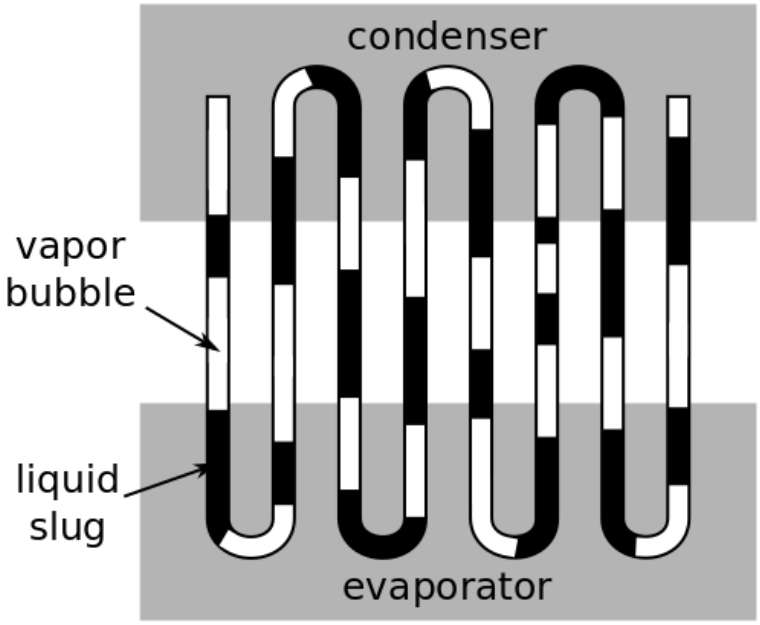

Schematic drawing of a pulsating heat pipe

In order to better understand the processes that govern the pulsating heat pipe, we are building a test bench that allows a great variability, while also granting optical access. The goal of our experiment is to obtain a rich data set on the movement and size of the bubbles and slugs and identify local heat transfer characteristics from the data. Local heat transfer characteristics are one of the missing links between previous numerical efforts and experimental results.

Another aspect that also can be investigated with our experiment is the mechanism of bubble formation. It is a general problem, that in the numerical models of pulsating heat pipes, it is possible to predict the event of bubble collapse, whereas it is not possible to predict the place and time of bubble formation. This often leads to conditions that are clearly more regular than experimental data show. A better understanding of the bubble formation mechanism is therefore another crucial step towards a proper modeling of pulsating heat pipes, which then enables tailored designs and safe operation for given applications.

Waste Heat Measurements from the Exhaust of a Ship Diesel Internal Combustion Engine

Roberto Pili[a], Manuel Jimenez-Arreola[b], Alessandro Romagnoli[c], Hartmut Spliethoff[d], Christoph Wieland[e]

[a]roberto.pili@tum.de, [b]manuel002@e.ntu.edu.sg, [c]a.romagnoli@ntu.edu.sg, [d]spliethoff@tum.de, [e]wieland@tum.de

The maritime propulsion is highly based on combustion of lower quality fuels in internal combustion engines (ICE). The European Environmental Agency reports that the international maritime sector in the EU emitted 135 Mio. tons of CO_2 in 2015, corresponding to 12.8 % of the total CO_2 emissions in the transportation sector [1]. Even though several efforts have been made to increase the efficiency of maritime ICEs, around 50 % of the fuel energy is still released to the environment as waste heat [2]. To quantify the available waste heat and the potential for waste heat recovery, a measurement device has been developed at the Institute for Energy Systems of the Technical University of Munich (TUM). The measurement device mainly focuses on gaseous waste heat, such as the exhaust gas of an ICE or the flue gas from an industrial process. It can measure the absolute pressure, the flow velocity and the temperature of the gas. The knowledge of these three variables, together with an estimation of the gas composition, can lead to an estimation of the mass flow rate and specific heat at constant pressure, and, in turn, to a quantification of the available waste heat. A thermocouple of type “K” is used for temperature measurement. A Pitot tube of type “L” is used instead for the measurement of the flow velocity given the differential pressure at the two tube outputs. From one of the connection outputs the absolute pressure is also read. Given the particle loading of the exhaust gases especially at low engine load, an air purging system has been also integrated to the measurement device. In this way, compressed air can flow at given time intervals in reverse direction to clean the probe orifices in the case they are blocked by the exhaust particles.

The potential of such measurement device is described in this contribution, based on measurements at the exhaust pipe of a ship 6-cylinder Diesel ICE (Daihatsu 6DK-26) located at the Maritime Energy Testbed (METB) at the Nanyang Technological University of Singapore (NTU) [3]. The engine load profile has been taken from [4], based on an average ship trip between Stockholm (Sweden) and Mariehamn (Finland). The profile has been rescaled in time in order to limit the total experiment time to 5 h.

The results show that a significant potential for waste heat recovery from the internal combustion engine is present. The temperature of the exhaust gas varied between 270 °C at idle mode up to 420 °C at higher load, whereas the velocity at the center of the pipe was found between 5 and 19 m/s. Accordingly, a volume flow rate between 2 500 and 10 000 m^3/h has been estimated.

The experiment has been affected by the high particle loading of the engine at low load. The purging system has allowed to temporarily clean the probe and evaluate some of the operating points, but it was not possible to clean the probe in long term. For future work, a Pitot tube of type “S” with larger orifices is recommended, not only for highly loaded gases from industrial processes, but also for ICEs similar to the one discussed in this work. This should avoid blocking of the probe and guarantee more reliable measurements and a larger spectrum of operating points. Waste heat from different applications is also planned in the close future.

References

[1] European Environment Agency (EEA). Greenhouse gas emissions from transport. https://www.eea.europa.eu/data-and-maps/indicators/transport-emissions-of-greenhouse-gases/transport-emissions-of-greenhouse-gases-10. (Published 11 July 2017, last modified 23 Oct 2017, accessed 03 May 2017).

[2] MAN Diesel & Turbo. Waste Heat Recovery Systems (WHRS) for Reduction of Fuel Consumption, Emissions and EEDI. https://turbomachinery.mandieselturbo.com/docs/librariesprovider4/Turbomachinery_doc/waste-heat-recovery-system-(whrs).pdf?sfvrsn=8 (accessed on 03 May 2017).

[3] Maritime Energy Test Bed (METB). http://mi.ntu.edu.sg/Research/About%20METB/Pages/Home.aspx (accessed on 03 May 2017).

[4] Mondejar, M. E.; Ahlgren, F.; Thern, M.; Genrup, M. Quasi steady-state simulation of an organic Rankine cycle for waste heat recovery in a passenger vessel. Applied Energy 2017; 185, pp. 1324-1335.

Method to monitor the function of electrostatic precipitators in biomass combustion plants by capturing the operation parameters

Bastian Alt[a], Matthias Gaderer[b]

[a]bastian.alt@tum.de, [b]gaderer@tum.de

Burning solid fuel, especially biomass produces a lot of solid particle emission. Usually, these are referred to as dust emissions. Depending on the particle size, the dust particles can be a severe threat to public health. Fine dust can enter the respiratory systems and damage the bronchial tubes and alveoli. Therefore, operators of biomass combustion plants are obligated to control and reduce dust emission. Usually, this can be done by installing flue gas cleaning equipment. Electrostatic precipitators are secondary equipment often used for reducing particle emissions in biomass combustion plants to achieve legislative limits. The national legislative dictates the permitted limits and inspection timeframes. Nevertheless, the EU defines guidelines on how to accomplish emission goals. One of these guidelines, the EU directive 2015/2193, demands for a continuous verification of the effective operation of medium combustion plants, which has to adhere to the national guidelines of every European country. This will only be the first step to implement a continuous surveillance system on all combustion plants. Even small-scale plants used for domestic or isolated supply will fall under this requirement in the near future. To fulfil this, operators will be forced to use online dust particle measurement techniques, using optical signals. The devices need to be able to withstand high temperatures in the flue gas and this increases the prize. A state of the art measurement system will cost from around 10.000 to over 100.000 euros, depending whether the particle size is measured as well or not. This additional investment will reduce the economic efficiency and therefore reduce the interest in using biomass fuel.

This project aims eliminate the need for additional investments by determining the emitted dust concentration solely from operation parameters already available at the precipitator itself.
This can be achieved by defining a method, which can calculate the dust concentration from the current value of the operating current and voltage of the precipitator. This will decrease the investment costs in the near future and increase the economic efficiency.
If the method delivers positive results in field test at real facilities, the national guidelines can accept it as a legit method.

Particle charging and movement inside an electrostatic precipitator is a complex mechanism with a variety of influences. Figure 1 shows a schematic description of the charging and transport mechanism that takes place inside the electrostatic precipitator. The emission electrode generates corona discharge and therefore free electrons. These rapidly moving electrons ionize air molecules. The charge air molecules adsorb at the particle surface witch leads the charging of the dust particles themselves. The electrostatic field now transports the particle out of the core stream to the connecting anode, where they can fall of in the mechanical cleaning interval.

The influences on the mechanism are mostly geometrical and kinematical factors that can be summarized in a single mathematical equation, the Deutsch equation. Given the assumption, that most variables, like collecting area and mean velocity, are constant under nominal conditions, there is a direct connection between the input and output dust concentration only depending on the operation current and voltage (Figure 1).

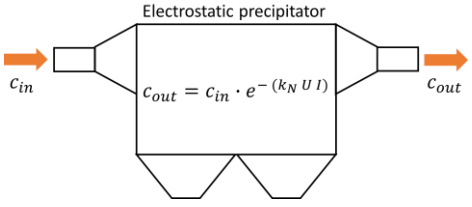

Figure 1: Schematic description

With this method, a continous survaillance of the precitipator can be achieved without further investment.

Detection of rotational periodic torque deviations in variable-speed wind turbine systems using disturbance observer and phase-locked loop

Korbinian Schechner[a], Christoph M. Hackl[b]

[a]korbinian.schechner@tum.de, [b]christoph.hackl@tum.de

Motivation

Condition monitoring and fault detection of wind turbines is an important task in the attempt of reducing failures and maintenance costs [1]. There is a huge variety of condition monitoring systems already available in the market. Most of the systems are based on vibration detection and require additional sensors and hardware installed in the wind turbine [2]. The purpose of these systems basically is to detect faults in the mechanical system of a wind turbine. Although stated to have relatively low costs (see [1]), the systems still cause additional expenses. To keep the costs of electricity—produced by wind turbine systems—at a minimum, while at the same time improving reliability of the system, condition monitoring techniques without the need of additional sensors seem to be an attractive choice. There are several faults which not only cause vibrations in the components of a wind turbine, but also cause rotational periodic deviations on the turbine shaft torque (see [3]). We present a method for detection of rotational periodic torque deviations in variable-speed wind turbine systems using disturbance observer and phase-locked loop.

Methodology

For fault detection, the turbine torque is estimated with an observer and an estimate of the aerodynamical torque is calculated. These torques are analysed using a phase-locked loop to detect deviations (see Fig. 1). The torque observer is based on the model of the turbine drive train. It is modelled as a two-mass-system with a flexible shaft. The design of the observer and the phase-locked loop are shown and their stability is discussed. Simulations show, that the presented concept is capable of detecting the amplitude of the deviations at different periodicities, online and at variable speed.

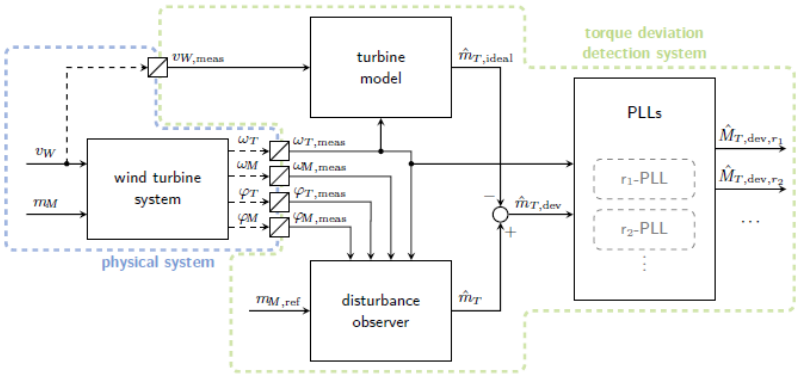

Figure 1: *Implementation of the torque deviation detection system.*

References

[1] W. Yang, P. J. Tavner, C. J. Crabtree, Y. Feng, and Y. Qiu, "Wind turbine condition monitoring: technical and commercial challenges," *Wind Energy*, vol. 17, no. 5, pp. 673–693, 2014.

[2] C. J. Crabtree, D. Zappalá, and P. J. Tavner, "Survey of commercially available condition monitoring systems for wind turbines." Durham University School of Engineering and Computing Sciences and the SUPERGEN Wind Energy Technologies Consortium, Tech. Rep., 2014.

[3] W. Qiao, "Recovery act: Online nonintrusive condition monitoring and fault detection for wind turbines," University of Nebraska - Lincoln, Tech. Rep., 2012.

Model predictive DC-link voltage control with disturbance observer for grid-connected power converters

Christian Dirscherl[1], Christoph M. Hackl[2]

Motivation

A raising amount of electrical systems are connected via power electronics to the electrical power grid (see [1]). Fig. 1 shows a grid-connected voltage source power converter (VSC) with DC-link, which is the most used topology of the installed power converters (see [1] and reference therein). The abilities to control the active and reactive power exchange with the grid independently and to support grid and frequency control are two important advantages of VSCs. To guarantee a reliable operation of such VSCs, it is necessary to achieve a stable DC-link voltage control. This is a non-trivial task, since the system is characterized by a non-minimum phase behavior when the load draws power from the VSC ([2],[3],[4],[5] and references therein).

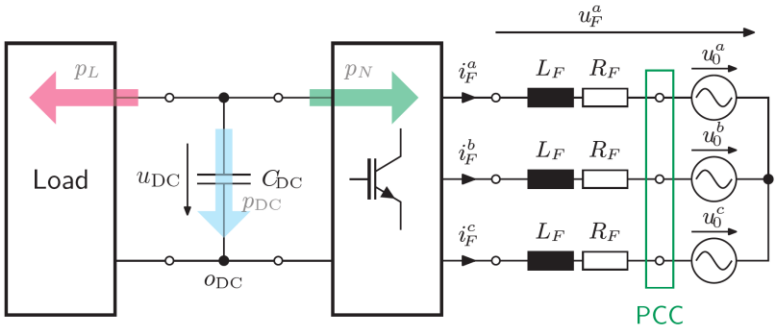

Figure 1: Grid-connected voltage source power converter with DC-link, RL-filter and load (based on [2]).

Methodology

For that, this poster discusses model predictive control (MPC) of the DC-link voltage. Compared with other multiple-objective MPC strategies, this poster presents a MPC method with explicit (analytical) solution. This allows for large prediction horizons, which (i) are beneficial for the control performance [6],[7]. and (ii) guarantee closed-loop stability [2]. Moreover, the system is augmented by a disturbance observer to estimate the load power. By feeding the load power estimation to the controller, an improvement of the steady state accuracy is achieved.

Results

Simulation results in Matlab/Simulink present the good control performance of the model predictive DC-link voltage controller with explicit solution (even for variations (a) in the load and (b) in the references of DC-link voltage and reactive power). In addition, the simulations illustrate the benefits from the disturbance observer which yields both a fast tracking of the real load and a better steady state accuracy of the DC-link voltage. Moreover, the impact of the length of the prediction horizon is highlighted—longer prediction horizons increase the control performance.

References

[1] F. Blaabjerg, Y. Yang, and K. Ma, „Power electronics – Key technology for renewable energy systems – Status and future,“in Proceedings of the 3rd International Conference on Electric Power and Energy Conversion Systems, 2013, pp. 1-6.

[2] C. Dirscherl, C. M. Hackl, and K. Schechner, „Explicit model predictive control with disturbance observer for grid-connected voltage source power converters,“ in Proceedings of the 2015 IEEE International Conference on Industrial Technology (ICIT 2015), 2015, pp. 999-1006.

[3] S. Heidary Yazdi, S. Fathi, G. Gharehpetian, and E. Ma'ali Amiri, „Regulation of DC link voltage in VSC-HVDC to prevent DC voltage instability based on accurate dynamic model,“in Proceedings of the 4th Power Electronics, Drive Systems and Technologies Conference, 2013, pp. 394-400.

[4] L. Zhang, H.-P. Nee, and L. Harnefors, „Analysis of stability limitations of a VSC-HVDC link using power-synchronization control,“IEEE Transactions on Power Systems, vol. 26, no. 3, pp. 1326-1337, 2011.

[5] R. K. Thakur, „Analysis and control of a variable speed wind turbine drive system dynamics,“in Proceedings of the International Conference on Power Systems, 2009, pp. 1-5.

[6] T. Geyer and D. E. Quevedo, „Multistep finite control set model predictive control for power electronics,“ Transactions on Power Electronics, vol. 29, no. 12, pp. 6836-6846, 2014.

[7] T. Geyer and D. E. Quevedo, „Performance of multistep finite control set model predictive control for power electronics,“ Transactions on Power Electronics, vol. 30, no. 3, pp. 1633-1644, 2015.

Design Sensitivities of Drag Power Kites

Florian Bauer[a], Ralph M. Kennel[b]

[a]florian.bauer@tum.de, [b]ralph.kennel@tum.de

A drag power kite [1] is a tethered electric aircraft which harvests wind energy by flying in crosswind motions such as figure eights or circles. The kite is like a tip of a rotor blade of a conventional wind turbine. Those blade tips harvest the majority of the energy, because they sweep the largest area and experience the highest (true) airspeed. Similar to the generative braking of the rotor of a conventional wind turbine, the kite brakes generatively, with small onboard wind turbines. Hence, a drag power kite uses only the most effective parts to harvest wind energy. Particularly the tower and the majority of the foundation are replaced by a lightweight tether, with which also higher altitudes with stronger and steadier winds are reachable. Electrical power is transferred between kite and ground via electrical cables integrated in the tether. The kite launches and lands like a multicopter, for which the onboard turbines and generators are reused as propellers and motors. A drag power kite with 600kW nominal power is currently under development at the company Makani/X Development [2].

A challenge is the design of the drag power kite plant. Not only the optimal flight altitude and tether length are obscure, but also many other design variables like the optimal voltage and diameter of the electrical cables in the tether. The latter incorporates e.g. the trade-off between low ohmic loss (large diameter optimal) and low overall aerodynamic tether drag (low diameter optimal). Similarly, a longer tether enables higher flight altitudes with stronger winds, but also increases the aerodynamic drag of the tether as well as the resistance of the electrical cables in the tether.

In this talk, the design sensitivities of an optimized MW-scale drag power kite plant are presented, with surprising and unexpected results. One example is, that the optimal tether voltage is around 7kV, but the optimum is very flat, i.e. the sensitivity is low. Therefore, also a much lower voltage may be used, which may greatly simplify the design of the power electronics at the negligible costs of an overall only slightly off-optimal power plant design. Such sensitivities can be of high value for a kite development team, because investment- and design decisions can be well-substantiated. The presented results are based on a comprehensive and multidisciplinary systems engineering model, which covers dominant effects of all involved disciplines: mechanical engineering (flight dynamics, aerodynamics, materials, structure, and thermodynamics), electrical engineering (power conversions through electrical drives and power electronics, and electricity transmission through tether), control engineering (power curve with actuator limitations, as well as reliability and safety issues due to rotor failures), meteorology (wind resource), and business administration (power plant economics). Preliminary results were presented in [3, 4]. All details on the model derivation, model validation, and results are currently being summarized in the corresponding author's dissertation.

[1] M. L. Loyd. “Crosswind kite power (for large-scale wind power production)”. In: Journal of Energy 4.3 (May 1, 1980), pp. 106–111. ISSN: 0146-0412. DOI: 10.2514/3.48021. URL: https://arc.aiaa.org/doi/10.2514/3.48021 (visited on Apr. 19, 2018).
[2] X Development LLC. “Makani”. URL: https://x.company/makani/ (visited on Apr. 19, 2018).
[3] F. Bauer, R. M. Kennel, C. M. Hackl, F. Campagnolo, M. Patt, and R. Schmehl. “Drag power kite with very high lift coefficient”. In: Renewable Energy (Elsevier) 118.Supplement C (2018), pp. 290–305. ISSN: 0960-1481. DOI: 10.1016/j.renene.2017.10.073. URL: http://www.sciencedirect.com/science/article/pii/S0960148117310285 (visited on Apr. 19, 2018).
[4] F. Bauer, R. M. Kennel, C. M. Hackl, F. Campagnolo, M. Patt, and R. Schmehl. “Power Curve and Design Optimization of Drag Power Kites”. In: Book of Abstracts of the Airborne Wind Energy Conference 2017. Ed. by Moriz Diehl, Rachel Leuthold, and Roland Schmehl. Freiburg, Germany: Albert Ludwigs University of Freiburg and Delft University of Technology, 2017, pp. 72–73. ISBN: 978-94-6186-846-6. DOI: 10.4233/uuid:4c361ef1-d2d2-4d14-9868-16541f60edc7. Conference video recording available from: www.awec2017.com (visited on Apr. 19, 2018).